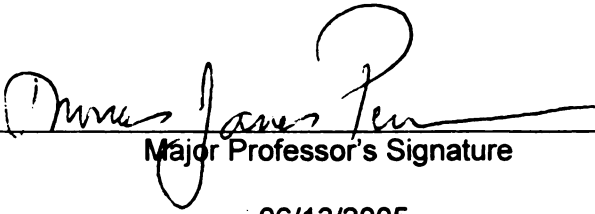This is to certify that the
dissertation entitled

Pure Azimuthal Shearing Deformations for an Extended Class
of Elastic Materials that are Characterized By a
Microstructurally Motivated Internal Balance Principle

presented by

Hasan Demirkoparan

has been accepted towards fulfillment
of the requirements for the

__Ph. D.__ degree in __Mathematics__

Major Professor's Signature

06/13/2005

Date

MSU is an Affirmative Action/Equal Opportunity Institution

PLACE IN RETURN BOX to remove this checkout from your record.
TO AVOID FINES return on or before date due.
MAY BE RECALLED with earlier due date if requested.

DATE DUE	DATE DUE	DATE DUE

Pure Azimuthal Shearing Deformations for an Extended Class
of Elastic Materials that are Characterized By a
Microstructurally Motivated Internal Balance Principle

By

Hasan Demirkoparan

A DISSERTATION

Submitted to
Michigan State University
in partial fulfillment of the requirements
for the degree of

DOCTOR OF PHILOSOPHY

Department of Mathematics

2005

ABSTRACT

Pure Azimuthal Shearing Deformations for an Extended Class of Elastic Materials that are Characterized By a Microstructurally Motivated Internal Balance Principle

By

Hasan Demirkoparan

In the event of certain substructural reconfiguration in solids, it is sometimes the case that the notion of simple deformation $\mathbf{X} \rightarrow \mathbf{x}$ must be broadened so as to incorporate a more detailed kinematic description. This typically involves new kinematic variables in addition to $\mathbf{x} = \mathbf{x}(\mathbf{X})$. Each new kinematic variable is in turn associated with an additional balance principle of the same tensor order as the new kinematic field variable. Gurtin's theory of configurational forces and the Ericksen model of liquid crystals are examples of such theories.

Recently a new constitutive framework for treating finite deformations when conventional elastic behavior is modified by the action of an additional microstructural balance requirement was proposed by Pence and Tsai. This framework offers interesting possibilities for the development of singular surfaces that can be interpreted as locations of concentrated microstructural rearrangement. This thesis investigates the solution of the pure azimuthal shear problem in this new framework.

To my parents and my wife,

ACKNOWLEDGMENTS

TABLE OF CONTENTS

LIST OF TABLES

LIST OF FIGURES

CHAPTER 1

Introduction

In the event of substructural reconfiguration in solids, it is sometimes the case that the notion of simple deformation $\mathbf{X} \to \mathbf{x}$ must be broadened so as to incorporate a more detailed kinematic description. This typically involves new kinematic variables in addition to $\mathbf{x} = \mathbf{x}(\mathbf{X})$. Each new kinematic variable is in turn associated with an additional balance principle of the same tensor order as the new kinematic field variable. The continuum mechanical theory known variously as "continua with microstructure" [9] or "multi-field theory" [18] gives insight into the role of such additional balance equations. Gurtin's theory of configurational forces provides a related type of description [12]. A well-known example of such a theory is the Ericksen model of liquid crystals [10]. In the liquid crystal theory, the additional field is a (unit) vector that describes the liquid crystal orientation.

A new constitutive framework for treating finite deformations when conventional elastic behavior is modified by substructural reconfiguration has recently been proposed by Pence and Tsai [22]. Energy minimization then leads to an additional balance principle that is associated with the richer kinematics. In this thesis, we investigate the solution of the pure azimuthal shear problem in this new framework. Azimuthal shear is most simply conceived as a twisting deformation of a circular cylinder due to an imposed difference in twist Ψ between in the inner and outer

1

radii. The constitutive model has, among other things, a natural parameter $k \geq 0$ such that the neo-Hookean material in standard nonlinear elasticity is retrieved in the limit $k \to 0$. In Chapter 2 the solution of the pure azimuthal shear problem is summarized for a neo-Hookean material in standard nonlinear elasticity theory. The methodology and results of the pure azimuthal shear problem for a neo-Hookean material are well-known and will serve as a basis for comparison with the new results described in this thesis. The new content of the thesis is divided into two parts as presented in Chapters 3 and 4.

The first part of this thesis, Chapter 3, is concerned with a material model such that the stored energy to be minimized is the sum of two terms. One term can be viewed as penalizing macroscopic elastic deformation and the strength of this penalization is described by a positive constant $\hat{\alpha}$. The second term can be viewed as penalizing elastic substructural reconfiguration and its strength is described by a positive constant α^*. The parameter k is the ratio $\hat{\alpha}/\alpha^*$. In the first section of Chapter 3 the pure azimuthal shear problem in this new framework is formulated. It is confirmed that if the parameter k goes to zero, then the pure azimuthal shear problem in the new framework reduces to the standard pure azimuthal shear problem for a neo-Hookean material. Since the governing field equations are complicated for a general k, it does not seem feasible to get a closed form solution for arbitrary k. Hence, in Section 3.2, the pure azimuthal shear problem is studied for small k by a perturbation expansion about the base neo-Hookean solution. The torque-twist relation is also presented for small k. An interesting aspect of the torque-twist relation as determined by the perturbation analysis is that torque is not an increasing function of twist for all values of twist if $k \neq 0$. The pure azimuthal shear problem is then solved numerically for any k in Section 3.3. When $k \neq 0$ the numerical solution reveals evidence of a threshold value for twist at which smooth solutions

are no longer available. In Section 3.4 the pure azimuthal shear problem is solved analytically in the special value $k = 1$ and a restriction in the form $|\Psi| \leq \Psi_{\text{max}}$ on the imposed twist Ψ is obtained for a classically smooth solution. With the exception of $k = 0$ and $k = 1$ it does not seem likely that analytic solutions can be constructed explicitly. In Section 3.5 the pure azimuthal shear problem is derived by minimizing an appropriately reduced stored energy function which acknowledges the symmetries inherent in the solution. In particular, we prove that the exact solution that is derived in Section 3.4, is indeed an absolute minimum for the energy integral when $k = 1$. In Section 3.6 direct methods of calculus of variations are used to investigate solution possibilities for arbitrarily large twist Ψ when $k = 1$. A minimizing curve is obtained among a collection of test curves for the parametric energy integral when the twist is arbitrarily large. Indeed we prove that this minimizing curve is an absolute minimum of the parametric energy integral in the class of piecewise-smooth curves such that, once restricted to the interior, their parametrization reduces to a function. The importance of such a result is that if we seek minimizers of the nonparametric energy integral for arbitrarily large twist Ψ in the space of piecewise-smooth functions, then the global minimum involves a discontinuity at the inner radius.

A more generalized material model is considered in the second part, Chapter 4. The strain-energy function for the new material model augments the strain-energy function of the first part by inclusion of an additional term. This additional term can be viewed as penalizing the overall deformation, as opposed to penalizing specific partial deformations. The strength of this penalization is described by a positive constant α. Thus there are now three terms to the stored energy with respective strengths $\hat{\alpha}$, α^* and α. The pure azimuthal shear problem subject to the same boundary conditions is studied in this extended material model when $\hat{\alpha} = \alpha^*$ $(k = 1)$. Our interest is in the extent to which $\alpha > 0$ gives different qualitative behavior from

the $\alpha = 0$ treatment of Chapter 3.

In the first section of Chapter 4, the pure azimuthal shear problem is formulated for the extended material model when $\hat{\alpha} = \alpha^*$. Moreover the resulting boundary value problem is expressed as an integral equation. In addition two modified boundary value problems are also defined. These *second boundary value problems* for the pure azimuthal shear problem are useful for obtaining existence and uniqueness results. The principle of contracting mapping is then used to prove an existence and uniqueness result for the pure azimuthal shear problem in Section 4.2. In Section 4.3 the pure azimuthal shear problem is solved numerically in the extended material model. In Section 4.4 a regular perturbation procedure is used to investigate the solution of the pure azimuthal shear problem when the material parameter $\alpha/\hat{\alpha}$ is small. It is observed that if $|\Psi| > \Psi_{\mathrm{max}}$, then the regular perturbation cannot be used. Further if $|\Psi| > \Psi_{\mathrm{max}}$ or $|\Psi| = (1 - \epsilon)\Psi_{\mathrm{max}}$ with $0 < \epsilon \ll 1$, then severe requirements are placed on the smallness of $\alpha/\hat{\alpha}$ in order to obtain a useful approximation near the inner radius. In Section 4.5 a boundary layer type analysis is developed in order to get a useful approximation in such cases. In particular, inner and outer solutions are obtained and a patching method is proposed for obtaining the full solution. This patching method is found to give satisfactory agreement with the numerical solution. The relation between torque, twist and energy in the extended material model is studied in Section 4.6, which is then followed by a concluding discussion in Chapter 5.

CHAPTER 2

Pure Azimuthal Shear Problem for a Neo-Hookean material

2.1   Introduction

This section provides preliminary discussion from the well known conventional theory of hyperelasticity in order to provide context for this thesis. Readers familiar with the pure azimuthal shear problem for a neo-Hookean material can, if they wish, proceed directly to Chapter 3.

2.2   Pure Azimuthal Shear Problem for a Neo-Hookean material

In standard nonlinear continuum mechanics it is the case that the continuity equation, the principles of linear and angular momentum, and the energy equation hold for any material regardless of its constitution. However, unless the body can be regarded as rigid, these equations are in general insufficient to determine the motion produced by given boundary conditions and body forces. They need to be supplemented by

a further set of equations, known as *constitutive equations*, which characterize the material composition of the body. Such a set of constitutive equations usually serves to define an ideal material, and much of the work on modern continuum mechanics has been concerned with the formulation of constitutive equations to model as closely as possible the behavior of real materials.

We consider a continuous body which occupies a connected open subset of a three-dimensional Euclidean point space, and we refer to such a subset as a *configuration* of the body. We identify a specific configuration as a *reference configuration* and denote this by B_r. Let points in B_r be labeled by their position vectors $\mathbf{X}$ relative to some chosen origin and let ∂B_r denote the boundary of B_r. Now suppose that the body is deformed quasi-statically from B_r so that it occupies a new configuration, B with boundary ∂B. We refer to B as the *current* or *deformed configuration* of the body. The deformation is represented by the mapping $\chi : B_r \rightarrow B$ which takes points $\mathbf{X}$ in B_r to points $\mathbf{x}$ in B, where $\mathbf{x}$ is the position vector corresponding to the point $\mathbf{X}$ in B_r. The mapping χ is called the *deformation* from B_r to B.

In this section we review the well known treatment of this deformation in the context of conventional continuum mechanics and hyperelasticity. In such a treatment the *equilibrium equations* in the absence of body forces are given by

$$div\, \boldsymbol{\sigma} = 0, \tag{2.1}$$

where $\boldsymbol{\sigma}$ is the *Cauchy stress tensor* and *div* is the divergence operator with respect to current coordinates. The constitutive equation of an elastic material is given in the form

$$\boldsymbol{\sigma} = G(\mathbf{F}), \tag{2.2}$$

where G is a symmetric tensor-valued function defined on the space of deformation

gradients $\mathbf{F}$. Here $\mathbf{F} = Grad\,\mathbf{x}$ or in component form

$$F_{i\alpha} = \frac{\partial x_i}{\partial X_\alpha},\tag{2.3}$$

where i and $\alpha \in \{1, 2, 3\}$. In general the form of G depends on the choice of reference configuration and G is referred to as the response function of the material relative to reference configuration B_r. A material whose constitutive law has the form (2.2) is referred to as a *Cauchy elastic material*. From the point of view of both theory and applications a more useful concept of elasticity, which is a special case of Cauchy elasticity, is *hyperelasticity* (or *Green elasticity*). In this theory there exists a *stored energy function* (or *strain-energy function*), denoted $W = W(\mathbf{F})$, defined on the space of deformation gradients such that the total stored energy is given by

$$E = \int W(\mathbf{F})\,dV.\tag{2.4}$$

Then for an unconstrained material

$$\boldsymbol{\sigma} = G(\mathbf{F}) = J^{-1}\frac{\partial W}{\partial \mathbf{F}}\,\mathbf{F}^T,\tag{2.5}$$

where $J = det\,\mathbf{F}$. The *Jacobian* J of the deformation gradient $\mathbf{F}$ determines the resulting volume change in the deformation. In this setting (2.1), (2.5) are the *Euler-Lagrange* equations associated with minimization of (2.4). For a volume preserving (*isochoric*) deformation

$$J = 1.\tag{2.6}$$

A material for which (2.6) is constrained to be true for all deformation gradients $\mathbf{F}$ is said to be *incompressible*. The modification of (2.5) appropriate for incompressibility is

$$\boldsymbol{\sigma} = \frac{\partial W}{\partial \mathbf{F}}\,\mathbf{F}^T - p\,\mathbf{I},\tag{2.7}$$

where $\mathbf{I}$ is the *identity tensor* and the scalar p is an arbitrary *hydrostatic pressure*, that is formally the Lagrange multiplier associated with the constraint (2.6).

7

A standard model for an incompressible material is given by the neo-Hookean stored energy density W in the form

$$W = \frac{1}{2}\mu \left(I_1 - 3\right), \tag{2.8}$$

where $\mu > 0$ is the *shear modulus* of the material in the reference configuration, $I_1 = tr(\mathbf{B})$ and $\mathbf{B} = \mathbf{F}\mathbf{F}^T$, the *left Cauchy-Green tensor* of the deformation, and tr denotes the trace. More detailed explanation of the above concepts, including restrictions upon W motivated by observer invariance and material symmetry requirements, can be found in any standard nonlinear elasticity book [2], [3], [11], [21].

Consider a nonlinearly elastic thick-walled circular cylindrical tube whose natural (unstressed) configuration is defined by

$$0 < R_i \leq R \leq R_o,\ 0 \leq \Theta < 2\pi,\ 0 \leq Z \leq h, \tag{2.9}$$

where (R, Θ, Z) are cylindrical polar coordinates. Consider the following deformation

$$r = R,\ \theta = \Theta + g(R),\ z = Z, \tag{2.10}$$

where (r, θ, z) are cylindrical polar coordinates associated with the deformed configuration. The deformation (2.10) is called a *pure azimuthal shear* (it is also called *gyroscopic, rotational* or *circumferential shear* in the finite elasticity literature [6], [15], [24], [26]). The deformation gradient $\mathbf{F}$ is given by

$$\mathbf{F} = \begin{bmatrix} 1 & 0 & 0 \\ rg' & 1 & 0 \\ 0 & 0 & 1 \end{bmatrix} = \mathbf{I} + rg'\,\mathbf{e}_\theta \otimes \mathbf{e}_R, \tag{2.11}$$

where $'$ denotes the derivative with respect to R. Since $r = R$ we may also consider that the derivative is with respect to r. Note that (2.6) is satisfied for this deformation.

The left Cauchy-Green tensor $\mathbf{B} = \mathbf{F}\,\mathbf{F}^T$ is

$$\mathbf{B} = \begin{bmatrix} 1 & rg' & 0 \\ rg' & 1 + (rg')^2 & 0 \\ 0 & 0 & 1 \end{bmatrix} \tag{2.12}$$

$$= \mathbf{I} + rg'\,(\mathbf{e}_\theta \otimes \mathbf{e}_r + \mathbf{e}_r \otimes \mathbf{e}_\theta) + (rg')^2\,\mathbf{e}_\theta \otimes \mathbf{e}_\theta.$$

For a neo-Hookean material the Cauchy stress tensor follows from (2.7), (2.8) as

$$\boldsymbol{\sigma} = -p\,\mathbf{I} + \mu\,\mathbf{B}. \tag{2.13}$$

The equilibrium equations (2.1) in cylindrical coordinates are

$$\frac{\partial \sigma_{rr}}{\partial r} + \frac{1}{r}\frac{\partial \sigma_{r\theta}}{\partial \theta} + \frac{\partial \sigma_{rz}}{\partial z} + \frac{1}{r}\,(\sigma_{rr} - \sigma_{\theta\theta}) = 0, \tag{2.14}$$

$$\frac{\partial \sigma_{\theta r}}{\partial r} + \frac{1}{r}\frac{\partial \sigma_{\theta\theta}}{\partial \theta} + \frac{\partial \sigma_{\theta z}}{\partial z} + \frac{1}{r}\,(\sigma_{r\theta} + \sigma_{\theta r}) = 0, \tag{2.15}$$

$$\frac{\partial \sigma_{zr}}{\partial r} + \frac{1}{r}\frac{\partial \sigma_{z\theta}}{\partial \theta} + \frac{\partial \sigma_{zz}}{\partial z} + \frac{1}{r}\,\sigma_{zr} = 0. \tag{2.16}$$

We will impose boundary conditions of prescribed twist

$$g(R_i) = \psi_i, \quad g(R_o) = \psi_o. \tag{2.17}$$

We also consider the boundary condition

$$\sigma_{rr}(R_o) = \sigma_{rr}^0, \tag{2.18}$$

meaning that the outer surface $R = R_o$ supports a radial traction σ_{rr}^0. Replacing the components of $\boldsymbol{\sigma}$ in equilibrium equations (2.14)–(2.16) gives

$$\frac{\partial(\mu - p)}{\partial r} + \frac{1}{r}\frac{\partial(\mu rg')}{\partial \theta} + \frac{1}{r}[-\mu(rg')^2] = 0, \tag{2.19}$$

$$\frac{\partial(\mu rg')}{\partial r} + \frac{1}{r}\frac{\partial(\mu + \mu(rg')^2 - p)}{\partial \theta} + \frac{1}{r}(2\mu rg') = 0, \tag{2.20}$$

$$\frac{\partial(\mu - p)}{\partial z} = 0. \tag{2.21}$$

Since g is a function of r only, it follows from (2.19)–(2.21) that

$$\frac{\partial p}{\partial r} + \mu r (g')^2 = 0, \tag{2.22}$$

$$\mu \frac{\partial(rg')}{\partial r} - \frac{1}{r}\frac{\partial p}{\partial \theta} + 2\mu g' = 0, \tag{2.23}$$

$$\frac{\partial p}{\partial z} = 0. \tag{2.24}$$

Then equation (2.24) gives

$$p = p(r, \theta), \tag{2.25}$$

while equation (2.23) supplies

$$\frac{\partial p}{\partial \theta} = \mu r \frac{\partial(rg')}{\partial r} + 2\mu r g'. \tag{2.26}$$

Hence $\partial p/\partial \theta$ is a function of r only and so p must be linear in θ; i.e.,

$$p = c_0(r)\,\theta + \bar{p}(r). \tag{2.27}$$

On the other hand it is immediate from equation (2.22) that

$$\frac{\partial^2 p}{\partial r\,\partial \theta} = 0. \tag{2.28}$$

Hence $c_0(r)$ is a constant function and p becomes

$$p = c_0\,\theta + \bar{p}(r). \tag{2.29}$$

Because of the symmetry, for any θ

$$\sigma_{rr}(\theta) = \sigma_{rr}(\theta + 2\pi), \tag{2.30}$$

which gives

$$c_0 \equiv 0. \tag{2.31}$$

Consequently

$$p = p(r). \tag{2.32}$$

Using the above result in (2.26) gives

$$\frac{\partial (r^3 g')}{\partial r} = 0. \tag{2.33}$$

After integration and replacing r by R

$$g(R) = \frac{c_1}{R^2} + c_2, \tag{2.34}$$

where c_1 and c_2 are integration constants. Using the above result in (2.22)

$$p(R) = \frac{\mu c_1^2}{R^4} + c_3, \tag{2.35}$$

where c_3 is another integration constant. The boundary conditions (2.17) now give

$$c_1 = \frac{(\psi_o - \psi_i) R_i^2 R_o^2}{R_i^2 - R_o^2}, \tag{2.36}$$

$$c_2 = \psi_i + \frac{(\psi_i - \psi_o) R_o^2}{R_i^2 - R_o^2}. \tag{2.37}$$

Notice that $|g'(R)|$ is decreasing in R with finite maximum value

$$|g'(R_i)| = \frac{2 (\psi_i - \psi_o) R_o^2}{R_i (R_i^2 - R_o^2)}. \tag{2.38}$$

The boundary condition (2.18) supplies

$$c_3 = \frac{(\psi_i - \psi_o)^2 R_i^4}{(R_i^2 - R_o^2)^2} \mu - \mu + \sigma_{rr}^0. \tag{2.39}$$

This completes the solution of pure azimuthal shear problem for a neo-Hookean material. The methodology and results (2.9)–(2.39) are well-known and will serve as a basis for comparison with the new results described in this paper. We will compute some useful quantities for later use. The *normal traction* on the inner surface $R = R_i$ is

$$\sigma_{rr}(R_i) = -\mu \frac{R_o^2 + R_i^2}{R_o^2 - R_i^2} (\psi_o - \psi_i)^2 + \sigma_{rr}^0. \tag{2.40}$$

11

Note that $\sigma_{rr}(R_i) < \sigma_{rr}^0$. The *azimuthal component of the traction* on the inner and outer surfaces are given respectively by

$$\sigma_{\theta r}(R_i) = 2\mu \, \frac{R_o^2}{R_o^2 - R_i^2} \, (\psi_o - \psi_i), \tag{2.41}$$

$$\sigma_{\theta r}(R_o) = 2\mu \, \frac{R_i^2}{R_o^2 - R_i^2} \, (\psi_o - \psi_i). \tag{2.42}$$

Torques, M_i and M_o acting on inner and outer surfaces are

$$M_i = h \int_0^{2\pi} -R_i^2 \, \sigma_{\theta r}(R_i) \, d\theta = -\frac{4\,\pi\,\mu\,h\,R_i^2\,R_o^2}{R_o^2 - R_i^2} \, (\psi_o - \psi_i), \tag{2.43}$$

$$M_o = h \int_0^{2\pi} R_o^2 \, \sigma_{\theta r}(R_o) \, d\theta = \frac{4\,\pi\,\mu\,h\,R_i^2\,R_o^2}{R_o^2 - R_i^2} \, (\psi_o - \psi_i). \tag{2.44}$$

Note that $M_i + M_o = 0$, which is expected from the general theory. Let $M = M_o = -M_i$. *Twist* Ψ is defined to be the difference between angular displacements at $R = R_o$ and $R = R_i$:

$$\Psi = (\psi_o - \psi_i). \tag{2.45}$$

The *Torque-Twist* relation now follows from (2.44), (2.45) as

$$M = \frac{4\,\pi\,\mu\,h\,R_i^2\,R_o^2}{R_o^2 - R_i^2} \, \Psi. \tag{2.46}$$

Note from (2.12) that, $I_1 = 3 + (rg')^2$ which in turn gives $W = \mu\,(rg')^2/2$. The energy E stored by this deformation follows from (2.4) and (2.34) as

$$E = \frac{2\,\pi\,\mu\,h\,R_i^2\,R_o^2}{R_o^2 - R_i^2} \, \Psi^2. \tag{2.47}$$

The work of the torque (2.44) is defined to be

$$\check{W} = \int_0^{\Psi} M(\psi) \, d\psi, \tag{2.48}$$

where $M = M(\psi)$ is given by (2.46) with ψ replacing Ψ. By direct calculation it is found that

$$\check{W} = E, \tag{2.49}$$

12
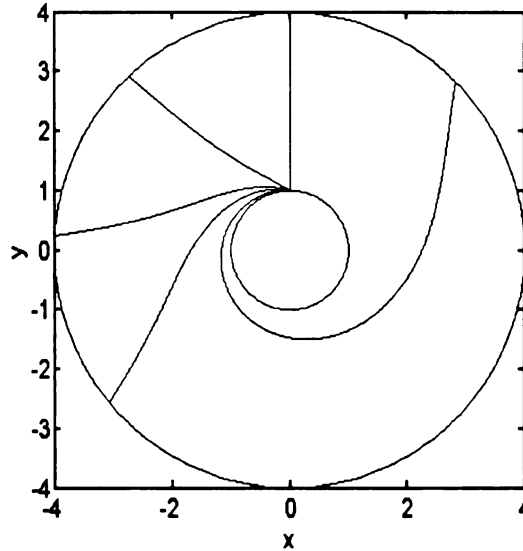
Figure 2.1: Deformation of an originally vertical line segment for different amount of twist ψ_o and $\psi_i = 0$. Specifically shown are $\psi_o = .75413$, 1.50826, 3.0165, 5.49779 corresponding respectively to $43.20°$, $86.41°$, $129.62°$, $315°$ for a neo-Hookean material in standard nonlinear elasticity theory. Note that $R_i = 1$ and $R_o = 4$ are used and multiples of $\arccos(R_i^2/R_o^2) = 1.50826$ are selected in order to provide correspondence with results of the more general theory that is the object of this thesis

which is also to be expected from the general theory.

We will conclude this section by considering the cross-section $R_i = 1$, $R_o = 4$ and sketching the deformation of the line segment given by $\{(R, \Theta)|1 \leq R \leq 4, \Theta = \pi/2\}$ in the reference configuration. Suppose $\psi_i = 0$ so that deformation is governed by ψ_o whereupon $g(R) = ((-16/15R^2) + 16/15) \psi_o$, $g'(R) = (32/15R^3) \psi_o$. Figure 2.1 shows the deformed location of the line segment for four values ψ_o:

$\psi_o = 0.5 \arccos(R_i^2/R_o^2) = 0.75413$, $\psi_o = \arccos(R_i^2/R_o^2) = 1.50826$, $\psi_o = 1.5 \arccos(R_i^2/R_o^2) = 3.0165$, $\psi_o = (7/4)\pi = 5.49779$. Multiples of $\arccos(R_i^2/R_o^2) = 1.50826$ are selected in order to provide correspondence with results of the more general theory as later considered in Section 3.4.

13

CHAPTER 3

The Internally Balanced Material

3.1 Formulation of the Problem for the Internally Balanced Material

The constitutive framework that we consider in this thesis is due to Pence and Tsai [22] and is based on multiplicative decomposition of the deformation gradient

$$\mathbf{F} = \hat{\mathbf{F}}\mathbf{F}^*, \tag{3.1}$$

where $\hat{\mathbf{F}}$ and $\mathbf{F}^*$ are respectively the conventional elastic part of the deformation and a precursor internal deformation that we will term pre-elastic. A full discussion of the rationale and motivation for this theory is given by Pence and Tsai [22]. In this thesis we will consider materials that admit only volume preserving deformations; hence

$$\det \mathbf{F} = 1. \tag{3.2}$$

Further, the elastic part itself is also taken to be volume preserving and thus

$$\det \hat{\mathbf{F}} = 1. \tag{3.3}$$

Note that (3.2), (3.3) in turn give

$$\det \mathbf{F}^* = 1, \tag{3.4}$$

and that any two of (3.2), (3.3), (3.4) implies the third. Equilibrium in this theory is based on minimizing the potential energy functional

$$E = \int W(\hat{\mathbf{F}}, \mathbf{F}^*) \, dX,$$ (3.5)

where W is a general storage energy function. The energy considered here is taken to have the following form

$$W = \frac{\alpha^*}{2}(I_1^* - 3) + \frac{\hat{\alpha}}{2}(\hat{I}_1 - 3),$$ (3.6)

where $\alpha^* \geq 0$ is the *internal modulus*, $\hat{\alpha} \geq 0$ is the *shear modulus* and $I_1^* = tr\,\mathbf{B}^*$ and $\hat{I}_1 = tr\,\hat{\mathbf{B}}$ with $\mathbf{B}^* = \mathbf{F}^*(\mathbf{F}^*)^T$ and $\hat{\mathbf{B}} = \hat{\mathbf{F}}(\hat{\mathbf{F}})^T$. Note that both $\hat{\mathbf{B}}$ and $\mathbf{B}^*$ are symmetric positive-definite with

$$\det \hat{\mathbf{B}} = 1,$$ (3.7)

and

$$\det \mathbf{B}^* = 1.$$ (3.8)

As discussed by Pence and Tsai [22] minimization of the potential energy functional involves separate independent variations with respect to both $\mathbf{x}$ and $\mathbf{F}^*$. Minimization with respect to $\mathbf{x}$ at fixed $\mathbf{F}^*$ gives

$$div\,\boldsymbol{\sigma} = 0,$$ (3.9)

$$\boldsymbol{\sigma} = \hat{\alpha}\,\hat{\mathbf{B}} - p\,\mathbf{I}.$$ (3.10)

Here p is a Lagrange multiplier associated with the constraint (3.2). Minimization with respect to $\mathbf{F}^*$ at fixed $\mathbf{x}$ gives the *internal balance*

$$\hat{\alpha}\,\hat{\mathbf{B}}^2 + q\,\hat{\mathbf{B}} = \alpha^*\,\mathbf{B},$$ (3.11)

where q is a Lagrange multiplier associated with the constraint (3.4). Equation (3.11) is the additional internal balance principle that serves to generalize the present treatment. It is a natural consequence of the energetic dependence on the decomposition

(3.1) which, as discussed Pence and Tsai, is motivated by the need to characterize materials with complex microstructural features.

Pence and Tsai prove for arbitrary symmetric positive-definite tensor $\mathbf{B}$ obeying $\det \mathbf{B} = 1$ that equations (3.7) and (3.11) can be solved uniquely for a symmetric positive-definite tensor $\hat{\mathbf{B}}$ and scalar q [22]. The proof given by Pence and Tsai is not fully constructive, in that the analysis generates a sixth order polynomial equation for q that may not have a closed form expression for the root of interest. The root itself however is guaranteed to exist and selected by a bound requirement.

We now formulate the pure azimuthal shear problem for this material. This deformation is again assumed to be in the form (2.10) so that (2.11), (2.12) continue to hold. This in turn ensures (3.2). We seek scalar functions $g(r)$, $p(r, \theta, z)$, $q(r, \theta, z)$ and a symmetric positive-definite tensor function $\hat{\mathbf{B}}(r, \theta, z)$ such that equations (3.7), (3.9), (3.10), (3.11) hold where $\mathbf{B}$ is given by (2.12). We again consider boundary conditions (2.17), (2.18).

Since $\mathbf{B}$ is given by (2.12), equations (3.7) and (3.11) can in principal be solved for $\hat{\mathbf{B}}$ and q in terms of rg', implying, in particular, that $q = q(r)$ and $\hat{\mathbf{B}} = \hat{\mathbf{B}}(r)$. Once $\hat{\mathbf{B}}$ is known the components of $\boldsymbol{\sigma}$ follow from (3.10) whereupon the equilibrium equation (3.9) is anticipated to first require $p = p(r)$ and second provide $g(R)$ and $p(R)$. This is the strategy in what follows.

By using the argument given by Pence and Tsai, it can be shown that $\hat{\mathbf{B}}$ and q are independent of θ and z by the following argument. Let $\mathbf{b}_i$ and $\hat{\mathbf{b}}_i$ be the eigenvectors of $\mathbf{B}$ and $\hat{\mathbf{B}}$, respectively, corresponding to the eigenvalues λ_i^2 and $\hat{\lambda}_i^2$ respectively. The internal balance (3.11) gives that $\mathbf{B}$ and $\hat{\mathbf{B}}$ have common principal frames whence $\mathbf{b}_i = \hat{\mathbf{b}}_i$. Thus by principal frame calculations

$$\lambda_i^2 = (\alpha^*)^{-1} (\hat{\alpha} \, \hat{\lambda}_i^4 + q \, \hat{\lambda}_i^2), \tag{3.12}$$

16

and

$$\hat{\lambda}_i^2 = \frac{-q + \sqrt{q^2 + 4\,\alpha^*\,\hat{\alpha}\,\lambda_i^2}}{2\,\hat{\alpha}}. \tag{3.13}$$

Since (3.7) gives $\hat{\lambda}_1^2\,\hat{\lambda}_2^2\,\hat{\lambda}_3^2 = 1$, it follows from (3.13) that

$$\prod_{i=1}^{3}\left(-q + \sqrt{q^2 + 4\,\hat{\alpha}\,\alpha^*\,\lambda_i^2}\right) = 8\,\hat{\alpha}^3. \tag{3.14}$$

By using the definition of $\mathbf{B}$

$$\lambda_1^2 = 1, \tag{3.15}$$

$$\lambda_2^2 = \frac{1}{2}\left(2 + (rg')^2 - \sqrt{-4 + (2 + r^2 g'^{\,2})^2}\right), \tag{3.16}$$

$$\lambda_3^2 = \frac{1}{2}\left(2 + (rg')^2 + \sqrt{-4 + (2 + r^2 g'^{\,2})^2}\right), \tag{3.17}$$

and corresponding eigenvectors are

$$\mathbf{b}_1 = \mathbf{e}_z, \tag{3.18}$$

$$\mathbf{b}_2 = -\frac{(rg')^2 + \sqrt{-4 + (2 + r^2 g'^{\,2})^2}}{2rg'}\,\mathbf{e}_r + \mathbf{e}_\theta, \tag{3.19}$$

$$\mathbf{b}_3 = -\frac{(rg')^2 - \sqrt{-4 + (2 + r^2 g'^{\,2})^2}}{2rg'}\,\mathbf{e}_r + \mathbf{e}_\theta. \tag{3.20}$$

Note from (3.14)–(3.17) that q is independent of θ and z. Since $\mathbf{b}_i = \hat{\mathbf{b}}_i$, we can write

$$\hat{\mathbf{B}} = \hat{\lambda}_1^2\,\mathbf{b}_1 \otimes \mathbf{b}_1 + \hat{\lambda}_2^2\,\mathbf{b}_2 \otimes \mathbf{b}_2 + \hat{\lambda}_3^2\,\mathbf{b}_3 \otimes \mathbf{b}_3, \tag{3.21}$$

and conclude that $\hat{\mathbf{B}}$ is independent of θ and z with $\hat{B}_{rz} = 0$ and $\hat{B}_{\theta z} = 0$. Thus $\hat{\mathbf{B}}$ can be written as

$$\hat{\mathbf{B}} = \begin{bmatrix} \hat{B}_{rr} & \hat{B}_{r\theta} & 0 \\ \hat{B}_{r\theta} & \hat{B}_{\theta\theta} & 0 \\ 0 & 0 & \hat{B}_{zz} \end{bmatrix}, \tag{3.22}$$

and by (3.7)

$$\hat{B}_{zz}\left(\hat{B}_{rr}\,\hat{B}_{\theta\theta}-\hat{B}_{r\theta}^2\right)=1. \tag{3.23}$$

Now, using (3.22) in (3.10) the Cauchy stress tensor $\boldsymbol{\sigma}$ can be written as

$$\boldsymbol{\sigma}=\begin{bmatrix} \hat{\alpha}\hat{B}_{rr}-p & \hat{\alpha}\hat{B}_{r\theta} & 0 \\ \hat{\alpha}\hat{B}_{r\theta} & \hat{\alpha}\hat{B}_{\theta\theta}-p & 0 \\ 0 & 0 & \hat{\alpha}\hat{B}_{zz}-p \end{bmatrix}. \tag{3.24}$$

The equilibrium equations (3.9) become

$$\frac{\partial(\hat{\alpha}\hat{B}_{rr}-p)}{\partial r}+\frac{1}{r}\frac{\partial(\hat{\alpha}\hat{B}_{r\theta})}{\partial\theta}+\frac{1}{r}(\hat{\alpha}\hat{B}_{rr}-\hat{\alpha}\hat{B}_{\theta\theta})=0, \tag{3.25}$$

$$\frac{\partial(\hat{\alpha}\hat{B}_{r\theta})}{\partial r}+\frac{1}{r}\frac{\partial(\hat{\alpha}\hat{B}_{\theta\theta}-p)}{\partial\theta}+\frac{1}{r}(2\hat{\alpha}\hat{B}_{r\theta})=0, \tag{3.26}$$

$$\frac{\partial(\hat{\alpha}\hat{B}_{zz}-p)}{\partial z}=0. \tag{3.27}$$

Since $\hat{\mathbf{B}}$ is a function of r only, the equations (3.25)–(3.27) reduce to

$$\hat{\alpha}\frac{\partial\hat{B}_{rr}}{\partial r}-\frac{\partial p}{\partial r}+\frac{\hat{\alpha}}{r}(\hat{B}_{rr}-\hat{B}_{\theta\theta})=0, \tag{3.28}$$

$$\hat{\alpha}\frac{\partial\hat{B}_{r\theta}}{\partial r}-\frac{1}{r}\frac{\partial p}{\partial\theta}+\frac{2\hat{\alpha}}{r}\hat{B}_{r\theta}=0, \tag{3.29}$$

$$\frac{\partial p}{\partial z}=0. \tag{3.30}$$

From (3.30) it follows that p is a function of r and θ, and from (3.29) it follows that $\partial p/\partial\theta$ is a function of r only. Hence p must be linear in θ. By using similar arguments as in the neo-Hookean case (Chapter 2), equations (3.24) and (3.28) lead again to the conclusion that p is a function of r only. Then (3.29) gives

$$\hat{\alpha}\frac{\partial\hat{B}_{r\theta}}{\partial r}+\frac{2\hat{\alpha}}{r}\hat{B}_{r\theta}=0, \tag{3.31}$$

18

and hence

$$\hat{B}_{r\theta} = \frac{d_1}{r^2},$$ (3.32)

where d_1 is an integration constant. Moreover (3.28) can be written as

$$\frac{dp}{dr} = \hat{\alpha}\frac{\partial \hat{B}_{rr}}{\partial r} + \frac{\hat{\alpha}}{r}(\hat{B}_{rr} - \hat{B}_{\theta\theta}).$$ (3.33)

The internal balance equation (3.11) can be written in the following form

$$k\hat{\mathbf{B}}^2 + \rho\,\hat{\mathbf{B}} = \mathbf{B},$$ (3.34)

where we introduce the normalized parameter k and the normalized function $\rho = \rho(r)$ via

$$k = \frac{\hat{\alpha}}{\alpha^*}, \quad \rho(r) = \frac{q(r)}{\alpha^*}.$$ (3.35)

Then the four nontrivial components of (3.34) generate

$$k\,(\hat{B}_{rr}^2 + \hat{B}_{r\theta}^2) + \rho\,\hat{B}_{rr} - 1 = 0,$$ (3.36)

$$k\,(\hat{B}_{rr}\,\hat{B}_{r\theta} + \hat{B}_{r\theta}\,\hat{B}_{\theta\theta}) + \rho\,\hat{B}_{r\theta} - rg' = 0,$$ (3.37)

$$k\,(\hat{B}_{r\theta}^2 + \hat{B}_{\theta\theta}^2) + \rho\,\hat{B}_{\theta\theta} - (1 + (rg')^2) = 0,$$ (3.38)

$$k\,\hat{B}_{zz}^2 + \rho\,\hat{B}_{zz} - 1 = 0.$$ (3.39)

Therefore, in this new framework, the pure azimuthal shear problem reduces to the following.

Find scalar functions $p = p(r)$, $\rho = \rho(r)$, $g = g(r)$, $\hat{B}_{rr} = \hat{B}_{rr}(r)$, $\hat{B}_{\theta\theta} = \hat{B}_{\theta\theta}(r)$, $\hat{B}_{zz} = \hat{B}_{zz}(r)$ such that equations (3.23), (3.33), (3.36), (3.37), (3.38), (3.39) are satisfied. Here $\hat{B}_{r\theta}$ is given by (3.32) in terms of as yet undetermined constant d_1. This constant and any other integration constants will be determined from boundary conditions (2.17) and (2.18).

We conclude this section by showing that this boundary value problem reduces to the pure azimuthal shear problem for the standard neo-Hookean material in the limit $k \to 0$. As k goes to zero it follows from (3.36) that

$$\hat{B}_{rr} = \frac{1}{\rho} + o(1), \tag{3.40}$$

from (3.37) that

$$\hat{B}_{r\theta} = \frac{rg'}{\rho} + o(1), \tag{3.41}$$

from (3.38) that

$$\hat{B}_{\theta\theta} = \frac{1 + r^2 g'^2}{\rho} + o(1), \tag{3.42}$$

and from (3.39) that

$$\hat{B}_{zz} = \frac{1}{\rho} + o(1). \tag{3.43}$$

Substituting from (3.40)–(3.43) into (3.23) and retaining only $O(1)$ terms gives

$$\frac{1}{\rho} \left(\frac{1}{\rho} \frac{1 + r^2 g'^2}{\rho} - \frac{r^2 g'^2}{\rho^2} \right) = 1. \tag{3.44}$$

After simplifying, equation (3.44) reduces to $\rho^3 = 1$ which gives

$$\rho = 1 + o(1) \tag{3.45}$$

independent of r. Therefore in the $k \to 0$ limit it follows to leading order that

$$\hat{B}_{rr} = 1, \quad \hat{B}_{r\theta} = rg', \quad \hat{B}_{\theta\theta} = 1 + r^2 g'^2, \quad \hat{B}_{zz} = 1. \tag{3.46}$$

Using the above results in (3.32) and in (3.33), give respectively to leading order that

$$r^3 g' = d_1, \tag{3.47}$$

and

$$\frac{dp}{dr} = -\hat{\alpha} r (g')^2. \tag{3.48}$$

Observe now that equation (3.47) is equivalent to equation (2.33) from the neo-Hookean case. Similarly equation (3.48) retrieves equation (2.22) from the neo-Hookean case. Hence as $k \to 0$ the results of the neo-Hookean analysis are obtained. For future use we note that (3.45) implies $\rho \to 1$ in this limit, which by virtue of (3.35) gives that $q(r) \to \alpha^*$.

3.2 Solution for Small k $\left(\hat{\alpha} \ll \alpha^* \right)$

At the end of the last section it was shown that the present theory with $k = 0$ reduces to the problem for the neo-Hookean type material of standard nonlinear finite elasticity. In this section we will study the pure azimuthal shear problem for small k by a perturbation expansion about the base neo-Hookean solution.

If $k = 0$, then the neo-Hookean solution applies. From equations (2.34) and (2.35) this solution is given by

$$g_0(R) = \frac{c_{10}}{R^2} + c_{20},$$ (3.49)

and

$$p_0(R) = \frac{\hat{\alpha} c_{10}^2}{R^4} + c_{30},$$ (3.50)

where c_{10}, c_{20}, c_{30} are the constants computed from boundary conditions (2.17), (2.18) and given by (2.36), (2.37), (2.39) respectively. Note that instead of c_1, c_2, c_3, the constants c_{10}, c_{20}, c_{30} are used respectively to emphasize that these are the constants corresponding to zeroth order solution. The subscript $_0$ is used to denote the zeroth order approximations for the unknown functions and tensor quantities. Moreover from (3.46) the base neo-Hookean value of $\hat{\mathbf{B}}$ is

$$\hat{\mathbf{B}}_0 = \begin{bmatrix} 1 & rg_0{}' & 0 \\ rg_0{}' & 1 + (rg_0{}')^2 & 0 \\ 0 & 0 & 1 \end{bmatrix},$$ (3.51)

21

and from the remark after (3.48)

$$q_0 = \alpha^*. \qquad (3.52)$$

Assume that there is a small k solution in the form of following expansions for $g(R)$, $p(R)$, $q(R)$, $\hat{\mathbf{B}}(R)$ for the given problem:

$$g(R) = g_0(R) + \Sigma_{n=1}^{\infty} k^n \, g_n(R), \qquad (3.53)$$

$$p(R) = p_0(R) + \Sigma_{n=1}^{\infty} k^n \, p_n(R), \qquad (3.54)$$

$$q(R) = q_0 + \Sigma_{n=1}^{\infty} k^n \, q_n(R), \qquad (3.55)$$

$$\hat{\mathbf{B}}(R) = \hat{\mathbf{B}}_0(R) + \Sigma_{n=1}^{\infty} k^n \, \hat{\mathbf{B}}_n(R), \qquad (3.56)$$

where $g_0(R)$, $p_0(R)$, q_0 and $\hat{\mathbf{B}}_0(R)$ are as given above. Note that by using the expansion (3.53) the *left cauchy-green tensor*, $\mathbf{B}$, given by (2.12), can be written as:

$$\mathbf{B} = \begin{bmatrix} 1 & r(g_0' + kg_1' + \ldots) & 0 \\ r(g_0' + kg_1' + \ldots) & 1 + r^2(g_0' + kg_1' + \ldots)^2 & 0 \\ 0 & 0 & 1 \end{bmatrix}, \qquad (3.57)$$

or equivalently,

$$\mathbf{B} = \begin{bmatrix} 1 & rg_0' & 0 \\ rg_0' & 1 + r^2(g_0')^2 & 0 \\ 0 & 0 & 1 \end{bmatrix} + k \begin{bmatrix} 0 & rg_1' & 0 \\ rg_1' & 2r^2g_0'g_1' & 0 \\ 0 & 0 & 0 \end{bmatrix} + \ldots \qquad (3.58)$$

giving that

$$\mathbf{B}_0 = \begin{bmatrix} 1 & rg_0' & 0 \\ rg_0' & 1 + r^2(g_0')^2 & 0 \\ 0 & 0 & 1 \end{bmatrix}, \qquad (3.59)$$

and

$$\mathbf{B}_1 = \begin{bmatrix} 0 & rg_1{}' & 0 \\ rg_1{}' & 2r^2 g_0{}' g_1{}' & 0 \\ 0 & 0 & 0 \end{bmatrix}. \tag{3.60}$$

Substituting from expansions (3.53)–(3.56) into the internal balance (3.34) gives

$$k(\hat{\mathbf{B}}_0 + k\hat{\mathbf{B}}_1 + \dots)^2 + \frac{(\alpha^* + kq_1 + \dots)}{\alpha^*}(\hat{\mathbf{B}}_0 + k\hat{\mathbf{B}}_1 + \dots)$$

$$-(\mathbf{B}_0 + k\mathbf{B}_1 + \dots) = 0, \tag{3.61}$$

or equivalently,

$$(\hat{\mathbf{B}}_0 - \mathbf{B}_0) + k\left(\hat{\mathbf{B}}_0^2 - \mathbf{B}_1 + \hat{\mathbf{B}}_1 + \frac{q_1}{\alpha^*}\hat{\mathbf{B}}_0\right) + O(k^2) = 0. \tag{3.62}$$

The $O(1)$ terms of (3.62) give

$$\hat{\mathbf{B}}_0 = \mathbf{B}_0, \tag{3.63}$$

which was already evident from (3.51) and (3.59), while the $O(k)$ terms give

$$\hat{\mathbf{B}}_0^2 + \frac{q_1}{\alpha^*}\hat{\mathbf{B}}_0 + \hat{\mathbf{B}}_1 - \mathbf{B}_1 = 0. \tag{3.64}$$

Therefore

$$\hat{\mathbf{B}}_1 = \mathbf{B}_1 - \hat{\mathbf{B}}_0^2 - \frac{q_1}{\alpha^*}\hat{\mathbf{B}}_0. \tag{3.65}$$

By using (3.59), (3.60) and (3.63)

$$\hat{\mathbf{B}}_1 = \begin{bmatrix} -1 - (q_1/\alpha^*) - r^2(g_0{}')^2 & (\hat{B}_1)_{r\theta} & 0 \\ \dots & (\hat{B}_1)_{\theta\theta} & 0 \\ \dots & \dots & -1 - (q_1/\alpha^*) \end{bmatrix}, \tag{3.66}$$

where

$$(\hat{B}_1)_{r\theta} = rg_1{}' - 2rg_0{}' - r^3(g_0{}')^3 - \frac{q_1}{\alpha^*}rg_0{}', \tag{3.67}$$

23

$$(\hat{B}_1)_{\theta\theta} = 2r^2 g_0'g_1' - 1 - 3r^2(g_0')^2 - r^4(g_0')^4 - \frac{q_1}{\alpha^*} - \frac{q_1}{\alpha^*}r^2(g_0')^2, \quad (3.68)$$

and the other components of $\hat{B}_1$ follow from the symmetry of $\hat{B}_1$. To find the complete solution up to the order k, it is necessary to find q_1, g_1 and p_1. If the components of $\hat{B}_0$ and $\hat{B}_1$, given by (3.59) and (3.66)–(3.68) respectively, are substituted into (3.23), then it follows that

$$1 + k\left(-3 - \frac{3\,q_1}{\alpha^*} - r^2(g_0')^2\right) + O(k^2) = 1, \quad (3.69)$$

from which it is immediate that

$$q_1 = \frac{-\alpha^*}{3}\,(3 + r^2(g_0')^2). \quad (3.70)$$

If $g_0'(r)$ is computed from (3.49) and used in (3.70), then q_1 is found as

$$q_1 = -\alpha^*\left(1 + \frac{4c_{10}^2}{3r^4}\right), \quad (3.71)$$

where c_{10} is the constant given by (2.36). By using the reduced equilibrium equations (3.32) and (3.33) it follows that g_1 and p_1 are given by

$$g_1 = \frac{8\,c_{10}^3}{9\,r^6} + \frac{2\,c_{10} - c_{11}}{2\,r^2} + c_{21}, \quad (3.72)$$

and

$$p_1 = \frac{(11\,c_{10}^2 - 3\,c_{10}\,c_{11})\,\hat{\alpha}}{3r^4} + \frac{4\,c_{10}^4\,\hat{\alpha}}{r^8} + c_{31}. \quad (3.73)$$

The constants c_{11}, c_{21}, c_{31} are determined by requiring $g_1(R_i) = g_1(R_o) = 0$ and $\sigma_{rr}(R_o) = \sigma_{rr}^0$. Hence

$$c_{11} = 2\,c_{10} + \frac{16\,(R_i^4 + R_i^2\,R_o^2 + R_o^4)\,c_{10}^3}{9\,R_i^4\,R_o^4}, \quad (3.74)$$

$$c_{21} = \frac{8\,(R_i^2 + R_o^2)\,c_{10}^3}{9\,R_i^4\,R_o^4}, \quad (3.75)$$

$$c_{31} = \frac{c_{10}\,[-4\,c_{10}^3 + R_o^4(3\,c_{11} - 19\,c_{10})]\,\hat{\alpha}}{3\,R_o^8}. \quad (3.76)$$

The *azimuthal component of the traction* on the inner and outer surfaces are respectively given by

$$\sigma_{\theta r}(R_i) = 2\,c_{10}\frac{\hat{\alpha}}{R_i^2} - k\,c_{11}\frac{\hat{\alpha}}{R_i^2} + O(k^2), \tag{3.77}$$

$$\sigma_{\theta r}(R_o) = -2\,c_{10}\frac{\hat{\alpha}}{R_o^2} + k\,c_{11}\frac{\hat{\alpha}}{R_o^2} + O(k^2). \tag{3.78}$$

By using (3.78) the *Torque* can be computed from

$$M = h \int_0^{2\pi} R_o^2\,\sigma_{\theta r}(R_o)\,d\theta. \tag{3.79}$$

Then *Torque-Twist* relation is given by

$$M = \frac{4\,\pi\,h\,\hat{\alpha}\,R_i^2\,R_o^2}{R_o^2 - R_i^2}\,\Psi -$$

$$k\,\frac{4\,\pi\,h\,\hat{\alpha}\,R_i^2\,R_o^2}{R_o^2 - R_i^2}\,\frac{[9(R_i^2 - R_o^2)^2 + 8(R_i^4 + R_i^2\,R_o^2 + R_o^4)\,\Psi^2]}{9\,(R_i^2 - R_o^2)^2}\,\Psi + O(k^2). \tag{3.80}$$

Note from equation (3.80) that $M(-\Psi) = -M(\Psi)$ by the terms thus far computed.

The torque can be normalized by dividing $4\,\pi\,h\,\hat{\alpha}\,R_i^2\,R_o^2$. The normalized Torque-Twist relation up to $O(k)$ as given by (3.80) is displayed in Figure 3.1. Here $R_i = 1$, $R_o = 4$ and the solid line shows the neo-Hookean case $k = 0$. The dashed line shows the case $k = 0.02$. Figure 3.1 shows that increasing $k = \hat{\alpha}/\alpha^*$ results in a relative softening.

Perhaps the most interesting aspect of (3.80) is that, to within the terms thus far computed, M is not an increasing function of Ψ when $k > 0$ for all Ψ.

By using (3.80) it is immediate that

$$\frac{dM}{d\Psi} = \frac{4\,\pi\,h\,\hat{\alpha}\,R_i^2\,R_o^2\,(k-1)}{(R_i^2 - R_o^2)} \tag{3.81}$$

$$+\frac{32\,\pi\,h\,\hat{\alpha}\,R_i^2\,R_o^2\,(R_i^4 + R_i^2 R_o^2 + R_o^4)\,k\,\Psi^2}{3(R_i^2 - R_o^2)^3} + o(k^2).$$
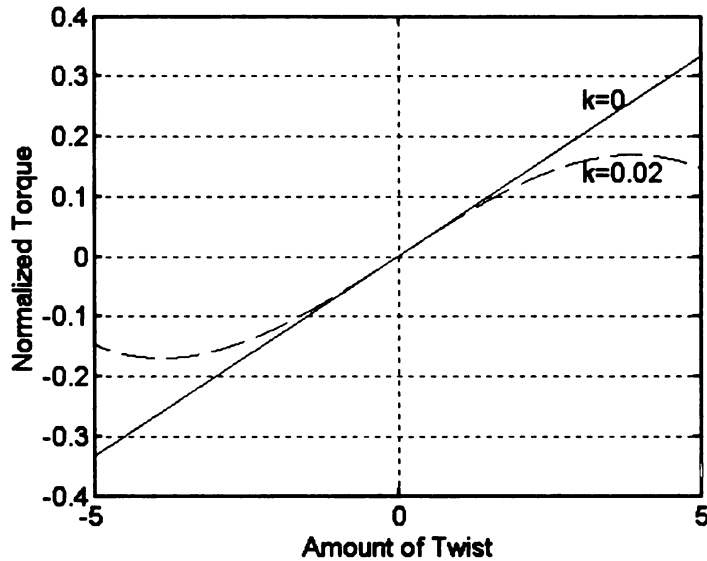
Figure 3.1: Comparison of normalized torque-twist relation when $k = 0$ and $k = 0.02$ for $R_i = 1$ and $R_o = 4$. The dashed line shows the case $k = 0.02$. The normalized torque is $M/(4\pi h \hat{\alpha} R_i^2 R_o^2)$

On the basis of the terms thus far computed one can solve $dM/d\Psi = 0$ for Ψ and hence M takes its extremum values at

$$\Psi = \pm\Psi_{\text{ext}}(k), \quad \Psi_{\text{ext}}(k) := \frac{\sqrt{3}(R_o^2 - R_i^2)\sqrt{1-k}}{\sqrt{8}\sqrt{k(R_i^4 + R_i^2 R_o^2 + R_o^4)}}. \tag{3.82}$$

Also note from (3.82) that

$$\lim_{k \to 0} \Psi_{\text{ext}}(k) = \infty, \tag{3.83}$$

and that

$$\frac{d\Psi_{\text{ext}}}{dk} = -\frac{\sqrt{3}\,(R_o^2 - R_i^2)}{\sqrt{32}\,\sqrt{1-k}\,k\,\sqrt{k(R_i^4 + R_i^2 R_o^2 + R_o^4)}}. \tag{3.84}$$

Restricting attention to small k, and in particular taking $0 < k < 1$ it follows that $d\Psi_{\text{ext}}/dk < 0$. It will indeed be shown analytically in Section 3.4 that loss of resistance occurs for $k = 1$ at sufficiently large Ψ. On the other hand, this thesis

26

will show that the subsequent decrease in M with Ψ for $\Psi > \Psi_{\text{ext}}$ is not found analytically. Presumably this decrease is an artifact of the expansion procedure that would be corrected by invoking a Ψ dependent criterion for determination of the number of terms necessary for a uniformly valid approximation. These issues will be clarified in the following development.

3.3 Numerical Solution

In this section we present a numerical solution procedure for the pure azimuthal shear problem which does not require an assumption of small k. The solution reveals evidence of a threshold value for Ψ at which smooth solutions no longer are available.

We begin with some additional reduction of the governing equations. Post-multiplying (3.34) with $\hat{\mathbf{B}}^{-1}$ gives

$$k\hat{\mathbf{B}} + \rho\,\mathbf{I} = \mathbf{B}\,\hat{\mathbf{B}}^{-1}. \tag{3.85}$$

Since the product of two symmetric matrices need not be symmetric, there are five nontrivial components of (3.85) as follows

$$k\,\hat{B}_{rr} + \rho = \hat{B}_{zz}[\hat{B}_{\theta\theta} - rg'\hat{B}_{r\theta}], \tag{3.86}$$

$$k\,\hat{B}_{r\theta} = \hat{B}_{zz}[rg'\hat{B}_{rr} - \hat{B}_{r\theta}], \tag{3.87}$$

$$k\,\hat{B}_{r\theta} = \hat{B}_{zz}[rg'\hat{B}_{\theta\theta} - (1 + (rg')^2)\hat{B}_{r\theta}], \tag{3.88}$$

$$k\,\hat{B}_{\theta\theta} + \rho = \hat{B}_{zz}[(1 + (rg')^2)\hat{B}_{rr} - rg'\hat{B}_{r\theta}], \tag{3.89}$$

$$k\,\hat{B}_{zz} + \rho = \frac{1}{\hat{B}_{zz}}. \tag{3.90}$$

The values $\hat{B}_{rr}$ and $\hat{B}_{\theta\theta}$ can now be obtained from (3.87) and (3.88) respectively in terms of $\hat{B}_{r\theta}$ and $\hat{B}_{zz}$, providing

$$\hat{B}_{rr} = \left[\frac{k}{\hat{B}_{zz}} + 1\right]\frac{\hat{B}_{r\theta}}{rg'}, \tag{3.91}$$

$$\hat{B}_{\theta\theta} = \left[\frac{k}{\hat{B}_{zz}} + 1 + (rg')^2\right]\frac{\hat{B}_{r\theta}}{rg'}. \tag{3.92}$$

Note, if $\hat{B}_{rr}$ as determined from (3.91) and $\hat{B}_{\theta\theta}$ as determined from (3.92) are both substituted into (3.86) and (3.89) respectively, then the resulting equations are equivalent. Therefore only four of the five equations in (3.86)–(3.90) are independent. In addition $\hat{B}_{zz}$ can be obtained uniquely from (3.90) in terms of ρ by using the positive-definiteness of $\hat{\mathbf{B}}$;

$$\hat{B}_{zz} = \frac{-\rho + \sqrt{\rho^2 + 4k}}{2k}. \tag{3.93}$$

The constraint (3.23) yields

$$\hat{B}_{r\theta}^2 = \hat{B}_{rr}\,\hat{B}_{\theta\theta} - \frac{1}{\hat{B}_{zz}}. \tag{3.94}$$

Taken together (3.91)–(3.94) indicates that $\hat{B}_{r\theta}$ can be found as a function of g' and ρ. Indeed it is given by

$$\hat{B}_{r\theta} = \frac{\sqrt{2k}\,r\,g'}{\sqrt{2k^2(r^2g'^2 + 2) + (k^3 - 1)\rho + \sqrt{4k + \rho^2}(1 + k^3)}}. \tag{3.95}$$

By using (3.93), (3.95) in (3.91), (3.92) the nontrivial components of $\hat{\mathbf{B}}$ can be found in terms of g' and ρ. In principal (3.86), or equivalently (3.89), now supply an equation relating ρ and g'.

To get a numerical solution observe first from (3.32) and (3.95) that

$$\frac{2kr^2g'^2}{2k^2(r^2g'^2 + 2) + (k^3 - 1)\rho + \sqrt{4k + \rho^2}(1 + k^3)} - \frac{d_1^2}{r^4} = 0. \tag{3.96}$$

Secondly upon substituting from (3.91), (3.92), (3.93), (3.95) into (3.86) and manipulating the resulting equation it is found that

$$k^3\rho^6 - (k^3 - 1)k^2(r^2g'^2 + 3)\rho^5 + [1 - (r^2g'^2 + 1)k^3 + k^6](r^2g'^2 + 3)k\,\rho^4 +$$

28

$$(1 + 5k^3 - 5k^6 - k^9)\rho^3 + 2(k^3 - 1)^2 k^2 (r^2 g'^2 + 3)\rho^2 + (k^3 - 1)^4 = 0. \quad (3.97)$$

Let k be fixed and choose a trial value for d_1. Then at a given radial location $r = r_j$ the equations (3.96) and (3.97) can be solved simultaneously for $\rho_j \equiv \rho(r_j)$ and $g'_j \equiv g'(r_j)$. Once g'_j is known the *tangent line approximation* can be used to estimate $g(r)$ at a nearby point r provided that $g(r_j)$ is also known. This is the strategy we will follow. At issue is the proper value of d_1. Divide the interval $[R_i, R_o]$ into N equal subintervals and label the end points as $R_i = r_0, r_1, \ldots, r_N = R_o$. One of the boundary conditions in (2.17) can be used as starting point, say $g(r_0) = \psi_i$. Then by the tangent line approximation

$$g(r_1) \approx g(r_0) + (g'(r_0)\,\Delta r), \quad (3.98)$$

where $\Delta r = (R_o - R_i)/N$. In general

$$g_j = g(r_j) \approx g(r_0) + \sum_{l=0}^{j-1}(g'(r_l)\,\Delta r), \quad (3.99)$$

for $j = 1, 2, \ldots, N$. Since $g(R_0) = \psi_o$, it is therefore necessary to choose d_1 so that

$$\psi_o - \psi_i = \sum_{l=0}^{j-1}(g'(r_l)\,\Delta r). \quad (3.100)$$

That is, d_1 can be used as a shooting parameter. Using this numerical scheme it is found that d_1 and the overall solution curves are robust with respect to finer and finer discretization (increase in N).

However it is found that the $R = R_i$ end point value of g'; that is, $g'(R_i)$, is very sensitive to change in N when ψ_o is sufficiently large. For example take $k = 0.1$, $R_i = 1$, $R_o = 4$, and $\psi_i = 0$. Then for $\psi_o = 2$ it is found that $d_1 = 2.84365$ for $N = 300$ and that $d_1 = 2.86951$ for $N = 3000$. The associated numerical values of $g'(R)$ at $R_i = 1$ are found to be $g'(1) = 8.54856$ and $g'(1) = 9.05256$ respectively. On the other hand for $\psi_o = 10$ it is found that $d_1 = 3.1621814432$ for $N = 300$ and that $d_1 = 3.162276607355$ for $N = 3000$. The associated numerical value of $g'(R)$

at $R_i = 1$ are found to be $g'(1) = 736.36329$ and $g'(1) = 7101.95319$ respectively. We also find for $\psi_o = 2$ that the numerical value of the derivatives at $R = 1.01$ are given by $g'(1.01) = 7.56906$ and $g'(1.01) = 7.94672$ respectively for $N = 300$ and $N = 3000$. For $\psi_o = 10$ it is found that $g'(1.01) = 23.48574$ and $g'(1.01) = 23.50641$ respectively for $N = 300$ and $N = 3000$. Therefore only $g'(R_i)$ is very sensitive to change in N when ψ_o is sufficiently large. In general, if $j \neq 0$, then g'_j values are quite stable to increase in N even for large ψ_o values. In particular for sufficiently large ψ_o, the numerically computed value of $g'(R_i)$ increases without apparent bound as N gets larger. We speculate that this is numerical evidence for a lack of smooth solutions at $R = R_i$ when ψ_o is sufficiently large.

For $k = 0.1$ Figure 3.2 shows the graph of $g(R)$ for five values of ψ_o: $\psi_o = 1$, $\psi_o = 2$, $\psi_o = 3$, $\psi_o = 5$ and $\psi_o = 10$ when $R_i = 1$, $R_o = 4$, $\psi_i = 0$ from the numerical procedure outlined above. For $\psi_o = 5$ and $\psi_o = 10$ the numerical procedure does not converge to a finite value for $g'(R_i)$ and the associated graphs for $g(R)$ show an apparent discontinuity at $R = R_i$. Figure 3.3 shows the corresponding $\rho(R)$ for the same parameter values. The graphs of $\rho(R)$ are ordered from top to bottom for $\psi_o = 1$, $\psi_o = 2$ and $\psi_o = 3$ and they are almost identical for $\psi_o = 3$, $\psi_o = 5$ and $\psi_o = 10$. For $\psi_o = 1$ and $\psi_o = 2$ we find that $\rho(R_o) = 0.89962$ and $\rho(R_o) = 0.89903$ respectively. For $\psi_o = 3, 5, 10$ we find that $\rho(R_o) = 0.89883$. However $\rho(R_i) = 0.790, 0.490, 0.064, 0.005, 0.001$ for $\psi_o = 1, 2, 3, 5, 10$ respectively.

For $k = 0.5$ Figure 3.4 shows the graph of $g(R)$ for five values of ψ_o: $\psi_o = 1$, $\psi_o = 2$, $\psi_o = 3$, $\psi_o = 5$ and $\psi_o = 10$ when $R_i = 1$, $R_o = 4$, $\psi_i = 0$. For $\psi_o = 2$, $\psi_o = 3$, $\psi_o = 5$ and $\psi_o = 10$ the numerical procedure does not converge to a finite value for $g'(R_i)$ and the associated graphs for $g(R)$ show an apparent discontinuity at $R = R_i$. Figure 3.5 shows the corresponding $\rho(R)$ for the same parameter values. The top curve corresponds to $\psi_o = 1$. The graphs of $\rho(R)$ are almost identical for

Figure 3.2: Graphs of $g(R)$ for five values of ψ_o: $\psi_o = 1$, $\psi_o = 2$, $\psi_o = 3$, $\psi_o = 5$ and $\psi_o = 10$ when $R_i = 1$, $R_o = 4$, $\psi_i = 0$ and $k = 0.1$. For $\psi_o = 5$ and $\psi_o = 10$ there is an apparent discontinuity at $R_i = 1$

Figure 3.3: Graphs of $\rho(R)$ for five values of ψ_o: $\psi_o = 1$, $\psi_o = 2$, $\psi_o = 3$, $\psi_o = 5$ and $\psi_o = 10$ when $R_i = 1$, $R_o = 4$, $\psi_i = 0$ and $k = 0.1$. The top curve corresponds to $\psi_o = 1$ and the middle one corresponds to $\psi_o = 2$. The graphs of $\rho(R)$ are almost identical for $\psi_o = 3$, $\psi_o = 5$ and $\psi_o = 10$ and so generates an essentially common lower curve

31
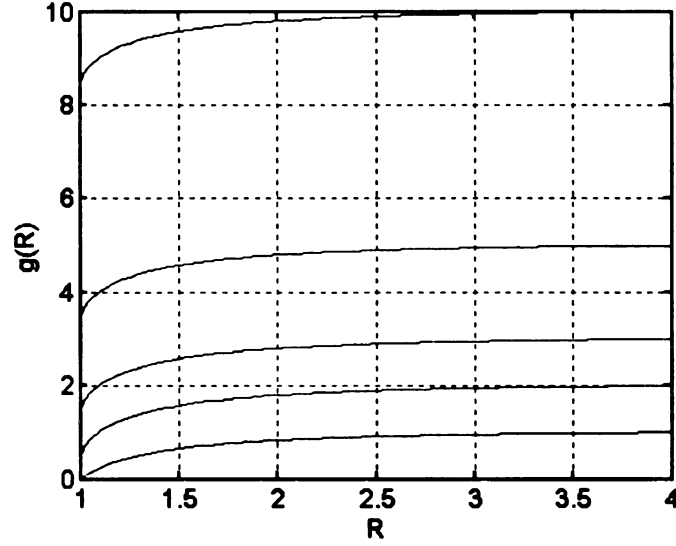
Figure 3.4: Graphs of $g(R)$ for five values of ψ_o: $\psi_o = 1$, $\psi_o = 2$, $\psi_o = 3$, $\psi_o = 5$ and $\psi_o = 10$ when $R_i = 1$, $R_o = 4$, $\psi_i = 0$ and $k = 0.5$. For $\psi_o = 2$, $\psi_o = 3$, $\psi_o = 5$ and $\psi_o = 10$ there is an apparent discontinuity at $R_i = 1$

$\psi_o = 2$, $\psi_o = 3$, $\psi_o = 5$ and $\psi_o = 10$ and so generates an essentially common lower curve. For $\psi_o = 2, 3, 5, 10$ we find that $\rho(R_o) = 0.49934$ and for $\psi_o = 1$ we find that $\rho(R_o) = 0.49955$. However $\rho(R_i) = 0.3252, 0.0042, 0.0012, 0.0005, 0.0002$ for $\psi_o = 1, 2, 3, 5, 10$ respectively.

For $k = 1$ Figure 3.6 shows the graph of $g(R)$ for five values of ψ_o: $\psi_o = 1$, $\psi_o = 2$, $\psi_o = 3$, $\psi_o = 5$ and $\psi_o = 10$ when $R_i = 1$, $R_o = 4$, $\psi_i = 0$. The associated graphs for $g(R)$ again show an apparent discontinuity at $R = R_i$ when $\psi_o = 2$, $\psi_o = 3$, $\psi_o = 5$ and $\psi_o = 10$. Figure 3.7 shows the corresponding $\rho(R)$ for the same parameter values. Note from the scale that this numerical solution gives $0 < \rho(R) \ll 1$ for $R > R_i = 1$. The top curve corresponds to $\psi_o = 1$. The graphs of $\rho(R)$ are almost identical for $\psi_o = 2$, $\psi_o = 3$, $\psi_o = 5$ and $\psi_o = 10$ and so generates an essentially common lower curve. For each ψ_o we find that $\rho(R_o) = 0.000422356$. However $\rho(R_i) = 0.0001$, $0.000001, 0.0000003, 0.0000001, 0.000000056$ for $\psi_o = 1, 2, 3, 5, 10$ respectively.
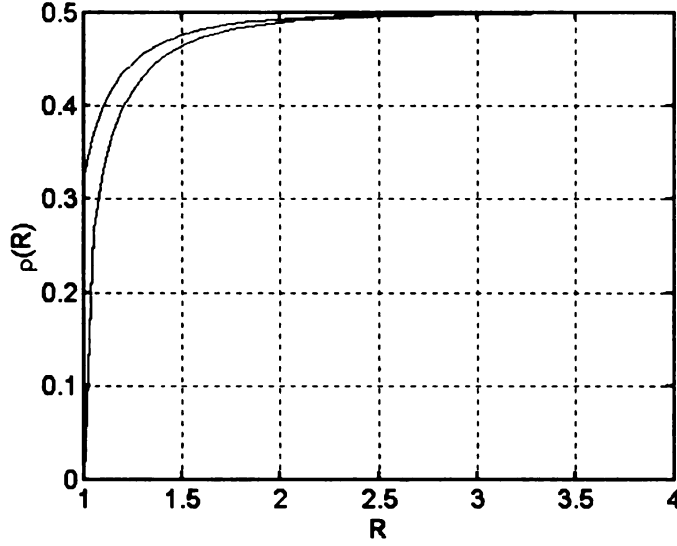
Figure 3.5: Graphs of $\rho(R)$ for five values of ψ_o: $\psi_o = 1$, $\psi_o = 2$, $\psi_o = 3$, $\psi_o = 5$ and $\psi_o = 10$ when $R_i = 1$, $R_o = 4$, $\psi_i = 0$ and $k = 0.5$. The top curve corresponds to $\psi_o = 1$. The graphs of $\rho(R)$ are almost identical for $\psi_o = 2$, $\psi_o = 3$, $\psi_o = 5$ and $\psi_o = 10$ and so generates an essentially common lower curve
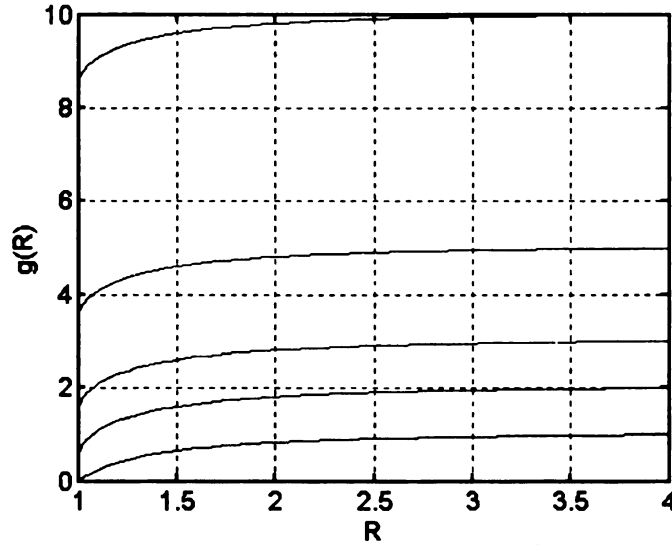
Figure 3.6: Graphs of $g(R)$ for five values of ψ_o: $\psi_o = 1$, $\psi_o = 2$, $\psi_o = 3$, $\psi_o = 5$ and $\psi_o = 10$ when $R_i = 1$, $R_o = 4$, $\psi_i = 0$ and $k = 1$. For $\psi_o = 2$, $\psi_o = 3$, $\psi_o = 5$ and $\psi_o = 10$ there is an apparent discontinuity at $R_i = 1$
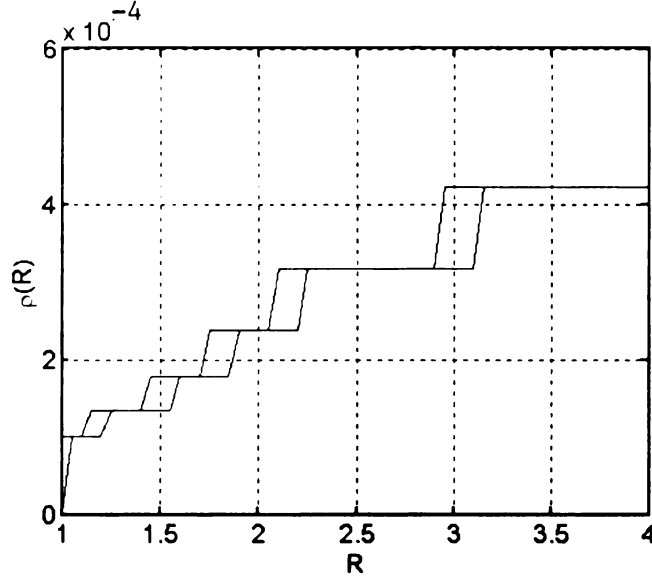
Figure 3.7: Graphs of $\rho(R)$ for five values of ψ_o: $\psi_o = 1$, $\psi_o = 2$, $\psi_o = 3$, $\psi_o = 5$ and $\psi_o = 10$ when $R_i = 1$, $R_o = 4$, $\psi_i = 0$ and $k = 1$. The top curve corresponds to $\psi_o = 1$. The graphs of $\rho(R)$ are almost identical for $\psi_o = 2$, $\psi_o = 3$, $\psi_o = 5$ and $\psi_o = 10$ and so generates an essentially common lower curve

For $k = 2$ Figure 3.8 shows the graph of $g(R)$ for five values of ψ_o: $\psi_o = 1$, $\psi_o = 2$, $\psi_o = 3$, $\psi_o = 5$ and $\psi_o = 10$ when $R_i = 1$, $R_o = 4$, $\psi_i = 0$. The associated graphs for $g(R)$ again show an apparent discontinuity at $R = R_i$ when $\psi_o = 2$, $\psi_o = 3$, $\psi_o = 5$ and $\psi_o = 10$. Figure 3.9 shows the corresponding $\rho(R)$ for the same parameter values. The lower curve corresponds to $\psi_o = 1$ and graphs of $\rho(R)$ are almost identical for $\psi_o = 2$, $\psi_o = 3$, $\psi_o = 5$ and $\psi_o = 10$ and so generates an essentially common top curve. For $\psi_o = 2, 3, 5, 10$ we find that $\rho(R_o) \approx -0.9987$ and $\rho(R_o) = -0.9991$ when $\psi_o = 1$. However $\rho(R_i) = -0.6505, -0.0080, -0.0025, -0.0011, -0.0010$ for $\psi_o = 1, 2, 3, 5, 10$ respectively.

It is tempting to seek a correlation between the issue of an apparent discontinuity at $R = R_i$ for sufficiently large ψ_o and the previously obtained $\Psi_{ext}(k)$ in Section 3.2. This gives rise to the notion of a smooth solution region in (ψ_o, k)-space for
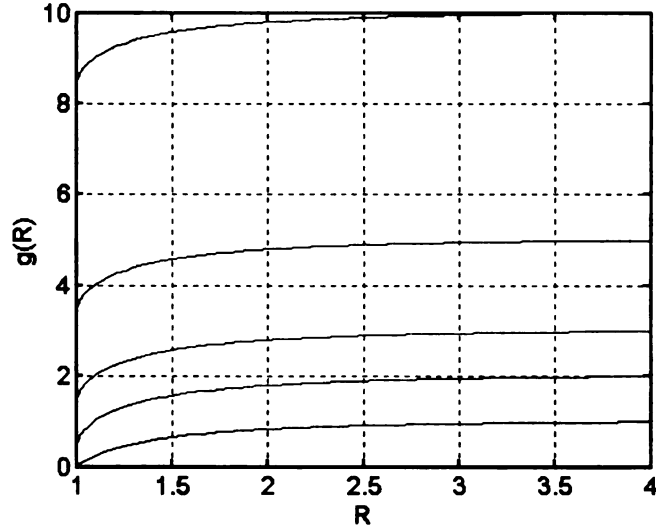
Figure 3.8: Graphs of $g(R)$ for five values of ψ_o: $\psi_o = 1$, $\psi_o = 2$, $\psi_o = 3$, $\psi_o = 5$ and $\psi_o = 10$ when $R_i = 1$, $R_o = 4$, $\psi_i = 0$ and $k = 2$. For $\psi_o = 2$, $\psi_o = 3$, $\psi_o = 5$ and $\psi_o = 10$ there is an apparent discontinuity at $R_i = 1$
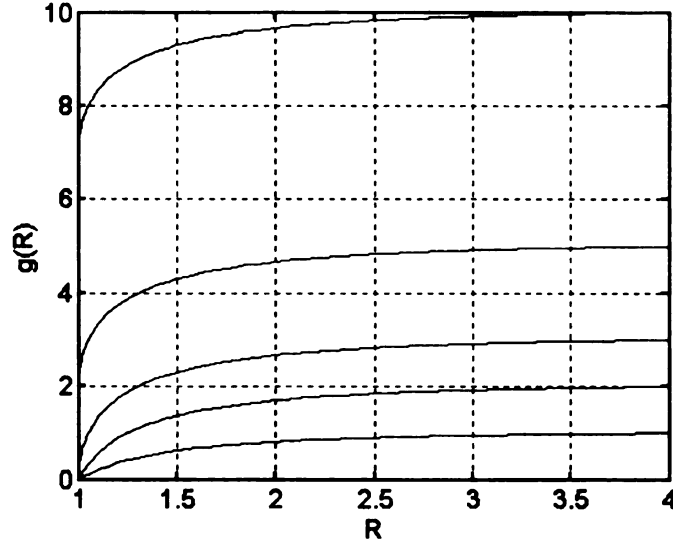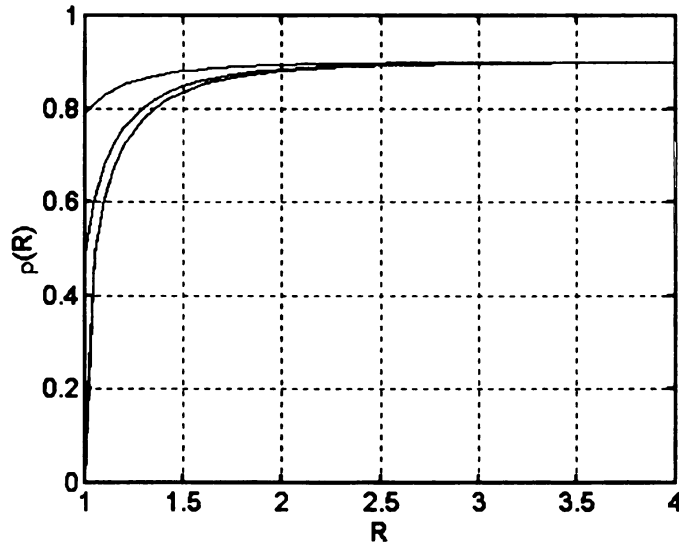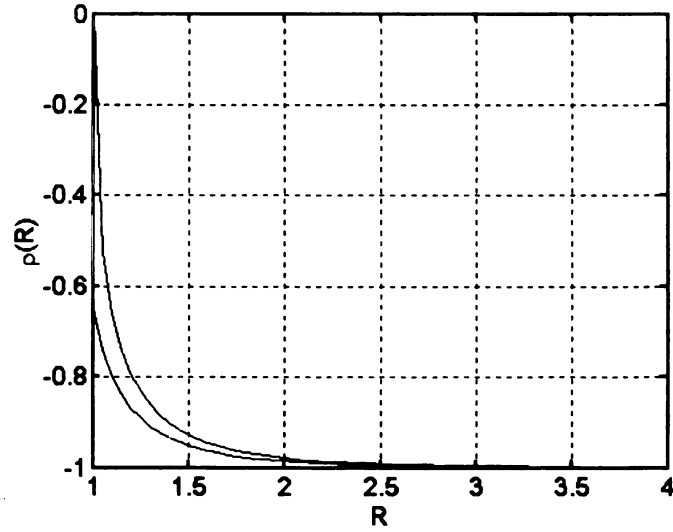

Figure 3.9: Graphs of $\rho(R)$ for five values of ψ_o: $\psi_o = 1$, $\psi_o = 2$, $\psi_o = 3$, $\psi_o = 5$ and $\psi_o = 10$ when $R_i = 1$, $R_o = 4$, $\psi_i = 0$ and $k = 2$. The top curve corresponds to $\psi_o = 1$. The graphs of $\rho(R)$ are almost identical for $\psi_o = 2$, $\psi_o = 3$, $\psi_o = 5$ and $\psi_o = 10$ and so generates an essentially common lower curve

35

fixed R_i, R_o, ψ_i. Using $R_i = 1$ and $R_o = 4$ in (3.82) gives

$$\Psi_{\text{ext}}(k) := \frac{15\sqrt{3}\sqrt{1-k}}{\sqrt{8}\sqrt{273\,k}}.$$ (3.101)

Let $\psi_i = 0$. Then the curve (3.101) can be used to estimate the boundary for the proposed smooth solution region in (ψ_o, k)-space. On the basis of following the argument it is found that smooth solution region is in fact somewhat larger than that predicted by (3.101). Based on the numerical solutions presented above it can be assumed for a given k that there is an $\Psi_{\text{crit}}(k)$ for which $g'(R_i) \to \infty$. Equivalently there is a critical value of shooting parameter d_1, say $d_{\text{crit}}(k)$, for which $g'(R_i) \to \infty$. Indeed it can be seen from (3.96) that

$$d_{\text{crit}}(k) = \frac{R_i^2}{\sqrt{k}}.$$ (3.102)

Then for a given R_o and N equation (3.96) with $d_1 = d_{\text{crit}}$ in conjunction with and (3.97) can be solved simultaneously for $\rho_j \equiv \rho(r_j)$ and $g'_j \equiv g'(r_j)$ as before. In principle $\Psi_{\text{crit}}(k)$ can now be approximated by (3.100). However the sensitivity of $g'(R_i)$ to N gives difficulty. Since ρ_j $(j = 0, \ldots, N)$ has no such sensitivity, an alternative is to find a good fitting polynomial for $\rho(r)$. Once a closed form approximating function for $\rho(r)$ is available, equation (3.96) can be solved for $g'(r)$ giving

$$g'(r) = \pm \frac{\sqrt{4\,k^2\,d_1^2 + (k^3 - 1)\,d_1^2\,\rho(r) + (1 + k^3)\,d_1^2\,\sqrt{4\,k + \rho(r)^2}}}{\sqrt{2\,k\,r^6 - 2\,k^2\,d_1^2\,r^2}}.$$ (3.103)

Note that since $\psi_o > \psi_i$ it is the positive root of (3.103) that is of interest. If the positive root of (3.103) is integrated numerically from R_i to R_o with $d_1 = d_{\text{crit}}$, one then obtains an estimate for $\Psi_{\text{crit}}(k)$.

By using the outlined method, the maximum amount of twist versus k is depicted in Figure 3.10. Note that $\Psi_{\text{crit}}(k)$ apparently takes its minimum when $k = 1$. The graph of $\Psi_{\text{ext}}(k)$ is also depicted in the same figure. Note that $\Psi_{\text{ext}}(k)$ is defined if

36
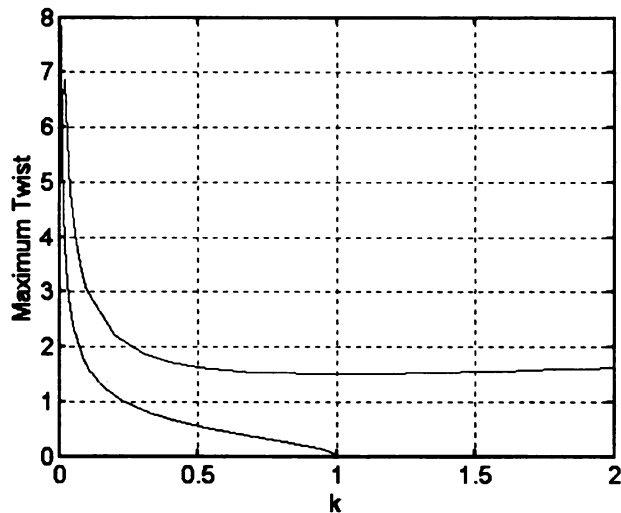
Figure 3.10: The lower curve is the graph of $\Psi_{\mathrm{ext}}(k)$ and the upper curve is the numerically estimated $\Psi_{\mathrm{crit}}(k)$ when $R_i = 1$, $R_o = 4$. Note that $\Psi_{\mathrm{crit}}(k)$ appears to take its minimum when $k = 1$

$k \in (0, 1]$ and that it gives a reasonable estimate for the critical amount of twist only if k is sufficiently small.

For $k = 0.1$, $R_i = 1$, $R_o = 4$, $\psi_i = 0$, we find that $\Psi_{\mathrm{crit}}(0.1) = 3.030996$. Note in comparison that $\Psi_{\mathrm{ext}}(0.1) = 1.667811 < \Psi_{\mathrm{crit}}(0.1)$. While (3.101) could likely be improved by computing more terms in the perturbation expansion, the central issue of an apparent threshold angle ψ_o remains. Namely, both the perturbation expansion and the numerical solution procedure give evidence that there is a maximum amount of twist above which there is no smooth solution for the pure azimuthal shear problem under consideration.

With respect to the later development of Section 6, it is useful to remark that the numerical estimate for $\Psi_{\mathrm{crit}}(1)$ is 1.50826 when $R_i = 1$, $R_o = 4$.

Note that the energy density (3.6) is separable in $\hat{I}_1$ and I_1^*. Hence the potential
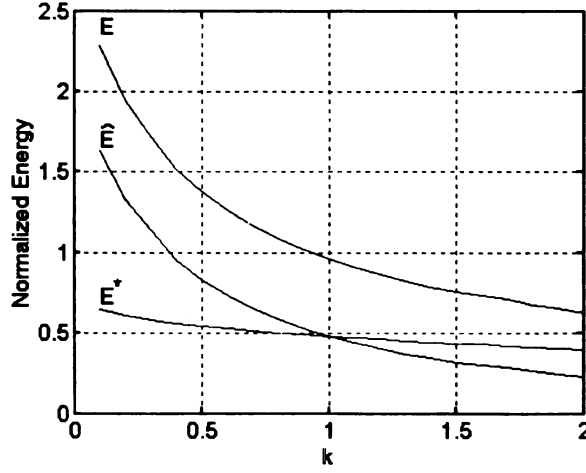
Figure 3.11: Graphs of the normalized total energy, normalized $\hat{E}$ and normalized E^* as a function of k when $R_i = 1$, $R_o = 4$ and $\psi_o - \psi_i = 1$

energy functional (3.5) can be decomposed into two parts

$$E = \hat{E} + E^*, \tag{3.104}$$

where

$$\hat{E} = \int \frac{\hat{\alpha}}{2}(\hat{I}_1 - 3) \, dX \tag{3.105}$$

is the energy corresponding to elastic part of the deformation and

$$E^* = \int \frac{\alpha^*}{2}(I_1^* - 3) \, dX \tag{3.106}$$

is the energy corresponding to pre-elastic part of the deformation.

Let $\psi_o - \psi_i$ be fixed. For given R_i, R_o and k the numerical solution presented in this section can be computed numerically to find (3.105) and (3.106). This numerical computation reveals the following relation between $\hat{E}$ and E^* for a fixed amount of twist. If $0 < k < 1$ then $\hat{E} > E^*$ and if $k > 1$ then $\hat{E} < E^*$. Moreover $\hat{E} = E^*$ when $k = 1$ meaning that the energies corresponding to elastic and pre-elastic part of the deformation are equal.

For $\psi_o - \psi_i = 1$, Figure 3.11 shows the numerically estimated graphs of the normalized total energy, normalized $\hat{E}$ and normalized E^* as a function of k when $R_i = 1$, $R_o = 4$. Energies are normalized by dividing $\pi h \hat{\alpha}$.

3.4 Explicit Solution when $\hat{\alpha} = \alpha^*$ $\left(k = 1 \right)$

In this section we will show for $k = 1$ that the governing field equations for azimuthal shear can be solved explicitly up to integration constants. Then using the boundary conditions we will show that the pure azimuthal shear problem for $k = 1$ has a unique solution provided that the twist Ψ is not too large thereby verifying the notion of a threshold twist as described above.

Recall from Section 3.3 that (3.97) supplies an equation relating ρ and g'. However it is only for $k = 1$ that ensuing algebraic simplifications as given next will take place. That $k = 1$ is special in this regard could have been anticipated by the discussions in Pence and Tsai.

If (3.97) is used with $k = 1$, then ρ is a root of the equation

$$64 \, \rho^4 \left[\rho^2 - ((rg')^4 + 2(rg')^2 - 3) \right] = 0. \tag{3.107}$$

Hence

$$\rho = 0, \pm\sqrt{(rg')^4 + 2(rg')^2 - 3}. \tag{3.108}$$

However if components of $\hat{\mathbf{B}}$ are computed from (3.91), (3.92), (3.93), (3.95) by using either $\rho = \pm\sqrt{(rg')^4 + 2(rg')^2 - 3}$, then one finds that the component equations (3.36), (3.37), (3.38) of the internal balance equation (3.34) are not satisfied. Thus these roots are spurious and $\rho = 0$ is the only solution possibility for the internal balance equation (3.34). This is consistent with the uniqueness result for the solution of internal balance. For $\rho = 0$, it follows from (3.91), (3.92), (3.93), (3.95) that

$$\hat{B}_{r\theta} = \frac{rg'}{\sqrt{4 + (rg')^2}}, \tag{3.109}$$

$$\hat{B}_{rr} = \frac{2}{\sqrt{4 + (rg')^2}}, \tag{3.110}$$

$$\hat{B}_{\theta\theta} = \frac{2 + (rg')^2}{\sqrt{4 + (rg')^2}}, \tag{3.111}$$

$$\hat{B}_{zz} = 1, \tag{3.112}$$

and it is verified that (3.34) holds. Now equations (3.109) and (3.32) give

$$\frac{rg'}{\sqrt{4 + (rg')^2}} = \frac{d_1}{r^2}, \tag{3.113}$$

which in turn provides

$$g' = \frac{2d_1}{r\sqrt{r^4 - d_1^2}}. \tag{3.114}$$

After integration and replacing r by R it is found that

$$g(R) = \arctan\sqrt{\frac{R^4 - d_1^2}{d_1^2}} + d_2, \tag{3.115}$$

where d_2 is another constant. By applying the boundary conditions (2.17) and eliminating d_2 it follows that

$$\arctan\sqrt{\frac{R_o^4 - d_1^2}{d_1^2}} - \arctan\sqrt{\frac{R_i^4 - d_1^2}{d_1^2}} = (\psi_o - \psi_i). \tag{3.116}$$

Equation (3.116) can be solved for d_1 if and only if the twist Ψ as given by (2.44) obeys

$$|\Psi| \leq \Psi_{\max}, \quad \Psi_{\max} = \arccos(\frac{R_i^2}{R_o^2}). \tag{3.117}$$

By restricting the boundary values as indicated in equation (3.117) the constants d_1 and d_2 are found to be

$$d_1 = \frac{R_i^2 R_o^2 \sin\Psi}{\sqrt{R_i^4 + R_o^4 - 2R_i^2 R_o^2 \cos\Psi}}, \tag{3.118}$$

$$d_2 = \psi_i - \arctan\sqrt{\frac{R_i^4 - d_1^2}{d_1^2}}. \tag{3.119}$$

40

Note that $\cos \Psi_{\max} = R_i^2 / R_o^2$ implies $\sin \Psi_{\max} = \sqrt{R_o^4 - R_i^4} / R_o^2$ whereupon the associated values of d_1 and d_2 are

$$(d_1)_{max} = R_i^2, \quad (d_2)_{max} = \psi_i. \tag{3.120}$$

In particular $(3.120)_1$ shows that $(d_1)_{max} = d_{\text{crit}}(1)$ as given by (3.102). In addition $\Psi_{\max} = \arccos(1/16) = 1.50826$ when $R_i = 1$, $R_o = 4$ which is consistent with $\Psi_{\text{crit}}(1)$ as given at the end of Section 3.3.

Substituting for $\hat{B}_{rr}$, $\hat{B}_{\theta\theta}$, g' from (3.110), (3.111), (3.114), into the equilibrium equation (3.33) gives

$$\frac{dp}{dr} = \hat{\alpha} \frac{\partial}{\partial r} \left(\frac{2}{\sqrt{4 + (rg')^2}} \right) + \frac{\hat{\alpha}}{r} \left(\frac{-(rg')^2}{\sqrt{4 + (rg')^2}} \right). \tag{3.121}$$

This equation simplifies to

$$\frac{dp}{dr} = 0. \tag{3.122}$$

Using (3.122) and replacing r by R gives

$$p(R) = d_3, \tag{3.123}$$

where d_3 is another constant. This constant can be computed from the boundary condition (2.18) with the help of (3.24):

$$d_3 = \frac{\hat{\alpha}}{R_o^2} \sqrt{R_o^4 - d_1^2} - \sigma_{rr}^0, \tag{3.124}$$

where d_1 is the constant given by (3.118). Since $\rho = q/\alpha^*$ and $\rho = 0$ it is immediate that

$$q = 0. \tag{3.125}$$

Thus it has been shown that if $k = 1$ and Ψ obeys (3.117) then $\hat{B}$ is given from (3.22), (3.109)–(3.112), g is given by (3.115), p is given by (3.123) and q is given by (3.125), where the constants d_1, d_2, d_3 follow from (3.118), (3.119), (3.124). Note that (3.125) is consistent with the $k = 1$ numerical solution given in Section 3.3.

41

We remark that (3.114), (3.119) give

$$g'(R) = \frac{2R_i^2 R_o^2 \sin \Psi}{R\sqrt{R^4(R_i^4 + R_o^4 - 2R_i^2 R_o^2 \cos \Psi) - R_i^4 R_o^4 \sin^2 \Psi}}. \qquad (3.126)$$

Thus $|g'(R)|$ is decreasing in R with

$$g'(R_i) = \frac{2R_o^2 \sin \Psi}{R_i(R_o^2 \cos \Psi - R_i^2)}, \qquad (3.127)$$

$$g'(R_o) = \frac{2R_i^2 \sin \Psi}{R_o(R_o^2 - R_i^2 \cos \Psi)}. \qquad (3.128)$$

Observe also that

$$g'(R_i) \to \infty \quad \text{as} \quad \Psi \to \Psi_{\max}. \qquad (3.129)$$

The normal traction on the inner surface $R = R_i$ is

$$\sigma_{rr}(R_i) = \frac{\hat{\alpha}}{R_i^2} \sqrt{R_i^4 - d_1^2} - \frac{\hat{\alpha}}{R_o^2} \sqrt{R_o^4 - d_1^2} + \sigma_{rr}^0, \qquad (3.130)$$

and we observe again that $\sigma_{rr}(R_i) < \sigma_{rr}^0$. By using (3.24) and (3.32) the shear traction on the inner and outer surfaces are

$$\sigma_{r\theta}(R_i) = \hat{\alpha}\frac{d_1}{R_i^2}, \quad \sigma_{r\theta}(R_o) = \hat{\alpha}\frac{d_1}{R_o^2}. \qquad (3.131)$$

The Torque-Twist relations follows from (2.44), (3.118), (3.131) and is given by $M = M_o = -M_i$ where

$$M = \frac{2\pi h \hat{\alpha} R_i^2 R_o^2 \sin \Psi}{\sqrt{R_i^4 + R_o^4 - 2R_i^2 R_o^2 \cos \Psi}}, \quad |\Psi| \le \Psi_{\max}. \qquad (3.132)$$

Note that

$$\frac{\partial M}{\partial \Psi}(\pm \Psi_{\max}) = 0. \qquad (3.133)$$

Thus $\Psi_{\max}$ is similar to Ψ_{ext} as discussed in Section 3.2. More generally, the notion of a threshold value for Ψ has been verified.

To compute the total stored energy E first note from (3.22) that,

$$\hat{I}_1 = \hat{B}_{rr} + \hat{B}_{\theta\theta} + \hat{B}_{zz}. \qquad (3.134)$$

42
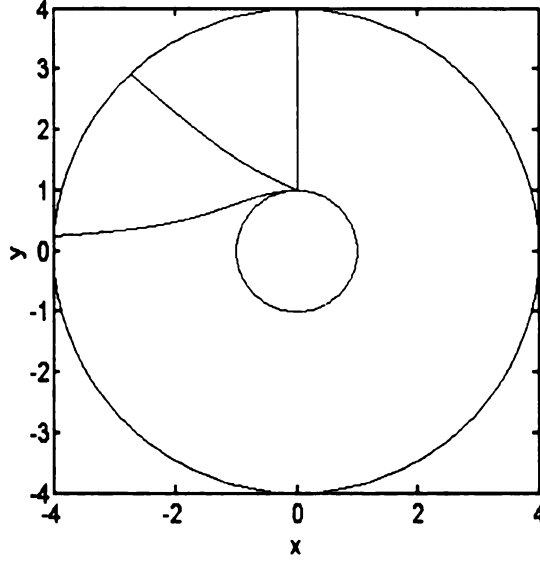
Figure 3.12: The deformation of an initially vertical line segment for a material with $k = 1$ for $\psi_o = .75413$ and $\psi_o = 1.50826 = \Psi_{max}$. These two values of ψ_o were also used in Figure 2.1 for the neo-Hookean material. Here $R_i = 1$, $R_o = 4$ and $\psi_i = 0$

By using $I_1^* = tr\, \mathbf{B}^* = tr\, \mathbf{C}^*$, where $\mathbf{C}^* = (\mathbf{F}^*)^T\, \mathbf{F}^*$ is the *right Cauchy-Green tensor* of the pre-elastic part of the deformation and $\mathbf{F}^* = \hat{\mathbf{F}}^{-1}\, \mathbf{F}$, one finds

$$\mathbf{C}^* = [\hat{\mathbf{F}}^{-1}\, \mathbf{F}]^T\, [\hat{\mathbf{F}}^{-1}\, \mathbf{F}] = \mathbf{F}^T\, \hat{\mathbf{B}}^{-1}\, \mathbf{F}. \tag{3.135}$$

Then by (2.11) and (3.22) it follows that

$$I_1^* = \frac{(1 + (rg')^2)\hat{B}_{rr} - 2rg'\,\hat{B}_{r\theta} + \hat{B}_{\theta\theta}}{\hat{B}_{rr}\hat{B}_{\theta\theta} - \hat{B}_{r\theta}^2} + \frac{1}{\hat{B}_{zz}}. \tag{3.136}$$

At this point an interesting observation following from (3.109)–(3.112), (3.134), (3.136) is that the values of $\hat{I}_1$ and I_1^* are equal for $k = 1$. This common value is given by

$$\hat{I}_1 = I_1^* = \sqrt{4 + (rg')^2} + 1. \tag{3.137}$$

The total stored energy E for this deformation follows from (3.5), (3.6), (3.136) as

$$E = \pi h\, (\hat{\alpha} + \alpha^*) \int_{R_i}^{R_o} (\sqrt{4 + (rg')^2} - 2)\, r\, dr. \tag{3.138}$$

43

Evaluating this integral with the aid of (3.114), (3.118) and using $\alpha^* = \hat{\alpha}$ (since $k = \hat{\alpha}/\alpha^* = 1$) gives

$$E = 2\pi h \, \hat{\alpha} \left(\sqrt{R_i^4 + R_o^4 - 2 R_i^2 R_o^2 \cos \Psi} + R_i^2 - R_o^2 \right). \tag{3.139}$$

Note as a result of (3.137) that the energies corresponding to elastic and pre-elastic part of the deformation are equal for $k = 1$; i.e.,

$$\int \frac{\alpha^*}{2} (I_1^* - 3) \, dX = \int \frac{\hat{\alpha}}{2} (\hat{I}_1 - 3) \, dX = \frac{E}{2}. \tag{3.140}$$

The work of the torque M follows from (2.48) and (3.133) as

$$\check{W} = 2\pi h \, \hat{\alpha} \left(\sqrt{R_i^4 + R_o^4 - 2 R_i^2 R_o^2 \cos \Psi} + R_i^2 - R_o^2 \right). \tag{3.141}$$

By direct comparison of (3.139) and (3.141) it is again found that

$$\check{W} = E. \tag{3.142}$$

We conclude this section by sketching three graphs for the deformation when $k = 1$. The first is analogous to Figure 2.1 which we recall corresponds to the neo-Hookean material ($k = 0$). Consider again the deformation of a line segment occupying $\{(R, \Theta) | 1 \leq R \leq 4, \; \Theta = \pi/2\}$ in the cross-section $R_i = 1$, $R_o = 4$ in the reference configuration. It now follows from (3.117) that the solution (3.115) holds only if $|\Psi| \leq \Psi_{\max} = \arccos(\frac{1}{16}) \simeq 1.50826$. Suppose $\psi_i = 0$ so that deformation is governed by ψ_o. Figure 3.12 shows the deformed location of the line segment for two values ψ_o: $\psi_o = 0.5\Psi_{\max} = 0.75413$ and $\psi_o = \Psi_{\max} = 1.50826$. Observe that $g'(R_i) = \infty$ for $\psi_o = \Psi_{\max}$.

For $\psi_o = .75413$ and $\psi_o = 1.50826 = \Psi_{\max}$ Figure 3.13 compares the deformation of an initially vertical line segment for a material with $k = 1$ to that of the neo-Hookean material ($k = 0$). Since it is possible to twist the neo-Hookean material beyond $\Psi_{\max}$, the deformation of the initially vertical line segment for the neo-Hookean material is also depicted for two more values of $\psi_o > \Psi_{\max}$.
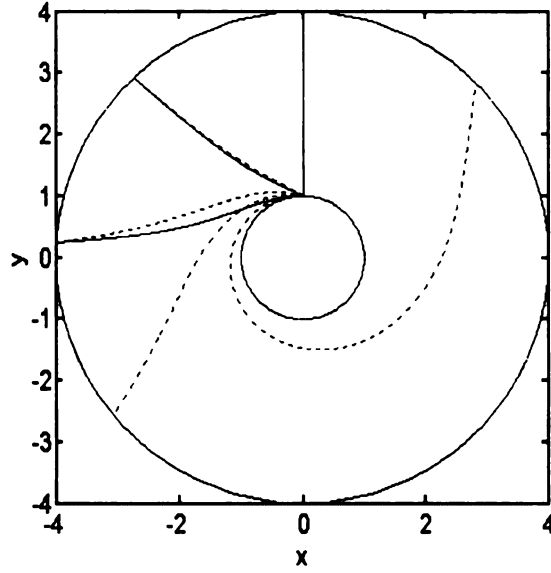
Figure 3.13: Comparison of the deformation of an initially vertical line segment for a material with $k = 1$ to that of the neo-Hookean material ($k = 0$)
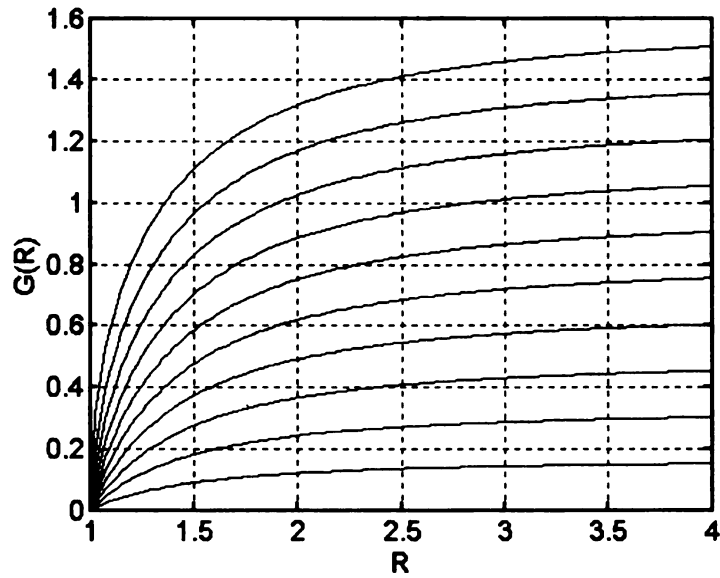
Figure 3.14: Graph of $g(R)$ when $k = 1$ for the following ten values of ψ_o, $\psi_o = 0.150826, 0.30165, 0.452475, 0.6033, 0.754125, 0.90495, 1.055775, 1.2066, 1.357425, 1.50826 = \Psi_{max}$. Here $R_i = 1$, $R_o = 4$ and $\psi_i = 0$

45

Figure 3.14 shows the graph of $g(R)$ for ten values of ψ_o: $\psi_o = \Psi_{\max} = 1.50826$, $\psi_o = 0.9\Psi_{\max} = 1.357425$, $\psi_o = 0.8\Psi_{\max} = 1.2066, \ldots$, $\psi_o = 0.1\Psi_{\max} = 0.150826$. It is again observed that $g'(R_i) \to \infty$ as $\psi_o \to \Psi_{\max}$.

3.5   Alternative Derivation from Energy

In this section it will be shown that the formulation for the pure azimuthal shear problem can be obtained directly by minimizing an appropriate energy functional that acknowledges the a-priori symmetries of azimuthal shear. This will serve as a basis for later developments and in particular will clarify the interpretation of the results of the previous section for the case $\psi > \Psi_{\max}$. Consider the deformation given by (2.10) for a material whose energy function is given by (3.6) and subject to constraint (3.7). Building the constraint into the minimization with Lagrange multiplier τ gives the functional

$$H = H(k) = \alpha^* \int_\Omega \frac{1}{2}(I_1^* - 3) + \frac{k}{2}(\hat{I}_1 - 3) - \tau(\det \hat{\mathbf{B}} - 1) \, dV. \qquad (3.143)$$

Upon use of the symmetries $g = g(r)$, $\tau = \tau(r)$, $\hat{B}_{rr} = \hat{B}_{rr}(r)$, $\hat{B}_{r\theta} = \hat{B}_{r\theta}(r)$, $\hat{B}_{\theta\theta} = \hat{B}_{\theta\theta}(r)$, $\hat{B}_{zz} = \hat{B}_{zz}(r)$, the functional H becomes

$$H = 2\pi h \alpha^* \int_{R_i}^{R_o} \left[\frac{1}{2}(I_1^* - 3) + \frac{k}{2}(\hat{I}_1 - 3) - \tau(\det \hat{\mathbf{B}} - 1) \right] r \, dr, \qquad (3.144)$$

with $\hat{I}_1$ and I_1^* given by (3.134) and (3.136) respectively. Thus (3.144) may be written as

$$H(r, \hat{B}_{rr}, \hat{B}_{r\theta}, \hat{B}_{\theta\theta}, \hat{B}_{zz}, \tau, g, g') =$$

$$\pi h \alpha^* \int_{R_i}^{R_o} \Lambda(r, \hat{B}_{rr}, \hat{B}_{r\theta}, \hat{B}_{\theta\theta}, \hat{B}_{zz}, \tau, g, g') dr, \qquad (3.145)$$

where

$$\Lambda = \left[k(\hat{B}_{rr} + \hat{B}_{\theta\theta} + \hat{B}_{zz} - 3) - 2\tau(\hat{B}_{zz}\hat{B}_{rr} \, \hat{B}_{\theta\theta} - \hat{B}_{zz}\hat{B}_{r\theta}^2 - 1) \right.$$

46

$$+\left(\frac{(1+(rg')^2)\hat{B}_{rr} - 2rg'\hat{B}_{r\theta} + \hat{B}_{\theta\theta}}{\hat{B}_{rr}\hat{B}_{\theta\theta} - \hat{B}_{r\theta}^2} + \frac{1}{\hat{B}_{zz}} - 3\right)\Big]r. \tag{3.146}$$

The *Euler-Lagrange* equations for minimization of (3.145) are

$$\frac{\partial\Lambda}{\partial\hat{B}_{rr}} = 0, \quad \frac{\partial\Lambda}{\partial\hat{B}_{r\theta}} = 0, \quad \frac{\partial\Lambda}{\partial\hat{B}_{\theta\theta}} = 0, \quad \frac{\partial\Lambda}{\partial\hat{B}_{zz}} = 0,$$

$$\frac{\partial\Lambda}{\partial\tau} = 0, \quad \frac{d}{dr}\left(\frac{\partial\Lambda}{\partial g'}\right) - \frac{\partial\Lambda}{\partial g} = 0. \tag{3.147}$$

The first five equations in (3.147) give

$$k + \hat{B}_{zz}^2(2rg'\hat{B}_{r\theta}\hat{B}_{\theta\theta} - \hat{B}_{\theta\theta}^2 - \hat{B}_{r\theta}^2 - (rg')^2\hat{B}_{r\theta}^2) - 2\tau\hat{B}_{zz}\hat{B}_{\theta\theta} = 0, \tag{3.148}$$

$$\hat{B}_{zz}\left[((rg')^2 + 1)\hat{B}_{rr}\hat{B}_{r\theta} + \hat{B}_{\theta\theta}\hat{B}_{r\theta} - rg'(\hat{B}_{r\theta}^2 + \hat{B}_{rr}\hat{B}_{\theta\theta})\right] \tag{3.149}$$

$$+ 2\tau\hat{B}_{r\theta} = 0,$$

$$k + \hat{B}_{zz}^2(2rg'\hat{B}_{rr}\hat{B}_{r\theta} - \hat{B}_{r\theta}^2 - \hat{B}_{rr}^2 - (rg')^2\hat{B}_{rr}^2) - 2\tau\hat{B}_{zz}\hat{B}_{rr} = 0, \tag{3.150}$$

$$k\hat{B}_{zz}^2 - 2\tau\hat{B}_{zz} - 1 = 0, \tag{3.151}$$

$$\hat{B}_{zz}(\hat{B}_{rr}\hat{B}_{\theta\theta} - \hat{B}_{r\theta}^2) - 1 = 0. \tag{3.152}$$

The last equation in (3.147) admits an immediate first integral by virtue of $\partial\Lambda/\partial g = 0$, the result being

$$\hat{B}_{zz}(r^3 g'\hat{B}_{rr} - r^2\hat{B}_{r\theta}) = \frac{\bar{d}}{\alpha^*}, \tag{3.153}$$

where $\bar{d}$ is an integration constant. Note that equation (3.152) is equivalent in form to (3.7). Moreover, if $\rho = -2\tau$, then equations (3.39) and (3.151) are also equivalent. It remains to show that (3.148), (3.149), (3.150), (3.153) provides the same completions as (3.36), (3.37), (3.38), (3.39) for suitably chosen d_1 and $\bar{d}$. Although we do not

have the proof of equivalency of these two systems for general k, such equivalency can be demonstrated for both $k = 0$ and $k = 1$.

Let us first consider the neo-Hookean limit case $k = 0$. By taking $k = 0$ and $\rho = -2\tau$, equations (3.148), (3.149), (3.150) reduce to

$$\hat{B}_{zz}^2(2rg'\hat{B}_{r\theta}\hat{B}_{\theta\theta} - \hat{B}_{\theta\theta}^2 - \hat{B}_{r\theta}^2 - (rg')^2\hat{B}_{r\theta}^2) + \rho\hat{B}_{zz}\hat{B}_{\theta\theta} = 0, \tag{3.154}$$

$$\hat{B}_{zz}[((rg')^2 + 1)\hat{B}_{rr}\hat{B}_{r\theta} + \hat{B}_{\theta\theta}\hat{B}_{r\theta} - rg'(\hat{B}_{r\theta}^2 + \hat{B}_{rr}\hat{B}_{\theta\theta})] - \rho\hat{B}_{r\theta} = 0, \tag{3.155}$$

$$\hat{B}_{zz}^2(2rg'\hat{B}_{rr}\hat{B}_{r\theta} - \hat{B}_{r\theta}^2 - \hat{B}_{rr}^2 - (rg')^2\hat{B}_{rr}^2) + \rho\hat{B}_{zz}\hat{B}_{rr} = 0, \tag{3.156}$$

and (3.153) reduces to

$$r^3g'\hat{B}_{rr} - r^2\hat{B}_{r\theta} = 0. \tag{3.157}$$

Moreover (3.151) gives

$$\hat{B}_{zz} = \frac{1}{\rho}. \tag{3.158}$$

Now substituting from (3.158) into (3.154)–(3.156) gives after some manipulation that

$$\rho^2\hat{B}_{\theta\theta} = [rg'\hat{B}_{r\theta} - \hat{B}_{\theta\theta}]^2 + \hat{B}_{r\theta}^2, \tag{3.159}$$

$$\rho^2\hat{B}_{r\theta} = [((rg')^2 + 1)\hat{B}_{rr}\hat{B}_{r\theta} + \hat{B}_{\theta\theta}\hat{B}_{r\theta} - rg'(\hat{B}_{r\theta}^2 + \hat{B}_{rr}\hat{B}_{\theta\theta})], \tag{3.160}$$

$$\rho^2\hat{B}_{rr} = [rg'\hat{B}_{rr} - \hat{B}_{r\theta}]^2 + \hat{B}_{rr}^2. \tag{3.161}$$

Now, (3.159) and (3.161) are quadratic equations for $\hat{B}_{\theta\theta}$ and $\hat{B}_{rr}$ respectively and using the positive-definiteness of $\hat{\mathbf{B}}$ can be solved uniquely in terms of $\hat{B}_{r\theta}$ and ρ. After substituting $\hat{B}_{\theta\theta}$ and $\hat{B}_{rr}$ in (3.160), the resulting equation is

$$\frac{(2\,\hat{B}_{r\theta} - r\,g'\,\rho^2)\,\sqrt{\rho^4 + 4\,\hat{B}_{r\theta}\,(r\,g'\,\rho^2 - \hat{B}_{r\theta})}}{2 + 2\,r^2\,(g')^2} - \tag{3.162}$$

$$\frac{r\,g'\,[\rho^4 \,+\, 4\,\hat{B}_{r\theta}\,(r\,g'\,\rho^2 \,-\, \hat{B}_{r\theta})]}{2 \,+\, 2\,r^2\,(g')^2} = 0,$$

which can be solved for $\hat{B}_{r\theta}$ in terms of ρ. By using the resulting expressions for $\hat{B}_{rr}$, $\hat{B}_{r\theta}$, $\hat{B}_{\theta\theta}$ as functions of ρ in (3.152) one obtains

$$\frac{\rho^3 + \rho\sqrt{\rho^4}\,(1 + 2\,r^2 g'^2)}{2 + 2\,r^2 g'^2} = 1, \tag{3.163}$$

which has root

$$\rho = 1, \tag{3.164}$$

and so retrieves the neo-Hookean limit (viz.(3.45).) If other roots of (3.163) are used to find the nontrivial components of $\hat{\mathbf{B}}$, it can be shown that the internal balance equation (3.34) is not satisfied. This is consistent with the uniqueness result for the solution of internal balance equation (3.34). It then follows that (3.148)--(3.153) again lead to (3.46). If (3.46) is used in (3.157), then (3.157) reduces to an identity. If (3.46) is used in (3.145) with $k = 0$, then H is a functional of g' only. Indeed it is the same energy integral (2.4) as given in the standard neo-Hookean case. By solving the *Euler-Lagrange* equations associated with this integral, one obtains $g(R)$ given by (2.34). This shows that the solution of the *Euler-Lagrange* equations associated with vanishing first variation to the functional (3.144) for $k = 0$ indeed retrieves the $k = 0$ neo-Hookean result.

Next we will consider the case $k = 1$ which corresponds to $\hat{\alpha} = \alpha^*$. By taking $k = 1$ and $\rho = -2\tau$, equations (3.148), (3.149), (3.150) reduce to

$$1 + \hat{B}_{zz}^2(2rg'\hat{B}_{r\theta}\hat{B}_{\theta\theta} - \hat{B}_{\theta\theta}^2 - \hat{B}_{r\theta}^2 - (rg')^2\hat{B}_{r\theta}^2) + \rho\hat{B}_{zz}\hat{B}_{\theta\theta} = 0, \tag{3.165}$$

$$\hat{B}_{zz}[((rg')^2 + 1)\hat{B}_{rr}\hat{B}_{r\theta} + \hat{B}_{\theta\theta}\hat{B}_{r\theta} - rg'(\hat{B}_{r\theta}^2 + \hat{B}_{rr}\hat{B}_{\theta\theta})] - \rho\hat{B}_{r\theta} = 0, \tag{3.166}$$

$$1 + \hat{B}_{zz}^2(2rg'\hat{B}_{rr}\hat{B}_{r\theta} - \hat{B}_{r\theta}^2 - \hat{B}_{rr}^2 - (rg')^2\hat{B}_{rr}^2) + \rho\hat{B}_{zz}\hat{B}_{rr} = 0, \tag{3.167}$$

and (3.153) does not change. An explicitly constructive solution procedure for obtaining ρ from (3.165)–(3.167) is not obvious. However it follows by direct verification that a solution of (3.165)–(3.167) is given by $\rho = 0$ in conjunction with components of $\hat{\mathbf{B}}$ given by (3.109)–(3.112). If (3.109)–(3.112) are substituted into (3.153), then resulting expression reduces to an identity provided that $\bar{d} = 0$. This shows that the *Euler-Lagrange* equations associated with the functional (3.144) for $k = 1$ retrieves the $k = 1$ result for the internally balanced elastic material model.

By using $k = 1$ with components of $\hat{\mathbf{B}}$ given by (3.109)–(3.112) in (3.145) we obtain

$$H_1 = 2\pi h\,\hat{\alpha} \int_{R_i}^{R_o} \left(r\sqrt{4 + (rg')^2} - 2r \right) dr. \tag{3.168}$$

Here the subscript 1 in H_1 is notation to indicate that $k = 1$. It therefore follows for $k = 1$ that if $|\Psi| \leq \Psi_{\max}$ then $g(r)$ as given by (3.115) is an extremal of (3.168) obeying (2.17). Indeed (3.113) is the first integral of the *Euler-Lagrange* equation for (3.168).

The formal theory of calculus of variations can now be used to prove that $g(r)$ given by (3.115) is in fact a strong local minimum of (3.168) if $|\Psi| \leq \Psi_{\max}$ (See Appendix A). Thus minimization of (3.168) is central to the $k = 1$ theory, suggesting that (3.168) can be used to investigate solution possibilities for $|\Psi| > \Psi_{\max}$. This will be the focus of the next section using direct methods of the calculus of variations.

We will close this section by proving that $g(r)$ given by (3.115) is indeed an absolute minimum of (3.168) if $|\Psi| \leq \Psi_{\max}$. We proceed on the basis of a convexity argument using standard procedures of the calculus of variations as reviewed next.

Consider the basic problem of calculus of variations: Find a function $y(x)$ on the interval $[a, b]$ that minimizes the definite integral

$$J[y] = \int_a^b F(x, y(x), y'(x))\, dx, \tag{3.169}$$

subject to

$$y(a) = A, \; y(b) = B. \tag{3.170}$$

In general, the minimum value of $J[y]$ depends on the eligible functions specified by the problem. Hence, the basic problem is stated more precisely as to find

$$\min_{y \in S} \{ J[y] \mid y(a) = A, \; y(b) = B \}, \tag{3.171}$$

where S is the collection of eligible functions specified by the problem. Any $y(x) \in S$ will be called as a test function. Given that y' appears in the integrand $F(x, y(x), y'(x))$ of $J[y]$, it is rather natural to use $S = C^1$, that is the space of smooth test functions. However for many problems, it is more useful to work with continuous and piecewise-smooth test functions, denoted by D^1. The following are well-known from the calculus of variations [1], [28].

Definition 3.5.1 *A test function is called an admissible test function if it also satisfies all the prescribed constraints on $y(x)$ such as the end conditions.*

Let $\hat{y}(x)$ be an admissible test function for minimizing $J[y]$ and introduce the notation $\hat{F}(x) := F(x, \hat{y}(x), \hat{y}'(x))$, $\hat{F}_{,y}(x) := \partial F(x, \hat{y}(x), \hat{y}'(x))/\partial y$, etc.

Theorem 3.5.2 *A C^1 solution $\hat{y}$ that minimizes $J[y]$ must be a solution of the Euler-Lagrange equation*

$$\hat{F}_{,y} - \frac{d}{dx}(\hat{F}_{,y'}) = 0. \tag{3.172}$$

Proof: See [28], page 13. □

Definition 3.5.3 *A smooth test function which satisfies (3.172) is called a smooth extremal for the basic problem (3.169)-(3.170).*

Definition 3.5.4 *An admissible test function $\hat{y}(x)$ is said to be a weak local minimum for the basic problem (3.169)-(3.170) if $J[y(x)] \geq J[\hat{y}(x)]$ for all admissible functions of the type $y(x) = \hat{y}(x) + \epsilon h(x)$ with $|h(x)| \leq 1$, $|h'(x)| \leq 1$, $h(a) = h(b) = 0$ and $\epsilon > 0$ sufficiently small.*

Definition 3.5.5 *An admissible test function $\hat{y}(x)$ is said to be a strong local minimum if $\exists\, \epsilon > 0$ such that $J[y(x)] \geq J[\hat{y}(x)]$ for any admissible y satisfying $|y(x) - \hat{y}(x)| < \epsilon$ in $[a, b]$.*

Weak and strong local minima can also be defined by using weak and strong neighborhoods of $\hat{y}(x)$ as described next

Definition 3.5.6 *For a given $\epsilon > 0$, the set of all piecewise-smooth test functions satisfying*

$$|y(x) - \hat{y}(x)| < \epsilon \tag{3.173}$$

for each $x \in [a, b]$, is called a strong ϵ-neighborhood of $\hat{y}(x)$ and denoted by $U_S(\epsilon, \hat{y}(x))$.

Definition 3.5.7 *For a given $\epsilon > 0$, the set of all piecewise-smooth test functions satisfying the inequality (3.173) and*

$$|y'(x) - \hat{y}'(x)| < \epsilon \tag{3.174}$$

for each $x \in [a, b]$, is called a weak ϵ-neighborhood of $\hat{y}(x)$ and denoted by $U_W(\epsilon, \hat{y}(x))$.

Definition 3.5.8 *An admissible test function $\hat{y}(x)$ is said to be a strong local minimum if $\exists\, \epsilon > 0$ such that $J[y(x)] \geq J[\hat{y}(x)]$ for all $y \in U_S(\epsilon, \hat{y}(x))$.*

Definition 3.5.9 *An admissible test function $\hat{y}(x)$ is said to be a weak local minimum if $\exists\, \epsilon > 0$ such that $J[y(x)] \geq J[\hat{y}(x)]$ for all $y \in U_W(\epsilon, \hat{y}(x))$.*

If $S = D^1$; i.e., the set of all piecewise-smooth functions in $[a, b]$, then the *Euler-Lagrange* equation (3.172) alone is not sufficient to characterize the minimization. The characterization needs to be modified as follows.

Theorem 3.5.10 *In order for the admissible piecewise-smooth test function $\hat{y}$ of the basic problem (3.169)–(3.170) to render the integral $J[y]$ a weak local minimum, it is necessary that*

$$\hat{F}_{,y'}(x) = c + \int_a^x \hat{F}_{,y}(t)\, dt, \tag{3.175}$$

for some constant c.

Proof: See [28], page 38. $\square$

Equation (3.175) is called the *integral* form of the Euler-Lagrange equation.

Corollary 3.5.11 *At any point x where $\hat{y}'$ is continuous, it is necessary that $\hat{y}$ satisfies the Euler-Lagrange equation (3.172).*

Definition 3.5.12 *A piecewise-smooth test function $\hat{y}(x)$ that satisfies (3.175) is called an extremal for the basic problem (3.169)–(3.170).*

It is more effective and convenient to work with the Euler-Lagrange equation (3.172). Hence, it is important to know whether the extremals for a basic problem are smooth and the locations of discontinuities of their derivative when they are not smooth. These discontinuities are known as corners of extremals. Information on discontinuities can be obtained from the so-called *Erdmann's corner conditions*.

Definition 3.5.13 *A corner point of a test function $\hat{y}(x)$ is a point x where the left derivative and right derivative of $\hat{y}(x)$ exist at x (and are denoted by y'_- and y'_+ respectively) but they are not equal.*

Theorem 3.5.14 *If $\hat{y}(x)$ is an extremal, then $\hat{F}_{,y'}(x)$ is continuous at a corner point.*

Proof: See [28], page 45. □

Theorem 3.5.15 *If $\hat{y}(x)$ is an extremal, then the quantity $(\hat{F} - \hat{y}'\hat{F}_{,y'})$ is continuous at a corner point.*

Proof: See [28], page 46. □

Theorem 3.5.16 *(Hilbert's Theorem)Suppose that $\hat{y}$ is an extremal, x_0 is not a corner point, and $\hat{F}_{,y'y'}(x_0) \neq 0$. Then $\hat{y}$ is C^2 and*

$$(\hat{F}_{,y'y'})\, y'' + (\hat{F}_{,y'y})\, y' + (\hat{F}_{,y'x} - \hat{F}_{,y}) = 0, \tag{3.176}$$

holds in some neighborhood of x_0.

Proof: See [28], page 48. □

Equation (3.176) is sometimes called the *ultradifferentiated* form of the Euler-Lagrange equation.

Definition 3.5.17 *A scalar valued function* $f : R^n \to R$ *is said to be convex if*

$$f(\lambda w + (1 - \lambda)z) \le \lambda f(w) + (1 - \lambda)f(z) \tag{3.177}$$

$\forall w, z \in R^n$, *and* $\forall \lambda \in [0, 1]$.

Theorem 3.5.18 *If* $F(x, y, y')$ *is differentiable in its arguments and convex in* y *and* y' *for each* x, *then any admissible extremal of the basic problem (3.169)–(3.170) renders* $J[y]$ *a global minimum and conversely.*

Proof: See [28], page 108. □

Theorem 3.5.19 *A scalar valued function of one variable* $f(y)$ *is convex if and only if* f'' *is everywhere non-negative.*

Proof: See [28], page 105. □

This completes the quick review of the appropriate machinery from the calculus of variations. We may now on this basis rapidly show that $g(r)$ as given by (3.115) is indeed an absolute minimum. For (3.168) the *Lagrangian* F is

$$F(r, g, g') = r\sqrt{4 + (rg')^2} - 2r. \tag{3.178}$$

From (3.178) it follows that

$$\frac{\partial^2 F}{\partial g'^2} = \frac{4r^3}{(4 + (rg')^2)^{3/2}} > 0. \tag{3.179}$$

Hence $F(r, g, g') = F(r, g')$ is convex in g' for each fixed r by Theorem 3.5.19. If $|\Psi| \le \Psi_{\text{max}}$, then it follows by the Theorem 3.5.18 that $g(r)$ given by (3.115), (3.118), (3.119) is an absolute minimum of (3.168) obeying (2.17).

3.6 Direct Methods for Minimization when $k = 1$

At the end of the last section it was shown that if $|\Psi|$ is restricted by $|\Psi| \leq \Psi_{max}$ where Ψ_{max} is given by (3.117), then $g(r)$ given by (3.115) provides an absolute minimum for (3.168) among functions obeying (2.17). The significance of this result is that minimization of (3.168) subject to (2.17) governs the $k = 1$ problem. In this section we will investigate the minimization of (3.168) subject to (2.17) for arbitrarily large twist Ψ. Since $g'(R_i) \to \infty$ as $\Psi \to \Psi_{max}$, it is conjectured that minimizers might involve vertical line segments. Since such a vertical line segment cannot be considered as a function of R, it is expedient to use the parametric form of the energy integral (3.168) for further investigation.

Consider the basic problem of calculus of variations in parametric form: Find a piecewise-smooth curve $C = \{(x, y) = (x(t), y(t)) : t_1 \leq t \leq t_2\}$ that minimizes the definite integral

$$J_C = \int_C f(t, x, y, \dot{x}, \dot{y})\, dt, = \int_{t-1}^{t-2} f(t, x, y, \dot{x}, \dot{y})\, dt, \tag{3.180}$$

subject to

$$(x(t_1), y(t_1)) = (x_1, y_1), \ (x(t_2), y(t_2)) = (x_2, y_2). \tag{3.181}$$

The dots indicate derivatives with respect to the parameter and f is a given function, continuous in all its arguments when $(x(t), y(t))$ lies in a given region G; $\dot{x}$, $\dot{y}$ have arbitrary values and are not zero simultaneously. The function f cannot be completely arbitrary because the integral under consideration must depend only on the curve C and not on any particular parametric representation of the curve. By the discussions given in [1], p 39–40 this independence of parametric representation will hold if and only if:

(i1) t does not appear explicitly in the integrand function f; that is,

$$f(t, x, y, \dot{x}, \dot{y}) = f(x, y, \dot{x}, \dot{y}). \tag{3.182}$$

(i2) The integrand function $f(x, y, \dot{x}, \dot{y})$ must be positively homogeneous and of the first degree relative to the second pair of arguments; that is,

$$f(x, y, m\dot{x}, m\dot{y}) = m\, f(x, y, \dot{x}, \dot{y}) \; \forall m > 0. \tag{3.183}$$

As a result of homogeneity

$$\frac{f_{\dot{x}\dot{x}}}{\dot{y}^2} = \frac{f_{\dot{x}\dot{y}}}{-\dot{x}\dot{y}} = \frac{f_{\dot{y}\dot{y}}}{\dot{x}^2}. \tag{3.184}$$

If the common ratio in (3.184) is denoted by $K = K(x, y, \dot{x}, \dot{y})$, then

$$f_{\dot{x}\dot{x}} = \dot{y}^2\, K, \; f_{\dot{x}\dot{y}} = -\dot{x}\dot{y}\, K, \; f_{\dot{y}\dot{y}} = \dot{x}^2\, K. \tag{3.185}$$

Suppose an admissible curve

$$\bar{C}: \quad x = \bar{\phi}(t), \quad y = \bar{\varphi}(t) \quad (t_1 \le t \le t_2) \tag{3.186}$$

gives the functional J_C a weak relative minimum. Then functions $\bar{\phi}(t)$, $\bar{\varphi}(t)$ must satisfy the *Euler-Lagrange equations in parametric form*

$$f_{\dot{x}} = A + \int_{t_1}^{t} f_x(\xi)\, d\xi, \; f_{\dot{y}} = B + \int_{t_1}^{t} f_y(\xi)\, d\xi, \tag{3.187}$$

in which A and B are constants.

If arc length s is used as parameter, then

$$\dot{x} = \frac{dx}{ds} = \cos\omega, \quad \dot{y} = \frac{dy}{ds} = \sin\omega, \tag{3.188}$$

where ω is the angle between the tangent to the curve and the x-axis. Along each smooth arc of a curve

$$\frac{d}{ds}f_{\dot{x}} - f_x = 0, \quad \frac{d}{ds}f_{\dot{y}} - f_y = 0, \tag{3.189}$$

and at a corner point $s = s_0$

$$f_{\dot{x}}(s_0^+) - f_{\dot{x}}(s_0^-) = 0, \quad f_{\dot{y}}(s_0^+) - f_{\dot{y}}(s_0^-) = 0. \tag{3.190}$$

57

(Here s_0^+ and s_0^- denote the one-sided limits $\lim_{s \to s_0^+}$ and $\lim_{s \to s_0^-}$ respectively.) A smooth solution of (3.189) is called an extremal and (3.190) express the *Weierstrass-Erdmann corner conditions*. Note that (3.190)$_1$ is equivalent to corner condition given by Theorem 3.5.15 and (3.190)$_2$ is equivalent to corner condition given by Theorem 3.5.14 for the nonparametric case.

If parametric forms of $r = x(t)$ and $g = y(t)$ are used, then the energy integral (3.168) becomes

$$H_p[x(t), y(t)] = 2\pi h \, \hat{\alpha} \int_{t_1}^{t_2} \left[\frac{x}{\dot{x}} \sqrt{4\dot{x}^2 + x^2 \dot{y}^2} - 2x \right] \dot{x} \, dt, \tag{3.191}$$

where the subscript p in H_p indicates that the parametric form of the energy is used, $\dot{x} = dx/dt$, $\dot{y} = dy/dt$, $(x(t_1), y(t_1)) = (R_i, \psi_i)$ and $(x(t_2), y(t_2)) = (R_o, \psi_o)$.

Note that the *Lagrangian* of (3.191) can be written as

$$f(x, y, \dot{x}, \dot{y}) = x \sqrt{4\dot{x}^2 + x^2 \dot{y}^2} - 2x\dot{x}. \tag{3.192}$$

Homogeneity of f in the last two variables is immediate since

$$f(x, y, m\dot{x}, m\dot{y}) = x \sqrt{4(m\dot{x})^2 + x^2(m\dot{y})^2} - 2x(m\dot{x}) \tag{3.193}$$

$$= x \sqrt{4m^2\dot{x}^2 + x^2 m^2 \dot{y}^2} - 2xm\dot{x}$$

$$= m[x\sqrt{4\dot{x}^2 + x^2\dot{y}^2} - 2x\dot{x}]$$

$$= m \, f(x, y, \dot{x}, \dot{y}).$$

Thus condition (i2) is satisfied. Moreover, condition (i1) is satisfied since t does not appear explicitly in the *Lagrangian* (3.192). Therefore the value of the energy integral (3.191) depends only on the curve C not on any particular parametric representation of the curve.

58

The *Euler-Lagrange* equations (3.187) are

$$\left[\frac{4x\dot{x}}{\sqrt{4\dot{x}^2 + x^2\dot{y}^2}} - 2x\right] - \int_{t_1}^{t} f_x(\xi)\,d\xi = \bar{c}_1, \tag{3.194}$$

and

$$\frac{x^3\dot{y}}{\sqrt{4\dot{x}^2 + x^2\dot{y}^2}} = \bar{c}_2, \tag{3.195}$$

where $\bar{c}_1$ and $\bar{c}_2$ are constants. Note that (3.195) is equivalent to (3.113) and by taking the derivative with respect to t in (3.194) the first *Euler − Lagrange* equation becomes

$$\frac{d}{dt}\left[\frac{4x\dot{x}}{\sqrt{4\dot{x}^2 + x^2\dot{y}^2}} - 2x\right] = \sqrt{4\dot{x}^2 + x^2\dot{y}^2} + \frac{x^2\dot{y}^2}{\sqrt{4\dot{x}^2 + x^2\dot{y}^2}} - 2\dot{x}. \tag{3.196}$$

From (3.195) and (3.196) it follows that $y(t) = constant$ and curves described by (3.115) are extremals whereas $x(t) = constant$ are not extremals. An extremal consisting of an arc of (3.115) and a straight line segment $y(t) = constant$ will not satisfy the *Erdmann's Corner Conditions* (3.190).

For $|\Psi| \leq \Psi_{\max}$, we consider the composite curve consisting of the curve obtained from (3.115) by vertical translation (with $d_1 = R_i^2$ and $d_2 = \psi_i$) in conjunction with the line segment $x = R_i$ between $y = \psi_i$ and $y = \psi_o - \Psi_{\max}$. This composite curve will be called Λ_1. Thus Λ_1 consists of a vertical translation of the $\Psi = \Psi_{\max}$ extremal so as to meet the $x = R_o$ end condition $y(R_o) = \psi_o$, along with an $x = R_i$ vertical segment so as to connect to the $x = R_i$ end condition $y(R_i) = \psi_i$. Since this vertical segment is confined to the boundary, it need not satisfy *Euler-Lagrange* condition (3.195) and (3.196).

We begin with some direct comparisons. In particular, it will now be shown that Λ_1 as described above provides a minimum to (3.191) among a collection test curves: Λ_{nH}, Λ_2, $\Lambda_3(n)$, $\Lambda_4(n)$ that we now define.

In the remainder of this section we will take $\psi_i = 0$ and $\psi_o > 0$. For $\psi_o \leq \Psi_{\max}$, we note that Λ_1 can be parameterized as follows

$$
x_1(t) = \begin{cases} R_i & \text{if } t \in [0, R_i] \\ t & \text{if } t \in [R_i, R_o], \end{cases}
$$

(3.197)

$$
y_1(t) = \begin{cases} (\psi_o - \Psi_{\max}) \, t \, / \, R_i & \text{if } t \in [0, R_i] \\ (\psi_o - \Psi_{\max}) + \arctan \sqrt{\left(t^4/R_i^4 \right) - 1} & \text{if } t \in [R_i, R_o], \end{cases}
$$

Then the corresponding energy can be computed from (3.191) as

$$
H_p[\Lambda_1] = E_d + E_s
$$

(3.198)

where

$$
E_d = 2\pi h \hat{a} R_i^2 \left[\psi_o - \Psi_{\max} \right], \quad E_s = 2\pi h \hat{a} \left[\sqrt{R_o^4 - R_i^4} + R_i^2 - R_o^2 \right].
$$

(3.199)

Note that first term E_d is the energy corresponding to vertical segment $x = R_i$ and second term E_s is the energy corresponding to the curve obtained from (3.115) by vertical translation. The associate matching requires that $d_1 = R_i^2$ and $d_2 = 0$ in (3.115). Since $\Psi_{\max} = \arccos(R_i^2/R_o^2)$, the energy expression (3.198) may also be written as

$$
H_p[\Lambda_1] = 2\pi h \hat{a} \left[R_i^2 \left(\psi_o - \arccos(\frac{R_i^2}{R_o^2}) \right) + \sqrt{R_o^4 - R_i^4} + (R_i^2 - R_o^2) \right]. (3.200)
$$

As $\psi_o \to \Psi_{\max} = \arccos(R_i^2/R_o^2)$ the energy associated with the discontinuity E_d goes to zero as expected.

Let Λ_{nH} be the curve corresponding to neo-Hookean solution (2.34), (2.36) and (2.37) with $\psi_i = 0$. Then it has the parametrization

$$
x_{nH}(t) = t \quad \text{if } t \in [R_i, R_o],
$$

(3.201)

$$
y_{nH}(t) = \frac{-R_i^2 R_o^2 \psi_o}{(R_o^2 - R_i^2) \, t^2} + \frac{\psi_o \, R_o^2}{(R_o^2 - R_i^2)} \quad \text{if } t \in [R_i, R_o].
$$

60

ψ_o	N. Energy for Λ_1	N. Energy for Λ_{nH}
2	1.4605	1.7056
2.5	1.9605	2.4835
3	2.4605	3.3440
3.5	2.9605	4.2720
4	3.4605	5.2570

Table 3.1: Normalized energies for Λ_1 and Λ_{nH} for several ψ_o values when $R_i = 1$, $R_o = 4$ and $\psi_i = 0$

Then the energy for the present case $k = 1$ using the $k = 0$ neo-Hookean deformation can be computed from (3.191) as

$$H_p[\Lambda_{nH}] = 2\,\pi\,h\,\hat{\alpha}\left\{ R_i^2 - R_o^2 + R_o^2\sqrt{1 + \frac{R_i^4\,\psi_o^2}{(R_i^2 - R_o^2)^2}} - \right.$$

$$R_i^2\sqrt{1 + \frac{R_o^4\,\psi_o^2}{(R_i^2 - R_o^2)^2}} + \frac{R_i^2 R_o^2 \psi_o}{(R_i^2 - R_o^2)^2}\log\left[\frac{R_o^2\,\psi_o}{R_i^2 - R_o^2} + \sqrt{1 + \frac{R_o^4\,\psi_o^2}{(R_i^2 - R_o^2)^2}}\right]$$

$$\left. -\frac{R_i^2 R_o^2 \psi_o}{(R_i^2 - R_o^2)^2}\,\log\left[\frac{R_i^2\,\psi_o}{R_i^2 - R_o^2} + \sqrt{1 + \frac{R_i^4\,\psi_o^2}{(R_i^2 - R_o^2)^2}}\right] \right\}. \tag{3.202}$$

Note that $H_p[\Lambda_{nH}] \approx 5.2570\,(2\,\pi\,h\,\hat{\alpha})$ when $R_i = 1$, $R_o = 4$ and $\psi_o = 4$. In the following table, Table 3.1, the normalized minimum energies for Λ_1 and Λ_{nH} are presented for several ψ_o values when $R_i = 1$, $R_o = 4$ and $\psi_i = 0$. The energy in this table is normalized via division by $2\,\pi\,h\,\hat{\alpha}$. It is consistently verified that $\Lambda_1 < \Lambda_{nH}$.

We now construct a broader class of comparison functions. Let Λ_2 be the straight line connecting $(R_i, 0)$ to (R_o, ψ_o). It is given by the parametrization

$$x_2(t) = t \quad \text{if } t \in [R_i, R_o], \tag{3.203}$$

$$y_2(t) = \frac{\psi_o\,(t - R_i)}{R_o - R_i} \quad \text{if } t \in [R_i, R_o].$$

The corresponding energy is computed from (3.191) to be

$$H_p[\Lambda_2] = 2\,\pi\,h\,\hat{a}\left[R_i^2 - R_o^2\right].\tag{3.204}$$

$$+2\,\pi\,h\,\hat{a}\left[\frac{[4\,(R_o - R_i)^2 + R_o^2\,\psi_o^2]^{3/2} - [4\,(R_o - R_i)^2 + R_i^2\,\psi_o^2]^{3/2}}{3\,(R_o - R_i)^2\,\psi_o^2}\right].$$

Let $\Lambda_3(n)$ be the family of curves given by the parametrization:

$$x_{3,n}(t) = t \quad \text{if } t \in [R_i, R_o],\tag{3.205}$$

$$y_{3,n}(t) = \psi_o\left[1 + \left(\arctan\frac{n\,(t - R_o)}{R_o - R_i}\right)\middle/\arctan n\right] \quad \text{if } t \in [R_i, R_o],$$

with $n \geq 0$ and not generally an integer.

Figure 3.15 shows 6 curves of this family for the case $R_i = 1$ and $R_o = 4$ (implying $\Psi_{\max} \approx 1.50826$) and $\psi_o = 4$, namely $n = 0, 1, 10, 100, 1000, 10000$. Note that in the limit as $n \to 0$ these rectifiable curves tend to Λ_2, and as $n \to \infty$ tend to the step function

$$x_{3,\infty}(t) = \begin{cases} t & \text{if } t \in [R_i, R_o] \\ R_o & \text{if } t \in [R_o, R_o + \psi_o], \end{cases}\tag{3.206}$$

$$y_{3,\infty}(t) = \begin{cases} 0 & \text{if } t \in [R_i, R_o] \\ (t - R_o) & \text{if } t \in [R_o, R_o + \psi_o]. \end{cases}$$

By numerical computation it is found that $H_p[\Lambda_3(n)]$ increases with n. The corresponding energy as $n \to \infty$ can be computed from (3.191) as

$$\lim_{n \to \infty} H_p[\Lambda_3(n)] = 2\,\pi\,h\,\hat{a}\,R_o^2\,\psi_o.\tag{3.207}$$

Let $\Lambda_4(n)$ be the family of curves given by the parametrization:

$$x_{4,n}(t) = t \quad \text{if } t \in [R_i, R_o],\tag{3.208}$$

$$y_{4,n}(t) = \psi_o\left[\left(\arctan\frac{n\,(t - R_i)}{R_o - R_i}\right)\middle/\arctan n\right] \quad \text{if } t \in [R_i, R_o],$$
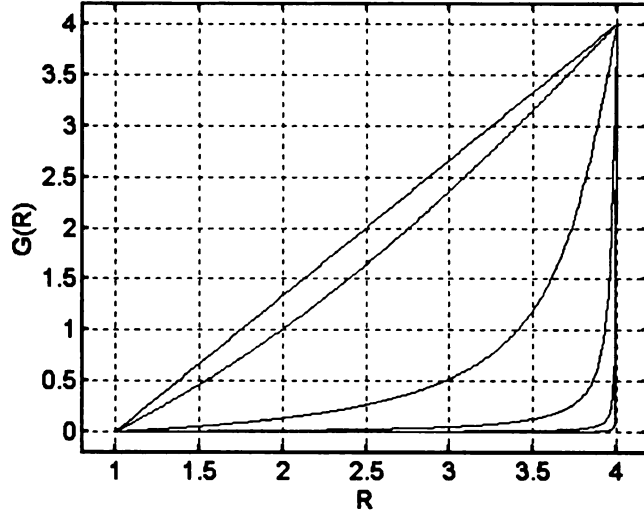
Figure 3.15: Graph of the family $\Lambda_3(n)$ with $R_i = 1$, $R_o = 4$, $\psi_i = 0$ and $\psi_o = 4$ for $n = 0$ (the diagonal line), and $1, 10, 100, 1000, 10000$

with $n \geq 0$. Figure 3.16 shows 7 curves of this family for the case $R_i = 1$ and $R_o = 4$ and $\psi_o = 4$, namely $n = 0, 1, 10, 83.1, 100, 1000, 10000$. The dashed line shows the case $n = 83.1$, the significance of which will shortly be made clear. In the limit as $n \rightarrow 0$ these rectifiable curves tend to Λ_2, and as $n \rightarrow \infty$ tend to the step function

$$x_{4,\infty}(t) = \begin{cases} R_i & \text{if } t \in [0, R_i] \\ t & \text{if } t \in [R_i, R_o], \end{cases}$$ (3.209)

$$y_{4,\infty}(t) = \begin{cases} \psi_o t & \text{if } t \in [0, R_i] \\ \psi_o & \text{if } t \in [R_i, R_o]. \end{cases}$$

In this case the corresponding energy as $n \rightarrow \infty$ can be computed from (3.191) as

$$\lim_{n \rightarrow \infty} H_p[\Lambda_4(n)] = 2 \pi h \, \hat{\alpha} \, R_i^2 \, \psi_o.$$ (3.210)

Numerical calculation shows for this family of curves that the corresponding energy $H_p[\Lambda_4(n)]$ initially decreases with n after which $H_p[\Lambda_4(n)]$ subsequently increases

63
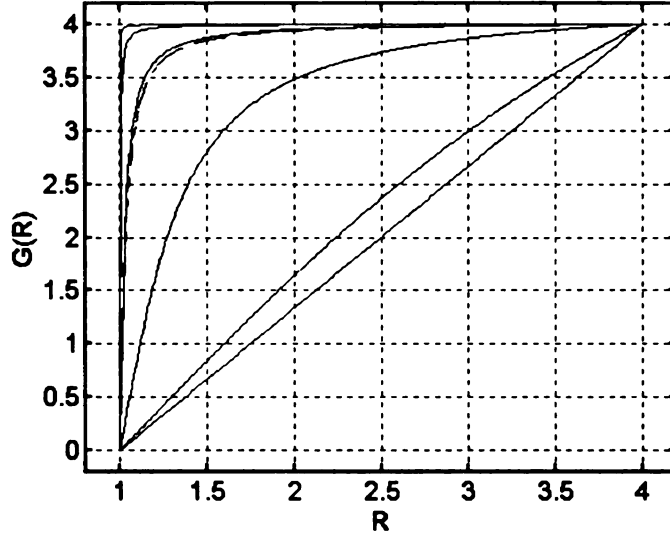
Figure 3.16: Graph of the family $\Lambda_4(n)$ with $R_i = 1$, $R_o = 4$, $\psi_i = 0$ and $\psi_o = 4$ for $n = 0$ (the diagonal line), and $1, 10, 83.1, 100, 1000, 10000$. The dashed line shows the case $n = 83.15$ which results the minimum energy among the family $\Lambda_4(n)$

with n. Let $n_{\min} = n_{\min}(R_i, R_o, \psi_o)$ denote the transition value of n between these two behaviors. We find for example $n_{\min}(1, 4, 4) \approx 83.15$ and the corresponding minimum energy among $\Lambda_4(n)$ is $H_p[\Lambda_4(83.15)] \approx 3.70242\,(2\,\pi\,h\,\hat{\alpha})$. In Table 3.2 the transition value of n and corresponding normalized minimum energies among $\Lambda_4(n_{\min})$ are presented for several ψ_o values when $R_i = 1$, $R_o = 4$ and $\psi_i = 0$. Once again the energy in this table is normalized via division by $2\,\pi\,h\,\hat{\alpha}$.

Taken together the family of curves $\Lambda_3(n)$ with n decreasing, the single curve Λ_2 and the family of curves $\Lambda_4(n)$ with n increasing form a larger continuous family of curves with minimum H_p at $\Lambda_4[n_{\min}(R_i, R_o, \psi_o)]$.

We find on the basis of extensive numerical calculation that the energy H_p at $\Lambda_4[n_{\min}(R_i, R_o, \psi_o)]$ is still greater than the energy corresponding to Λ_1 for the same values of R_i, R_o and ψ_o. In particular comparison of Tables 3.1 and 3.2 shows this for a few selected cases. Figure 3.17 for $R_i = 1$, $R_o = 4$ and $\psi_o = 4$ compares the

ψ_o	n	Normalized Energy
2	18.08	1.54436
2.5	28.14	2.10070
3	42.52	2.64498
3.5	61.00	3.17782
4	83.15	3.70242

Table 3.2: Normalized minimum energies $\Lambda_4(n_{\min})$ for several ψ_o values when $R_i = 1$, $R_o = 4$ and $\psi_i = 0$

graph of Λ_1 with the graph of $\Lambda_4(83.15)$ which gives the minimum energy in this extended family.

Consequently, for a given R_o and fixed $\psi_o \geq \Psi_{\max}$ the minimum among the computed energies remains $H_p[\Lambda_1]$.

Formally, Λ_1 and hence $H_p[\Lambda_1]$ is defined only if $\psi_o \geq \Psi_{\max}$. However it is natural to extend Λ_1 to $0 \leq \psi_o \leq \Psi_{\max}$ via (3.115) and this is understood in what follows. The graph in Figure 3.18 shows normalized energies E_1, E_2, E_3, E_4 and E_{nH} as a function of the amount of twist ψ_o corresponding to Λ_1, Λ_2, $\Lambda_{3,\infty}$, $\Lambda_{4,\infty}$ and Λ_{nH}, respectively, when $R_i = 1$ and $R_o = 4$. The normalized energy associated with $\Lambda_4[n_{\min}]$ as given in Table 3.2 is also indicated by stars for $\psi_o = 2, 2.5, 3, 3.5, 4$.

If $\psi_o \in [0, \Psi_{\max}]$ then the torque-twist relation is given by (3.132). If $\psi_o \geq \Psi_{\max}$ then we note from (2.48), (2.49) that it is enough to compute $\partial \check{W}/\partial \psi_o$ which can be computed from (3.200). Hence the torque-twist relation for Λ_1 is given by

$$M = \begin{cases} \dfrac{2\pi h \,\hat{\alpha}\, R_i^2\, R_o^2\, \sin\psi_o}{\sqrt{R_i^4 + R_o^4 - 2\,R_i^2\, R_o^2\, \cos\psi_o}} & \text{if } 0 \leq \psi_o \leq \Psi_{\max} \\[4mm] 2\pi h\, R_i^2\, \hat{\alpha} & \text{if } \psi_o \geq \Psi_{\max}. \end{cases} \tag{3.211}$$

The conspicuous feature of (3.211) is that the twisting moment associated with this extended deformation Λ_1 is monotonically increasing with ψ_o on $0 \leq \psi_o \leq \Psi_{\max}$ after which the twisting moment remains constant. The physical interpretation is

65
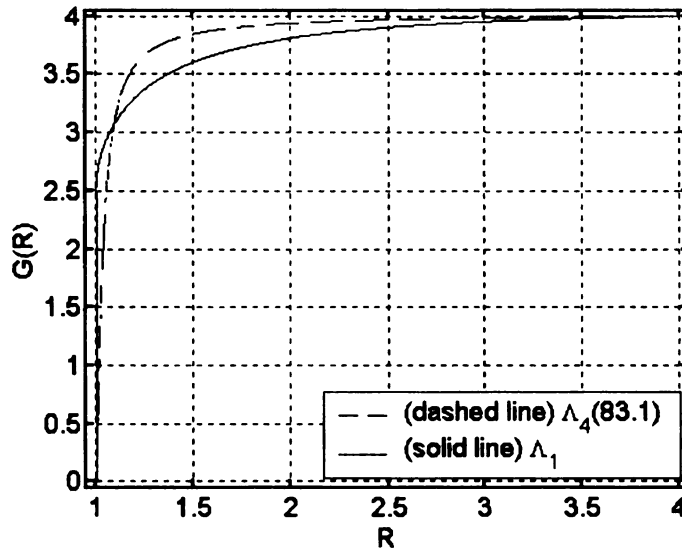
Figure 3.17: Graph of Λ_1 and $\Lambda_4(83.15)$ when $R_i = 1$, $R_o = 4$ and $\psi_o = 4$
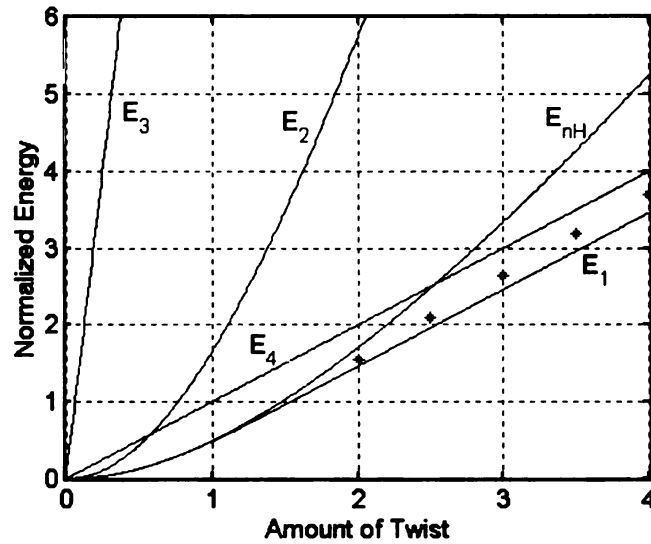
Figure 3.18: Normalized energy versus twist for $R_i = 1$, $R_o = 4$, $\psi_i = 0$ and varying ψ_o. Here $\Psi_{\max} = 1.50826$. The energies corresponding to Λ_1, Λ_2, $\Lambda_{3,\infty}$, $\Lambda_{4,\infty}$ and Λ_{nH} are normalized by dividing $2\pi h \hat{a}$. The normalized energy associated with $\Lambda_4[n_{\min}]$ is also indicated by stars for $\psi_o = 2, 2.5, 3, 3.5, 4$

that conventional macroelastic resistance to twist occurs until $\psi_o = \Psi_{\max}$ after which substructural rearrangement concentrates at the singular surface $R = R_i$ so as to relieve any further macroelastic resistance. This novel effect is not present in the conventional theory of hyperelasticity, although it is reminiscent of other phenomena in the conventional theory such as cavity formation and shear banding at critical load values [5], [14], [19], [23], [27].

It will now be proven that Λ_1 given by (3.197) provides a weak local minimum for the parametric energy integral (3.191) subject to $(x(t_1), y(t_1)) = (R_i, 0)$ and $(x(t_2), y(t_2)) = (R_o, \psi_o)$ in the family of piecewise-smooth curves lying in the closed region $G = \{(x, y) | R_i \leq x \leq R_o, \ 0 \leq y \leq \psi_o\}$.

To this end we begin with a technical detail. Namely we note that Λ_1 given by (3.197) is a differentiable curve only if $t \neq 1$. However the location of non-differentiability at $t = 1$ is an artifact of the parametrization. If Λ_1 is reparameterized in terms of arc length, then it is also differentiable at the location associated with the original $t = 1$. To this end let s be the arc length parameter. Then Λ_1 can be parameterized by

$$
\bar{x}_1(s) = \begin{cases} R_i & \text{if } s \in [0, \psi_o - \Psi_{\max}] \\ h(s) & \text{if } s \in [\psi_o - \Psi_{\max}, s_o], \end{cases} \tag{3.212}
$$

$$
\bar{y}_1(s) = \begin{cases} s & \text{if } s \in [0, \psi_o - \Psi_{\max}] \\ \psi_o - \Psi_{\max} + \arctan\sqrt{\left(h^4(s)/R_i^4\right) - 1} & \text{if } s \in [\psi_o - \Psi_{\max}, s_o], \end{cases}
$$

where s_o is the total arc length and

$$
s = \int_0^{h(s)} \sqrt{\dot{x}_1{}^2 + \dot{y}_1{}^2}\, dt. \tag{3.213}
$$

By using (3.197), it follows that (3.213) can be written as

$$
s = \psi_o - \Psi_{\max} + \int_{R_i}^{h(s)} \sqrt{1 + \frac{4\, R_i^4}{t^6 - R_i^4\, t^2}}\, dt. \tag{3.214}
$$

The integral in (3.214) does not have a readily explicit antiderivative hence there is no readily explicit form for $h(s)$. However using (3.214) it can be seen that parametrization of Λ_1 given by (3.212) is a C^1 parametrization.

Proposition 3.6.1 *The Λ_1 given by (3.197) is a weak local minimum of (3.191) subject to $(x(t_1), y(t_1)) = (R_i, 0)$ and $(x(t_2), y(t_2)) = (R_o, \psi_o)$ in the class of piecewise-smooth curves lying in the closed region $G = \{(x,y)|R_i \leq x \leq R_o,\ 0 \leq y \leq \psi_o\}$.*

Proof: Let $\epsilon \geq 0$ be a given small nonnegative number. Consider the curve defined by

$$\bar{x}(t) = x_1(t) + \epsilon\,\zeta(t), \tag{3.215}$$

$$\bar{y}(t) = y_1(t) + \epsilon\,\eta(t),$$

where $\zeta(0) = \eta(0) = 0$, $\zeta(R_o) = \eta(R_o) = 0$ and $\zeta(t) \geq 0$ if $0 \leq t \leq R_i$. Here $x_1(t)$ and $y_1(t)$ are given by (3.197); i.e., $(\bar{x}(t), \bar{y}(t))$ is a small perturbation of $(x_1(t), y_1(t))$ that is confined to lie in the closed region G.

Then the variation in H_p as a result of this perturbation is defined by

$$\Delta H_p = H_p[x_1(t) + \epsilon\,\zeta(t), y_1(t) + \epsilon\,\eta(t)] - H_p[x_1(t), y_1(t)], \tag{3.216}$$

or equivalently

$$\Delta H_p = (2\,\pi\,h\,\hat{\alpha}) \int_0^{R_o} \{f[x_1 + \epsilon\,\zeta, y_1 + \epsilon\,\eta, \dot{x}_1 + \epsilon\,\dot{\zeta}, \dot{y}_1 + \epsilon\,\dot{\eta}] - \tag{3.217}$$

$$f[x_1, y_1, \dot{x}_1, \dot{y}_1]\}\,dt,$$

where "dot" denotes d/dt. By using the *Taylor Series* expansion for the first term in the integrand, (3.217) becomes

$$\Delta H_p = (2\,\pi\,h\,\hat{\alpha}) \int_0^{R_o} \{f[x_1, y_1, \dot{x}_1, \dot{y}_1] + \tag{3.218}$$

68

$$\epsilon \left[\frac{\partial f}{\partial x_1} \zeta + \frac{\partial f}{\partial y_1} \eta + \frac{\partial f}{\partial \dot{x}_1} \dot{\zeta} + \frac{\partial f}{\partial \dot{y}_1} \dot{\eta} \right] + \epsilon^2 [\ldots] + \cdots - f[x_1, y_1, \dot{x}_1, \dot{y}_1] \} dt,$$

Hence (3.218) can be written as

$$\Delta H_p = (2\pi h \hat{\alpha}) \left[\epsilon \, \delta I + \frac{\epsilon^2}{2} \delta^2 I + \ldots \right], \tag{3.219}$$

where δI is the first variation given by

$$\delta I = \int_0^{Ro} \left[\frac{\partial f}{\partial x_1} \zeta + \frac{\partial f}{\partial y_1} \eta + \frac{\partial f}{\partial \dot{x}_1} \dot{\zeta} + \frac{\partial f}{\partial \dot{y}_1} \dot{\eta} \right] dt. \tag{3.220}$$

Since Λ_1 has a C^1 parametrization, $\partial f / \partial \dot{x}_1$ and $\partial f / \partial \dot{y}_1$ are differentiable with respect to t. Hence integrating by parts in (3.220) is permissible, which in turn gives

$$\delta I = \left[\frac{\partial f}{\partial \dot{x}_1} \zeta + \frac{\partial f}{\partial \dot{y}_1} \eta \right] \Big|_0^{Ro} + \tag{3.221}$$

$$\int_0^{Ro} \left\{ \left[\frac{\partial f}{\partial x_1} - \frac{d}{dt} (\frac{\partial f}{\partial \dot{x}_1}) \right] \zeta + \left[\frac{\partial f}{\partial y_1} - \frac{d}{dt} (\frac{\partial f}{\partial \dot{y}_1}) \right] \eta \right\} dt.$$

The boundary terms in (3.221) vanishes by virtue of $\zeta(0) = \eta(0) = 0$, $\zeta(R_o) = \eta(R_o) = 0$ so (3.221) reduces to

$$\delta I = \int_0^{Ro} \left\{ \left[\frac{\partial f}{\partial x_1} - \frac{d}{dt} (\frac{\partial f}{\partial \dot{x}_1}) \right] \zeta + \left[\frac{\partial f}{\partial y_1} - \frac{d}{dt} (\frac{\partial f}{\partial \dot{y}_1}) \right] \eta \right\} dt. \tag{3.222}$$

Note that the integral in (3.222) is naturally written as a sum of the two integrals associated with the different parts of the composite curve Λ_1:

$$\delta I = \int_0^{Ri} \left\{ \left[\frac{\partial f}{\partial x_1} - \frac{d}{dt} (\frac{\partial f}{\partial \dot{x}_1}) \right] \zeta + \left[\frac{\partial f}{\partial y_1} - \frac{d}{dt} (\frac{\partial f}{\partial \dot{y}_1}) \right] \eta \right\} dt. \tag{3.223}$$

$$+ \int_{Ri}^{Ro} \left\{ \left[\frac{\partial f}{\partial x_1} - \frac{d}{dt} (\frac{\partial f}{\partial \dot{x}_1}) \right] \zeta + \left[\frac{\partial f}{\partial y_1} - \frac{d}{dt} (\frac{\partial f}{\partial \dot{y}_1}) \right] \eta \right\} dt.$$

The second integral in (3.223) is identically zero as the portion of Λ_1 restricted to $[R_i, R_o]$ is the solution of the corresponding *Euler-Lagrange* equation for (3.168). Moreover since the *Lagrangian* (3.192) is independent of y, it follows that (3.223) reduces to

$$\delta I = \int_0^{Ri} \left\{ \left[\frac{\partial f}{\partial x_1} - \frac{d}{dt} (\frac{\partial f}{\partial \dot{x}_1}) \right] \zeta - \left[\frac{d}{dt} (\frac{\partial f}{\partial \dot{y}_1}) \right] \eta \right\} dt. \tag{3.224}$$

Since x_1, y_1 are given by (3.197), it follows that the integral in (3.224) simplifies to

$$\delta I = \int_0^{Ri} 2(\psi_o - \Psi_{\max}) \, \zeta(t) \, dt. \tag{3.225}$$

In view of the restriction $\zeta(t) \geq 0$, it is immediate that

$$\delta I \geq 0. \tag{3.226}$$

Consequently for a sufficiently small $\epsilon \geq 0$, the sign of ΔH_p is determined by the sign of δI which, in turn, is positive by virtue of (3.226). Thus

$$\Delta H_p = H_p[x_1(t) + \epsilon \, \zeta(t), y_1(t) + \epsilon \, \eta(t)] - H_p[x_1(t), y_1(t)] \geq 0, \tag{3.227}$$

which shows Λ_1 is a weak local minimum of (3.191). This completes the proof of Proposition 3.6.1. $\quad\Box$

We conclude this section by proving that Λ_1 is indeed an absolute minimum of (3.191) in the class of piecewise-smooth curves such that, once restricted to the interior of G, their parametrization reduces to a function $y = \tilde{f}(x)$. The importance of such a result is that if we seek minimizers of (3.168) when $\psi_o > \Psi_{\max}$ in the space of *piecewise-smooth functions* $g(R)$ then the global minimum involves a discontinuity at $R = R_i$ of magnitude $[[g]] = \psi_o - \Psi_{\max}$ such that $g(R)$ on $R_i < R \leq R_o$ is given by a vertical translate of the $\psi_o = \Psi_{\max}$ solution. The energy E_d associated with the discontinuity is given in $(3.199)_1$ and the energy E_s associated with the translation is given in $(3.199)_2$.

Proposition 3.6.2 *Let $y(x)$ be any given function $\in D^1([R_i, R_o])$ with $y(R_i) = \bar{\psi}_i$ and $y(R_o) = \psi_o$. Let $\hat{y}(x)$ be the function given by*

$$\hat{y}(x) = (\psi_o - \Psi_{\max}) + \arctan \sqrt{(\frac{x}{R_i})^4 - 1} \qquad x \in [R_i, R_o]. \tag{3.228}$$

Then

$$H_1[y(x)] - H_1[\hat{y}(x)] \geq R_i^2 \, (2 \, \pi \, h \, \hat{\alpha}) \, (\psi_o - \Psi_{\max} - \bar{\psi}_i), \tag{3.229}$$

70

where $H_1[y(x)]$ is given by (3.168) (x and $y(x)$ are used respectively instead of r and $g(r)$) and $\Psi_{\max}$ is given by (3.117).

Proof: Since the *Lagrangian* of (3.168), $F(x, y') = x\sqrt{4 + (xy')^2} - 2x$, is convex in y' for a fixed $x \in [R_i, R_o]$ it follows that

$$F(x, y') - F(x, \hat{y}') \geq \hat{F}_{,y'} (y' - \hat{y}'), \tag{3.230}$$

where

$$\hat{F}_{,y'} = F_{,y'}\Big|_{y=\hat{y}}. \tag{3.231}$$

Integrating (3.230) from R_i to R_o gives

$$\int_{R_i}^{R_o} F(x, y') - F(x, \hat{y}') \, dx \geq \int_{R_i}^{R_o} \hat{F}_{,y'} (y' - \hat{y}') \, dx, \tag{3.232}$$

whereupon

$$H_1[y(x)] - H_1[\hat{y}(x)] \geq (2\pi h\,\hat{\alpha}) \int_{R_i}^{R_o} \hat{F}_{,y'} (y' - \hat{y}') \, dx. \tag{3.233}$$

By integrating by parts from (3.233)

$$H_1[y(x)] - H_1[\hat{y}(x)] \geq (2\pi h\,\hat{\alpha})\Big\{ [\hat{F}_{,y'} (y - \hat{y})]\Big|_{R_i}^{R_o} - \tag{3.234}$$

$$\int_{R_i}^{R_o} \frac{d}{dx}[\hat{F}_{,y'}] (y - \hat{y}) \, dx\Big\}.$$

Since $\hat{y}(x)$ is the solution of the *Euler-Lagrange* equation for (3.168), $d[\hat{F}_{,y'}]/dx = 0$. Hence equation (3.234) reduces to

$$H_1[y(x)] - H_1[\hat{y}(x)] \geq (2\pi h\,\hat{\alpha}) [\hat{F}_{,y'} (y - \hat{y})]\Big|_{R_i}^{R_o}. \tag{3.235}$$

Moreover $\hat{y}(R_o) = y(R_o) = \psi_o$, so (3.235) reduces to

$$H_1[y(x)] - H_1[\hat{y}(x)] \geq -(2\pi h\,\hat{\alpha}) [\hat{F}_{,y'}\Big|_{x=R_i} (y(R_i) - \hat{y}(R_i))]. \tag{3.236}$$

71

Now $F_{,y'} = x^3y'/\sqrt{4 + (xy')^2}$ implies $\hat{F}_{,y'} = R_i^2$. Using this result in (3.236) in conjunction with the boundary values $y(R_i) = \bar{\psi}_i$ and $\hat{y}(R_i) = (\psi_o - \Psi_{\max})$, it follows that (3.236) becomes

$$H_1[y(x)] - H_1[\hat{y}(x)] \geq R_i^2 \, (2\,\pi\,h\,\hat{\alpha}) \, (\psi_o - \Psi_{\max} - \bar{\psi}_i). \tag{3.237}$$

This completes the proof of Proposition 3.6.2. $\quad\Box$

Theorem 3.6.3 *Let Λ_1 be the curve given by (3.197). Let C be any curve given by the following parametrization*

$$x(t) = \begin{cases} R_i & \text{if } t \in [0, R_i] \\[2mm] t & \text{if } t \in [R_i, R_o], \end{cases} \tag{3.238}$$

$$y(t) = \begin{cases} (\bar{\psi}_i \, t) \, / \, R_i & \text{if } t \in [0, R_i] \\[2mm] \varphi(t) & \text{if } t \in [R_i, R_o], \end{cases}$$

where $\varphi(t)$ is a piecewise-smooth function with $\varphi(R_i) = \bar{\psi}_i$ and $\varphi(R_o) = \psi_o$. Then

$$H_p[x(t), y(t)] - H_p[x_1(t), y_1(t)] \geq 0. \tag{3.239}$$

Proof: Note that

$$H_p[x(t), y(t)] = 2\,\pi\,h\,\hat{\alpha} \int_0^{R_o} f[x(t), y(t), \dot{x}(t), \dot{y}(t)] \, dt, \tag{3.240}$$

$$= 2\,\pi\,h\,\hat{\alpha} \left(\int_0^{R_i} f[x(t), y(t), \dot{x}(t), \dot{y}(t)] \, dt + \int_{R_i}^{R_o} F[x, y(x), y'(x)] \, dx \right),$$

where $F[x, y(x), y'(x)] = x\sqrt{4 + (xy')^2} - 2x$ is the nonparametric *Lagrangian*. Similarly

$$H_p[x_1(t), y_1(t)] = 2\,\pi\,h\,\hat{\alpha} \int_0^{R_i} f[x_1(t), y_1(t), \dot{x}_1(t), \dot{y}_1(t)] \, dt \tag{3.241}$$

72

$$+ 2\pi h\,\hat{\alpha} \int_{Ri}^{Ro} F[x, y_1(x), y_1'(x)]\, dx.$$

Therefore

$$H_p[x(t), y(t)] - H_p[x_1(t), y_1(t)] = \tag{3.242}$$

$$2\pi h\,\hat{\alpha} \int_0^{Ri} \{f[x, y, \dot{x}, \dot{y}] - f[x_1, y_1, \dot{x}_1, \dot{y}_1]\}\, dt +$$

$$2\pi h\,\hat{\alpha} \int_{Ri}^{Ro} \{F[x, y(x), y'(x)] - F[x, y_1(x), y_1'(x)]\}\, dx.$$

By Proposition 3.6.2, equation (3.242) gives

$$H_p[x(t), y(t)] - H_p[x_1(t), y_1(t)] \geq \tag{3.243}$$

$$2\pi h\hat{\alpha} \int_0^{Ri} f[x, y, \dot{x}, \dot{y}] - f[x_1, y_1, \dot{x}_1, \dot{y}_1]\, dt + R_i^2 2\pi h\hat{\alpha}(\psi_o - \Psi_{\max} - \bar{\psi}_i).$$

However after computing the integral in (3.243) it is found that

$$H_p[x(t), y(t)] - H_p[x_1(t), y_1(t)] \geq 2\pi h\,\hat{\alpha}\, R_i^2\, [\bar{\psi}_i - (\psi_o - \Psi_{\max})] \tag{3.244}$$

$$+ R_i^2\, 2\pi h\,\hat{\alpha}\, [(\psi_o - \Psi_{\max} - \bar{\psi}_i)],$$

or simply

$$H_p[x(t), y(t)] - H_p[x_1(t), y_1(t)] \geq 0. \tag{3.245}$$

This completes the proof of Theorem 3.6.3. □

CHAPTER 4

A More Generalized Class of

Material Models

4.1 Extended Material Model

We now extend the model in Chapter 3 along lines suggested by Pence and Tsai [22]. In particular, we consider an extended material model whose strain-energy function is given by

$$W = \frac{\alpha}{2}(I_1 - 3) + \frac{\alpha^*}{2}(I_1^* - 3) + \frac{\hat{\alpha}}{2}(\hat{I}_1 - 3), \tag{4.1}$$

where $\alpha \geq 0$, $\alpha^* \geq 0$, $\hat{\alpha} \geq 0$. The form (4.1) augments the previous form (3.6) by inclusion of the additional $I_1 - 3$ term. Our interest is in the extent to which $\alpha > 0$ gives different qualitative behavior from the $\alpha = 0$ treatment of Chapter 3. The boundary value problem for pure azimuthal shear with boundary conditions (2.17) is again the focus of study.

For the extended material (4.1) the minimization procedure again yields (3.9) where now the Cauchy stress (3.10) is given by

$$\boldsymbol{\sigma} = \alpha \mathbf{B} + \hat{\alpha} \hat{\mathbf{B}} - p \mathbf{I}. \tag{4.2}$$

In polar coordinates (3.9) again reduces to (2.14)–(2.16). The interstitial balance is still given by (3.11) namely

$$\alpha^* \, \mathbf{B} - \hat{\alpha} \, \hat{\mathbf{B}}^2 - q \, \hat{\mathbf{B}} = 0. \tag{4.3}$$

Here p is the hydrostatic pressure and q is the Lagrange multiplier associated with the constraint (3.4) and $\mathbf{B}$ is still the left Cauchy-Green tensor given by (2.12). When $\hat{\alpha} = \alpha^*$ the pure azimuthal shear problem reduces to the following first order nonlinear ordinary differential equation

$$\alpha \, r \, g' + \frac{\hat{\alpha} \, r \, g'}{\sqrt{4 + (rg')^2}} = \frac{d}{r^2}, \tag{4.4}$$

where d is an integration constant.

This result can be obtained as follows. Note from Section 6 that if $\hat{\alpha} = \alpha^*$ ($k = 1$) then $\rho = 0$ or equivalently $q = 0$. Therefore the nontrivial components of $\hat{\mathbf{B}}$ are still given by (3.109)–(3.112). The Cauchy stress tensor (4.2) can thus be expressed in terms of r and $g'(r)$. One now finds from (2.14)–(2.16) that $p = p(R)$ whereupon (2.16) is satisfied automatically and (2.14) yields (4.4). The remaining equation (2.15) then gives

$$\frac{dp}{dr} = 2 \, \hat{\alpha} \frac{d}{dr} \left(\frac{1}{\sqrt{4 + (rg')^2}} \right) - \alpha \, r \, (g')^2 - \frac{\hat{\alpha} \, r \, (g')^2}{\sqrt{4 + (rg')^2}}, \tag{4.5}$$

from which $p = p(r)$ can be computed once $g(r)$ is known.

Attention shall henceforth be restricted to this case $\hat{\alpha} = \alpha^*$. Note that (4.4) with $\alpha = 0$ and $d_1 = d/\hat{\alpha}$ retrieves (3.113) of the previous development.

Equation (4.4) when written as a polynomial in g' is quartic and hence can be solved for g'. It will be shown that if $\alpha > 0$ then equation (4.4) subject to boundary conditions (2.17) has a unique solution. Hence it is necessary to pick the correct root of the quartic polynomial. Even though it is possible to distinguish the correct root from extraneous ones, it does not seem feasible to integrate this root to get an explicit

form of $g(r)$. Therefore the solution of (4.4) subject to (2.17) will be investigated by alternate means.

Note that equation (4.4) can be written as

$$g' = \frac{1}{\alpha} \left[\frac{d}{r^3} - \frac{\hat{\alpha}\, g'}{\sqrt{4 + (rg')^2}} \right], \tag{4.6}$$

or equivalently

$$g(r) = g(R_i) + \frac{1}{\alpha} \int_{R_i}^r \frac{d}{\xi^3}\, d\xi - \frac{\hat{\alpha}}{\alpha} \int_{R_i}^r \frac{g'(\xi)}{\sqrt{4 + (\xi\, g'(\xi))^2}}\, d\xi. \tag{4.7}$$

By integrating the first integral in (4.7) and using the first boundary condition in (2.17), $g(R_i) = \psi_i$, equation (4.7) can be written as

$$g(r) = \psi_i + \frac{d}{\alpha} \frac{r^2 - R_i^2}{2\, R_i^2\, r^2} - \frac{\hat{\alpha}}{\alpha} \int_{R_i}^r F(\xi, g'(\xi))\, d\xi, \tag{4.8}$$

where

$$F(\xi, g'(\xi)) = \frac{g'(\xi)}{\sqrt{4 + (\xi\, g'(\xi))^2}}. \tag{4.9}$$

By using the other boundary condition in (2.17), $g(R_o) = \psi_o$, the constant d can be computed as

$$d = (\psi_o - \psi_i) \frac{2\, \alpha\, R_i^2\, R_o^2}{R_o^2 - R_i^2} + \frac{2\, \hat{\alpha}\, R_i^2\, R_o^2}{R_o^2 - R_i^2} \int_{Ri}^{Ro} F(\xi, g'(\xi))\, d\xi. \tag{4.10}$$

Therefore boundary value problem (4.4), (2.17) is equivalent to the following integral equation

$$g(r) = \psi_i + (\psi_o - \psi_i)\, P(r) +$$

$$\frac{\hat{\alpha}}{\alpha}\, (P(r) - 1) \int_{R_i}^r F(\xi, g'(\xi))\, d\xi + \frac{\hat{\alpha}}{\alpha}\, P(r) \int_r^{R_o} F(\xi, g'(\xi))\, d\xi, \tag{4.11}$$

where

$$P(r) = \frac{R_o^2\, (r^2 - R_i^2)}{(R_o^2 - R_i^2)\, r^2}. \tag{4.12}$$

76

By introducing

$$\bar{H}(r,\xi) = \begin{cases} P(r) - 1 & R_i \le \xi \le r \le R_o \\ P(r) & R_i \le r \le \xi \le R_o, \end{cases}$$
(4.13)

the integral equation (4.11) can be written in a more compact form

$$g(r) = \psi_i + (\psi_o - \psi_i)\, P(r) + \frac{\hat{\alpha}}{\alpha} \int_{Ri}^{Ro} \bar{H}(r,\xi)\, F(\xi, g'(\xi))\, d\xi.$$
(4.14)

The boundary value problem, (4.4), (2.17) is usually called the *first boundary value problem* (the value of the unknown function is prescribed at each end of the interval).

The *second boundary value problem* is a boundary value problem for which the value of the unknown function is prescribed at one end point and the slope is prescribed at the other end point. For latter purposes we will define the following second boundary value problems: Find a solution of (4.4) either subject to

$$g(R_i) = \psi_i, \quad g'(R_o) = m_o,$$
(4.15)

or else subject to

$$g'(R_i) = m_i, \quad g(R_o) = \psi_o.$$
(4.16)

Integral equation (4.8) also follows for the second boundary value problem (4.4), (4.15). However the constant d in (4.8) is now determined from the latter boundary condition in (4.15). By setting $g'(R_o) = m_0$ in (4.6) and solving for d it is found that

$$d = \alpha\, m_o\, R_o^3 + \frac{\hat{\alpha}\, m_o\, R_o^3}{\sqrt{4 + R_o^2\, m_o^2}}.$$
(4.17)

Consequently the second boundary value problem (4.4), (4.15) is equivalent to the following integral equation

$$g(r) = \psi_i + \left[m_o\, R_o^3 + \frac{\hat{\alpha}\, m_o\, R_o^3}{\alpha\, \sqrt{4 + R_o^2\, m_o^2}} \right] \frac{r^2 - R_i^2}{2\, R_i^2\, r^2}$$
(4.18)

$$- \frac{\hat{\alpha}}{\alpha} \int_{R_i}^{r} F(\xi, g'(\xi))\, d\xi,$$

where $F(\xi, g'(\xi))$ is still given by (4.9). Alternatively this second boundary value problem is equivalent to the initial value problem for

$$\alpha\, r\, g' + \frac{\hat{\alpha}\, r\, g'}{\sqrt{4 + (rg')^2}} = \frac{1}{r^2}\left(\alpha\, m_o\, R_o^3 + \frac{\hat{\alpha}\, m_o\, R_o^3}{\sqrt{4 + R_o^2\, m_o^2}}\right), \tag{4.19}$$

with initial condition

$$g(R_i) = \psi_i. \tag{4.20}$$

By a similar development the second boundary value problem (4.4), (4.16) gives

$$d = \alpha\, m_i\, R_i^3 + \frac{\hat{\alpha}\, m_i\, R_i^3}{\sqrt{4 + R_i^2\, m_i^2}} \tag{4.21}$$

and integral equation

$$g(r) = \psi_o - \left[m_i\, R_i^3 + \frac{\hat{\alpha}\, m_i\, R_i^3}{\alpha\, \sqrt{4 + R_i^2\, m_i^2}}\right]\frac{R_o^2 - r^2}{2\, R_o^2\, r^2} \tag{4.22}$$

$$+\frac{\hat{\alpha}}{\alpha}\int_r^{R_o} F(\xi, g'(\xi))\, d\xi.$$

The corresponding initial value problem is

$$\alpha\, r\, g' + \frac{\hat{\alpha}\, r\, g'}{\sqrt{4 + (rg')^2}} = \frac{1}{r^2}\left(\alpha\, m_i\, R_i^3 + \frac{\hat{\alpha}\, m_i\, R_i^3}{\sqrt{4 + R_i^2\, m_i^2}}\right), \tag{4.23}$$

subject to the initial condition

$$g(R_o) = \psi_o. \tag{4.24}$$

4.2   Existence and Uniqueness for the Extended Model

In this section it will be proven that the first order boundary value problem (4.4), (2.17) has a unique smooth solution on $[R_i, R_o]$ for every $0 < R_i < R_o < \infty$ whenever $\alpha > 0$.

Since it is more convenient to deal with integrals than derivatives, we will use the integral equation form (4.8) of the first boundary value problem (4.4), (2.17). Then the principle of contraction mapping will be used to prove existence and uniqueness.

Let S be a normed linear space with the norm denoted by $\|.\|$. A sequence of elements y_n of S is a Cauchy sequence if for every $\epsilon > 0$, there exist N such that $\|y_n - y_m\| < \epsilon$ whenever $n, m > N$. S is a complete space if every Cauchy sequence in S converges to a limit element in S.

An operator T mapping a normed space S into itself is said to be a contraction mapping on the space if there is a number λ, $0 < \lambda < 1$, such that for all $x, y \in S$

$$\|Tx - Ty\| \leq \lambda \|x - y\|. \tag{4.25}$$

The following theorem is well-known.

Theorem 4.2.1 *Principle of Contraction Mappings: Every contraction mapping T defined on a complete normed linear space S has one and only one fixed point (i.e., $y = Ty$ has exactly one solution). For any point $y_0 \in S$, the sequence of iterates $y_n = Ty_{n-1} = \cdots = T^n y_0$ converges to the fixed point y and*

$$\|y_n - y\| \leq \frac{\lambda^n}{1 - \lambda} \|y_1 - y_0\|. \tag{4.26}$$

Proof: See [4], page 26. $\square$

Lemma 4.2.2 *If*

$$\max \left\{ \frac{\hat{\alpha}}{2\,\alpha} (R_o - R_i)^2, \frac{\hat{\alpha}}{\alpha} \frac{(R_o - R_i)^2}{R_i} \right\} < 1, \tag{4.27}$$

then the first boundary value problem (4.4), (2.17) has one and only one solution.

Proof: Let S_0 be the space of continuously differentiable functions on $[R_i, R_o]$ with the norm

$$\|g(r)\| = \max \left\{ \max_{R_i \leq r \leq R_o} |g(r)|, \max_{R_i \leq r \leq R_o} \frac{|g'(r)|}{z(r)} \right\}, \qquad (4.28)$$

where $z(r)$ is the positive weight function given by

$$z(r) = \frac{R_o^2 - R_i^2}{r^2}. \qquad (4.29)$$

The space S_0 is complete with this norm, and convergence of a sequence $g_n(r)$ in this norm to $g(r)$ implies that $g(r)$ is continuously differentiable and that $g_n(r) \to g(r)$ and $g_n'(r) \to g'(r)$ uniformly.

Let $\bar{T}$ be the operator defined by the right side of (4.14). Observe that

$$\frac{d}{dr} \bar{T} g(r) = (\psi_o - \psi_i) P'(r) + \frac{\hat{\alpha}}{\alpha} \int_{R_i}^{R_o} \bar{H}_r(r, \xi) F(\xi, g'(\xi)) \, d\xi, \qquad (4.30)$$

where $\bar{H}_r(r, \xi) = \partial \bar{H} / \partial r$. Since $P'(r)$, $g'(r)$ and $\bar{H}_r(r, \xi)$ are continuous functions in r, the derivative of $\bar{T} g(r)$ with respect to r as given in (4.30) is continuous in r. Thus $\bar{T}$ maps S_0 into S_0.

To see when $\bar{T}$ is a contraction mapping consider

$$\bar{T} g_1(r) - \bar{T} g_2(r) = \frac{\hat{\alpha}}{\alpha} \int_{R_i}^{R_o} \bar{H}(r, \xi) \left(F(\xi, g_1'(\xi)) - F(\xi, g_2'(\xi)) \right) d\xi. \qquad (4.31)$$

Hence

$$|\bar{T} g_1(r) - \bar{T} g_2(r)| \leq \frac{\hat{\alpha}}{\alpha} \int_{R_i}^{R_o} |\bar{H}(r, \xi)| \, |F(\xi, g_1'(\xi)) - F(\xi, g_2'(\xi))| \, d\xi. \qquad (4.32)$$

Since $F(\xi, g'(\xi))$ is Lipshitz in g' with Lipshitz constant $1/2$, inequality (4.32) gives

$$|\bar{T} g_1(r) - \bar{T} g_2(r)| \leq \frac{\hat{\alpha}}{\alpha} \int_{R_i}^{R_o} |\bar{H}(r, \xi)| \, \frac{1}{2} |g_1'(\xi) - g_2'(\xi)| \, d\xi, \qquad (4.33)$$

which implies that

$$|\bar{T} g_1(r) - \bar{T} g_2(r)| \leq \frac{\hat{\alpha}}{2\,\alpha} \|g_1(r) - g_2(r)\| \int_{R_i}^{R_o} z(\xi) \, |\bar{H}(r, \xi)| \, d\xi. \qquad (4.34)$$

Since $0 \leq P(r) \leq 1$, it is clear that $|\bar{H}(r,\xi)| \leq 1$ for every $r \in [R_i, R_o]$. Therefore inequality (4.34) provides

$$|\bar{T}g_1(r) - \bar{T}g_2(r)| \leq \frac{\hat{\alpha}}{2\,\alpha} \int_{R_i}^{R_o} z(\xi)\,d\xi \ \|g_1(r) - g_2(r)\|. \tag{4.35}$$

Computing the integral in equation (4.35) gives

$$|\bar{T}g_1(r) - \bar{T}g_2(r)| \leq \frac{\hat{\alpha}}{2\,\alpha} \,(R_o - R_i)^2 \ \|g_1(r) - g_2(r)\|. \tag{4.36}$$

Similarly it can be shown that

$$\frac{1}{z(r)} \left| \frac{d}{dr} \{\bar{T}g_1(r) - \bar{T}g_2(r)\} \right| \leq$$

$$\frac{1}{z(r)} \frac{\hat{\alpha}}{2\alpha} \int_{R_i}^{R_o} z(\xi)\,|\bar{H}_r(r,\xi)|\,d\xi \ \|g_1(r) - g_2(r)\|, \tag{4.37}$$

and by using (4.13) it is clear that

$$|\bar{H}_r(r,\xi)| \leq \frac{2\,R_o^2}{R_i\,(R_o^2 - R_i^2)}, \tag{4.38}$$

for every $r \in [R_i, R_o]$. Thus

$$\frac{1}{z(r)} \left| \frac{d}{dr} \{\bar{T}g_1(r) - \bar{T}g_2(r)\} \right| \leq$$

$$\frac{1}{z(r)} \frac{\hat{\alpha}}{\alpha} \frac{R_o^2}{R_i\,(R_o^2 - R_i^2)} \int_{R_i}^{R_o} z(\xi)\,d\xi \ \|g_1(r) - g_2(r)\|. \tag{4.39}$$

Computing the integral in (4.39) gives

$$\frac{1}{z(r)} \left| \frac{d}{dr} \{\bar{T}g_1(r) - \bar{T}g_2(r)\} \right| \leq \frac{1}{z(r)} \frac{\hat{\alpha}}{\alpha} \frac{R_o^2(R_o - R_i)^2}{R_i\,(R_o^2 - R_i^2)} \|g_1(r) - g_2(r)\|. \tag{4.40}$$

After simplification equation (4.40) becomes

$$\frac{1}{z(r)} \left| \frac{d}{dr} \{\bar{T}g_1(r) - \bar{T}g_2(r)\} \right| \leq \frac{1}{z(r)} \frac{\hat{\alpha}}{\alpha} \frac{R_o^2(R_o - R_i)}{R_i\,(R_o + R_i)} \|g_1(r) - g_2(r)\|. \tag{4.41}$$

Note that

$$\max_{R_i \leq r \leq R_o} \left\{ \frac{1}{z(r)} \right\} = \frac{R_o^2 - R_i^2}{R_o^2}. \tag{4.42}$$

81

Consequently (4.28), (4.36), (4.41) and (4.42) together give

$$\|\bar{T}g_1(r) - \bar{T}g_2(r)\| \leq \qquad\qquad\qquad\qquad (4.43)$$

$$\max\left\{\frac{\hat{\alpha}}{2\alpha}(R_o - R_i)^2, \frac{\hat{\alpha}}{\alpha}\frac{(R_o - R_i)^2}{R_i}\right\} \ \|g_1(r) - g_2(r)\|.$$

Hence, if

$$M = \max\left\{\frac{\hat{\alpha}}{2\,\alpha}\,(R_o - R_i)^2, \frac{\hat{\alpha}}{\alpha}\,\frac{(R_o - R_i)^2}{R_i}\right\} < 1 \qquad\qquad (4.44)$$

then $\bar{T}$ is a contraction mapping on S_0. This completes the proof of Lemma 4.2.2.
□

The inequality (4.27) provides a restriction that can be interpreted in various ways. For example if $\hat{\alpha} > 0$, $R_o > R_i > 0$ are given then (4.27) requires sufficiently large positive α. Alternatively if $\alpha > 0$, $\hat{\alpha} > 0$, $R_i > 0$ are given then (4.27) requires that R_o is sufficiently close to R_i. It can also be shown upon modifying the norm (4.28) with a different positive weight function that it is possible to weaken the inequality (4.27) thereby making the result less restrictive. However such modification does not seem to give an existence and uniqueness result that applies to arbitrary $\alpha > 0$, $\hat{\alpha} > 0$, $R_o > R_i > 0$. As we now show, such a result is obtainable by bootstrapping the result with a development that first obtains an existence and uniqueness result for the second boundary value problem.

Theorem 4.2.3 *The Second boundary value problem, (4.4), (4.15) has a unique solution on $[R_i, R_o]$ for every $R_o > R_i > 0$.*

Proof: Recall that the second boundary value problem (4.4), (4.15) is equivalent to initial value problem (4.19), (4.20). Let $\bar{\alpha} = \alpha/\hat{\alpha}$ and $\bar{d} = d/\hat{\alpha}$. Then (4.19) is

$$\bar{\alpha}\,g' + \frac{g'}{\sqrt{4 + (rg')^2}} = \frac{\bar{d}}{r^3}, \qquad\qquad (4.45)$$

where $\bar{d}$ follows from (4.17).

Let

$$H(r, g(r), g'(r)) = \bar{\alpha} \, g' + \frac{g'}{\sqrt{4 + (rg')^2}} - \frac{\bar{d}}{r^3}. \tag{4.46}$$

Then initial value problem (4.19), (4.20) is equivalent to following initial value problem

$$H(r, g(r), g'(r)) = 0, \qquad g(R_i) = \psi_i. \tag{4.47}$$

Let $U = (0, \infty) \times (-\infty, \infty) \times (-\infty, \infty)$. Clearly U is an open convex region of the three dimensional Euclidean-space and H is defined and continuous on U. Moreover $\partial H / \partial g$ and $\partial H / \partial g'$ exist and are continuous on U. Additionally $H(R_i, g(R_i), g'(R_i)) = 0$ has a solution in U and the Jacobian $J = \partial H / \partial g'$ is not equal to zero at this point. Hence by the existence and uniqueness theorem for implicitly defined initial value problems (for example [20] pages 44-47) there is an interval containing R_i such that the initial value problem (4.47) has a unique solution on this interval.

Let the maximal solution domain for $g(r)$ be the interval (a, b). Clearly $R_i \in (a, b)$. It will now be established that $b \geq R_o$ by showing that the alternative assumption $b < R_o$ leads to a contradiction.

Note that (4.45) can be written as

$$g' = \frac{1}{\bar{\alpha}} (\frac{\bar{d}}{r^3} - \frac{g'}{\sqrt{4 + (rg')^2}}). \tag{4.48}$$

Integrating (4.48) from R_i to r provides

$$g(r) = g(R_i) + \frac{1}{\bar{\alpha}} \int_{R_i}^{r} (\frac{\bar{d}}{s^3} - \frac{g'(s)}{\sqrt{4 + (sg'(s))^2}}) \, ds. \tag{4.49}$$

Let R_1 and R_2 be any two numbers with $a < R_i < R_1 < R_2 < b$. Then

$$g(R_2) - g(R_1) = \frac{1}{\bar{\alpha}} \int_{R_1}^{R_2} (\frac{\bar{d}}{s^3} - \frac{g'(s)}{\sqrt{4 + (sg'(s))^2}}) \, ds. \tag{4.50}$$

83

Since

$$|\frac{\bar{d}}{r^3} - \frac{g'(r)}{\sqrt{4 + (rg'(r))^2}}| \leq |\frac{\bar{d}}{r^3}| + |\frac{g'(r)}{\sqrt{4 + (rg'(r))^2}}| \leq \frac{\bar{d}}{R_i^3} + \frac{1}{R_i} \qquad (4.51)$$

equation (4.50) implies that

$$|g(R_2) - g(R_1)| \leq (\frac{\bar{d}}{R_i^3} + \frac{1}{R_i})\frac{1}{\bar{\alpha}}|R_2 - R_1|. \qquad (4.52)$$

Assume that b is finite. Since $\bar{\alpha} > 0$, values of $g(r)$ for r near b and less than b satisfy a Cauchy condition and thus there exists $\lim_{r \to b} g(r)$. Call this limit g_b and let $g_{\text{new}}(r)$ be a solution of the initial value problem

$$H(r, g(r), g'(r)) = 0, \quad g(b) = g_b. \qquad (4.53)$$

Since H is independent of $g(r)$, it satisfies a global Lipschitz condition in g. Therefore the solution $g_{\text{new}}(r)$ is an extension of $g(r)$. Since the domain of this extension contains b, the domain (a, b) is not maximal. This contradiction comes from the assumption $b < R_o$. Hence the maximal solution domain for $g(r)$ can be extended to any $R_o < \infty$. Of course this means that the second boundary value problem, (4.4), (4.15) has a unique solution on $[R_i, R_o]$ for every $R_o > R_i > 0$. This completes the proof of Theorem 4.2.3. $\square$

Note that an alternative proof of the above theorem is presented in Appendix B. Similarly it can be shown that

Theorem 4.2.4 *The Second boundary value problem, (4.4), (4.16) has a unique solution on $[R_i, R_o]$ for every $R_o > R_i > 0$.*

To get the main result of this section, the following standard result from the theory of ordinary differential equations will be now utilized.

Theorem 4.2.5 *Uniqueness and Continuability of Solutions of Initial Value Problems: Consider the following initial value problem*

$$y''(t) + f(t, y(t), y'(t)) = 0, \tag{4.54}$$

$$y(t_0) = y_0, \tag{4.55}$$

$$y'(t_0) = y_0'. \tag{4.56}$$

If $f(t, y(t), y'(t))$ is continuous and satisfies a Lipschitz condition in a domain D which contains the point (t_0, y_0, y_0') then there is only one solution of (4.54), (4.55), (4.56). Furthermore, this solution can be uniquely continued arbitrarily close to the boundary of D.

Proof: See [4], page 10. □

Theorem 4.2.6 *The second order nonlinear boundary value problem (4.4), (2.17) has a unique solution on $[R_i, R_o]$ for every $0 < R_i < R_o < \infty$.*

Proof: According to Lemma 4.2.2 there is some finite length Δ such that all first boundary value problems for (4.4) on any interval of length less than Δ has a unique solution. Let n be an integer such that $(R_i - R_o)/2^n = \bar{\Delta} < \Delta$. Divide the interval $[R_i, R_o]$ into 2^n equal subintervals. Then by Lemma 4.2.2 on each subinterval all first boundary value problems for (4.4) have unique solutions. Now if it can be shown that first boundary value problem for (4.4) has a unique solution on an interval whose length is $2\bar{\Delta}$ then the same argument can be repeated for intervals whose length are $4\bar{\Delta}$, $8\bar{\Delta}$, etc. until $2^n \bar{\Delta} = (R_i - R_o)$. This in turn would establish that the first boundary value problem (4.4) has a unique solution on the interval $[R_i, R_o]$. Without

loss of generality we may assume that $n = 1$. Let R_m be the midpoint of the interval $[R_i, R_o]$. Then by Theorem 4.2.3 the second boundary value problem (4.4) subject to

$$g(R_i) = \psi_i, \quad g'(R_m) = m \tag{4.57}$$

has a unique solution. Moreover by Theorem 4.2.4 the second boundary value problem (4.4) subject to

$$g'(R_m) = m, \quad g(R_o) = \psi_o \tag{4.58}$$

also has a unique solution. To continue the proof of Theorem 4.2.6 we now consider the following claim

Claim 4.2.7 The solution $g_l(r, m)$ of (4.4), (4.57) and its derivative $g_l'(r, m) = \partial g_l / \partial r(r, m)$ are each strictly increasing in m. Namely, if $m_2 > m_1$, then

$$g_l'(r, m_2) > g_l'(r, m_1) \tag{4.59}$$

on $[R_i, R_m]$ and

$$g_l(r, m_2) > g_l(r, m_1) \tag{4.60}$$

on $(R_i, R_m]$.

Proof of Claim 4.2.7: Suppose $m_2 > m_1$. Clearly (4.59) is true for those $r \in (R_i, R_m]$ and sufficiently close to R_m. If

$$g_l'(R_n, m_2) = g_l'(R_n, m_1) \tag{4.61}$$

for some $R_n \in (R_i, R_m]$, then the second boundary value problem (4.4) subject to

$$g(R_i) = \psi_i, \quad g'(R_n) = g_l'(R_n, m_2) \tag{4.62}$$

has a unique solution by Theorem 4.2.3. This implies that $g_l(r, m_1) \equiv g_l(r, m_2)$ for every $r \in [R_i, R_n]$. Moreover since $f(r, g')$ is Lipshitz, then every initial value problem has a unique solution by the Theorem 4.2.5. Therefore $g_l(r, m_1) \equiv g_l(r, m_2)$

for every $r \in [R_n, R_m]$. In other words, branching of the solution at $r = R_n$ is not possible. Hence $g_l(r, m_1) \equiv g_l(r, m_2)$ for every $r \in [R_i, R_m]$. But this implies that $m_2 = g'_l(r, m_2) = g'_l(r, m_1) = m_1$ contrary to the assumption $m_2 > m_1$. Thus $g'_l(r, m)$ is a strictly increasing function in m. Moreover since $g_l(R_i, m_1) = g_l(R_i, m_2) = \psi_i$ and $g'_l(r, m_2) > g'_l(r, m_1)$ on $[R_i, R_m]$, we have $g_l(r, m)$ is also an increasing function in m for every $r \in (R_i, R_m]$. This completes the proof of Claim 4.2.7. $\square$

The proof of Theorem 4.2.6 now continues. It similarly can be shown that the solution $g_r(r, m)$ of (4.4), (4.58) and its derivative $g'_r(r, m)$ are respectively decreasing and increasing functions of m.

In particular $g_l(R_m, m)$ is an increasing function of m and $g_r(R_m, m)$ is a decreasing function of m. Since $g_l(r, m)$ and $g_r(r, m)$ are monotone functions of m without jump discontinuities, they are continuous in m on $[R_i, R_m]$ and $[R_m, R_o]$ respectively. Therefore every first boundary value problem (4.4) subject to

$$g(R_i) = \psi_i, \quad g(R_m) = \psi_m \tag{4.63}$$

and every first boundary value problem (4.4) subject to

$$g(R_m) = \psi_m, \quad g(R_o) = \psi_o \tag{4.64}$$

have continuous solutions in m. To continue the proof of Theorem 4.2.6 we now establish the following claim

Claim 4.2.8 If every first boundary value problem (4.4), (4.63) and every first boundary problem (4.4), (4.64) have continuous solutions in m, then these solutions both map the real line R onto itself.

Proof of Claim 4.2.8: Let $g_l(R_m, m)$ and $g_r(R_m, m)$ be the solutions of first boundary value problems (4.4), (4.63) and (4.4), (4.64) respectively. Consider the map $h : R \to R$ defined by $m \to g_l(R_m, m)$. Let ψ be any real number. To show surjectivity we need to show that there exists $m \in R$ such that $h(m) = g_l(R_m, m) =$

ψ. Since the first boundary value problem (4.4) subject to $g(R_i) = \psi_i$, $g(R_m) = \psi$ has a unique solution let m be the value of the derivative at R_m. For such an m it is clear that $h(m) = g_l(R_m, m) = \psi$. Therefore $h(m) = g_l(R_m, m)$ is onto. Similarly $g_r(R_m, m)$ is onto. This completes the proof of Claim 4.2.8. $\square$

The proof of Theorem 4.2.6 now continues. As a result of Claim 4.2.8, there must be exactly one number m_o for which

$$g_l(R_m, m_o) = g_r(R_m, m_o). \tag{4.65}$$

By definition

$$g_l'(R_m, m_o) = m_o = g_r'(R_m, m_o). \tag{4.66}$$

For $m = m_o$, the function $g(r)$ defined by

$$g(r) = \begin{cases} g_l(r, m) & r \in [R_i, R_m] \\ g_r(r, m) & r \in [R_m, R_o] \end{cases} \tag{4.67}$$

has a continuous derivative at $r = R_m$. Hence it is the only solution of the nonlinear boundary value problem (4.4), (2.17). This completes the proof of Theorem 4.2.6. $\square$

Theorem 4.2.6 establishes the existence of a unique classically smooth solution for the pure azimuthal shear problem in the extended material model ($\alpha > 0$, $\hat{\alpha} = \alpha^* > 0$) for all R_i, R_o, ψ_i, ψ_o. This contrasts with the lack of a classically smooth solution in the precursor model ($\alpha = 0$, $\hat{\alpha} = \alpha^* > 0$) whenever

$$|\psi_o - \psi_i| > \Psi_{\max} = \arccos(\frac{R_i^2}{R_o^2}). \tag{4.68}$$

Recall that in this case we found that a portion of the deformation localized at $R = R_i$. Thus the expectation for the extended theory is that $\alpha \to 0$ should in some sense retrieve the localized deformation studied in Section 3.4, suggesting a boundary layer type phenomena for sufficiently small $\alpha > 0$ whenever $|\psi_o - \psi_i|$ becomes sufficiently large.

4.3 Numerical Solution for the Extended Model

In this section we present a numerical solution procedure for the pure azimuthal shear problem in the extended material model. Note that for a fixed $\hat{\alpha} > 0$ the pure azimuthal shear problem is governed by (4.4) and boundary conditions are still given by (2.17). Note also that for a fixed $\hat{\alpha} > 0$ (4.4) can be written as

$$\bar{\alpha}\, r^3\, g' + \frac{r^3\, g'}{\sqrt{4 + (rg')^2}} = \bar{d}, \tag{4.69}$$

where

$$\bar{\alpha} = \alpha/\hat{\alpha}, \quad \bar{d} = d/\hat{\alpha}. \tag{4.70}$$

Differentiating (4.69) to eliminate $\bar{d}$ gives

$$g''(r) + f(r, g'(r), \bar{\alpha}) = 0, \tag{4.71}$$

where

$$f(r, g', \bar{\alpha}) = \frac{g'}{r} \left[3 + \frac{2\, r^2\, g'^2}{4 + \bar{\alpha}\, [4 + r^2\, g'^2\,]^{3/2}} \right]. \tag{4.72}$$

For a given $\bar{\alpha}$ the numerical solution of (4.71) subject to (2.17) can be found by various "shooting", "parallel shooting", "collocation" or "finite-difference" methods [16], [17]. Here we employ the finite-difference method to numerically solve (4.71) subject to (2.17).

Let $R_i = r_0 < r_1 < \cdots < r_{n-1} < r_n = R_o$ be an equally spaced partition of the interval $[R_i, R_o]$. The derivatives in (4.71) are replaced by suitably chosen difference quotients defined in terms of the points r_j. A typical choice is to use the *centered difference* approximations

$$g'(r_j) \approx \frac{g(r_{j+1}) - g(r_{j-1})}{2h}, \tag{4.73}$$

$$g''(r_j) \approx \frac{g(r_{j+1}) - 2\, g(r_j) + g(r_{j-1})}{h^2}. \tag{4.74}$$

When these approximations are used in (4.71), we obtain a system of equations of the form

$$\frac{g(r_{j+1}) - 2\,g(r_j) + g(r_{j-1})}{h^2} = f(r_j, \frac{g(r_{j+1}) - g(r_{j-1})}{2h}). \qquad (4.75)$$

for $j = 1, 2, \ldots, n-1$ where $g(r_0) = \psi_i, \ g(r_n) = \psi_o$.

In (4.75) the quantities $g(r_1), g(r_2), \ldots, g(r_{n-1})$ are unknown since any solution $g(r)$ of (4.71) will probably not satisfy (4.75) exactly. We think of the system (4.75) as an approximation to the equation in (4.71) and hope that for a sufficiently small spacing, $h = (R_o - R_i)/n$, the solutions $g(r_j)$ of (4.75) are good approximations to the exact values of $g(r_j)$.

Since the function $f(r, g', \bar{\alpha})$ is nonlinear in g', we are faced with solving a nonlinear system of $n-1$ equations in $n-1$ unknowns. Newton's method for several variables can be used to determine $g(r_1), g(r_2), \ldots, g(r_{n-1})$. Note that Newton's method applied to (4.75) takes the form

$$\mathbf{G}_{k+1} = \mathbf{G}_k - \mathbf{J}(\mathbf{G}_k)^{-1}\mathbf{P}(\mathbf{G}_k) \qquad (4.76)$$

where $\mathbf{G}_k = [g^{(k)}(r_1), g^{(k)}(r_2), \ldots, g^{(k)}(r_{n-1})]^T$ and where the jth component of the vector function $\mathbf{P}(\mathbf{G})$ is given by

$$P_j(\mathbf{G}) = g(r_{j+1}) - 2\,g(r_j) + g(r_{j-1}) - h^2 \ f\Big(r_j, \frac{g(r_{j+1}) - g(r_{j-1})}{2h}\Big). \qquad (4.77)$$

Since $\partial P_j / \partial g(r_l)$ is zero except for $l = j-1, j, j+1$, the $(n-1) \times (n-1)$ Jacobian Matrix $\mathbf{J}(\mathbf{G}_k)$ is tridiagonal; and it is relatively easy to apply Newton's method to (4.75) even for large n. The starting vector $\mathbf{G}_0$ could have components obtained by a linear interpolation of the boundary conditions:

$$g^{(0)}(r_j) = \frac{r_j - R_i}{R_o - R_i} \ \psi_o + \frac{R_o - r_j}{R_o - R_i} \ \psi_i, \quad 1 \leq j \leq n-1. \qquad (4.78)$$

There are several programs to solve boundary value problems based on finite-difference method. MATLAB's *bvp4c* is one such program and it is well explained in

90

Figure 4.1: Numerical solution when $R_i = 1$, $R_o = 4$, $\psi_i = 0$ and $\psi_o = 0.452478$ for three values of $\bar{\alpha}$, $\bar{\alpha} = 0.1, 0.01, 0.001$. Here $|\psi_o - \psi_i| = 0.3\Psi_{max}$

[25]. MATLAB's $bvp4c$ is utilized to solve (4.75) subject to (2.17) for several values of $\bar{\alpha}$. The specific problem that we consider involves $R_i = 1$, $R_o = 4$, $\psi_i = 0$ whereupon we consider the effect of increasing ψ_o for various $\bar{\alpha} > 0$. The limit $\bar{\alpha} \to 0$ should then retrieve the results of Chapter 3 wherein we recall that $\Psi_{max} \approx 1.50826$ for a geometry with $R_o = 4R_i$.

In the first case we investigate the solution of (4.75) when $R_i = 1$, $R_o = 4$, $\psi_i = 0$ and $\psi_o = 0.452478$. Values $\bar{\alpha} = 0.1$, $\bar{\alpha} = 0.01$ and $\bar{\alpha} = 0.001$ are used in Figure 4.1 and corresponding graphs are depicted by dotted, dashed and solid lines respectively. Note that $\psi_o - \psi_i = 0.452478 \ll \Psi_{max} = 1.50826$. In this case the three graphs are almost identical.

In the second case we investigate the solution of (4.75) when $R_i = 1$, $R_o = 4$, $\psi_i = 0$ and $\psi_o = 1.5$. Note that $\Psi_{max} \approx 1.50826$ when $R_i = 1$ and $R_o = 4$. Hence for this case $\psi_o \approx \Psi_{max}$. $\bar{\alpha} = 0.1$, $\bar{\alpha} = 0.01$ and $\bar{\alpha} = 0.001$ are used in Figure 4.2 and the corresponding graphs are depicted by dotted, dashed and solid lines respectively.

Figure 4.2: Numerical solution when $R_i = 1$, $R_o = 4$, $\psi_i = 0$ and $\psi_o = 1.5$ for three values of $\bar{\alpha}$, $\bar{\alpha} = 0.1, 0.01, 0.001$. Here $|\psi_o - \psi_i| = 0.995\Psi_{max}$

As $\bar{\alpha}$ tends to zero we observe that graph of the $g(R)$ moves upward meaning that smaller $\bar{\alpha}$ gives rise to more angular displacement on the interior $R_i < R < R_o$.

In the third case we investigate the solution of (4.75) when $R_i = 1$, $R_o = 4$, $\psi_i = 0$ and $\psi_o = 3$. Values $\bar{\alpha} = 0.1$, $\bar{\alpha} = 0.01$ and $\bar{\alpha} = 0.001$ are used in Figure 4.3 and corresponding graphs are depicted by dotted, dashed and solid lines respectively. Note that $\psi_o - \psi_i = 3 > \Psi_{max} = 1.50826$. Hence for this case $\psi_o > \Psi_{max}$. As suggested by the previous material model, $\bar{\alpha} = 0$, the graph of $g(R)$ converges to a vertical line segment near $r = R_i$ as $\bar{\alpha} \to 0$.

In Figure 4.4 the previous three graphs are superimposed. For $\psi_o > \Psi_{max}$, as suggested by previous material model, $\bar{\alpha} = 0$, the graph of $g(R)$ converges to a vertical line segment near $r = R_i$ as $\bar{\alpha} \to 0$.
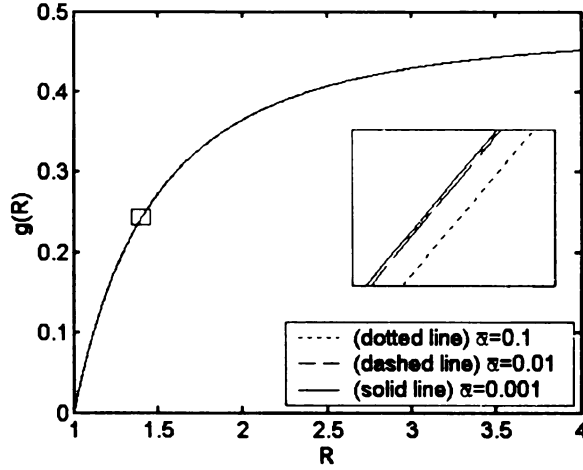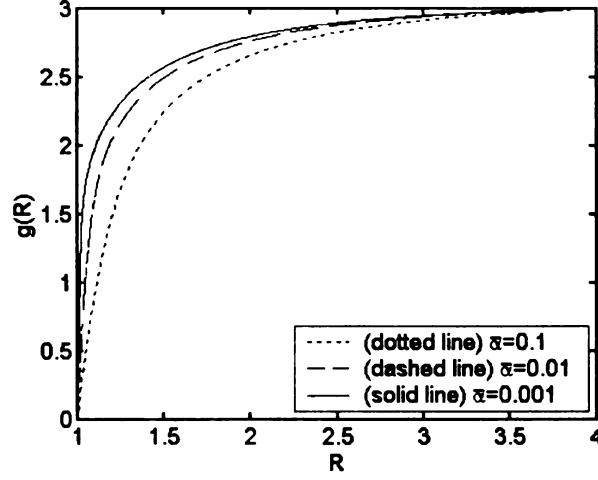
Figure 4.3: Numerical solution when $R_i = 1$, $R_o = 4$, $\psi_i = 0$ and $\psi_o = 3$ for three values of $\bar{\alpha}$, $\bar{\alpha} = 0.1, 0.01, 0.001$. Here $|\psi_o - \psi_i| = 1.989\Psi_{max}$
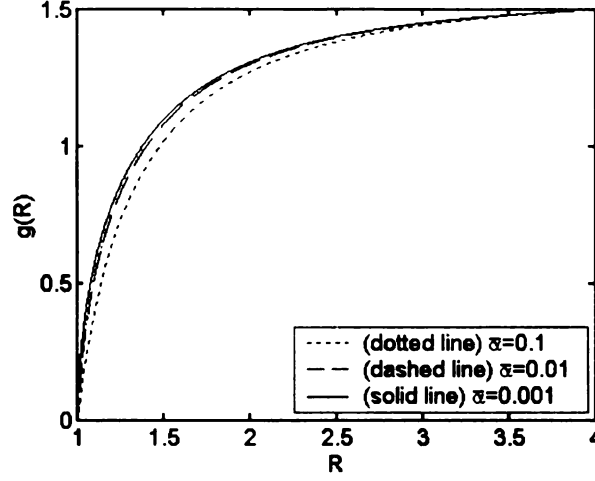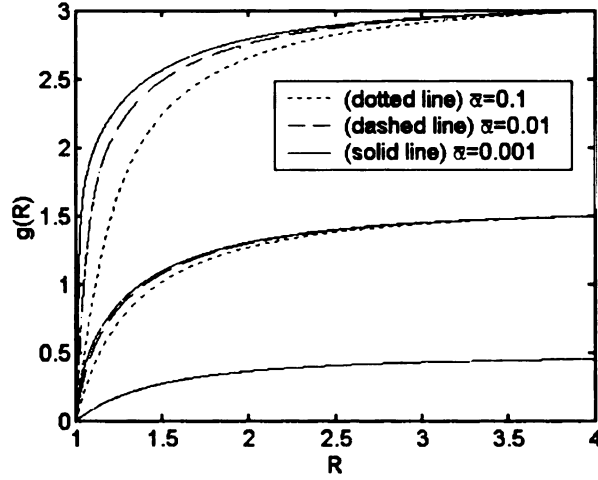

Figure 4.4: Numerical solution when $R_i = 1$, $R_o = 4$ and $\psi_i = 0$ and $\psi_o = 3$ for three values of $\bar{\alpha}$, $\bar{\alpha} = 0.1, 0.01, 0.001$ and three values of ψ_o, $\psi_o = 0.3\Psi_{max}$, $0.995\Psi_{max}$, $1.989\Psi_{max}$

93

4.4 Regular Perturbation Solution for the Extended Model

In this section it will be shown for small $\bar{\alpha} > 0$ that a regular perturbation can be used to get an approximate solution of (4.4) subject to (2.17) for the case $|\psi_o - \psi_i| < \Psi_{\max}$. If $|\psi_o - \psi_i| > \Psi_{\max}$ the technique presented here does not apply. Further if $|\psi_o - \psi_i| = (1 - \epsilon)\Psi_{\max}$ with $0 < \epsilon \ll 1$, i.e $|\psi_o - \psi_i|$ close to but less than $\Psi_{\max}$, then severe requirements are placed on the smallness of $\bar{\alpha}$ in order to obtain a useful regular perturbation solution approximation near $R = R_i$.

Let

$$g(r) = g_0(r) + \bar{\alpha}\, g_1(r) + \bar{\alpha}^2\, g_2(r) + \dots, \tag{4.79}$$

and

$$\bar{d} = \bar{d}_0 + \bar{\alpha}\, \bar{d}_1 + \bar{\alpha}^2\, \bar{d}_2 + \dots. \tag{4.80}$$

Then equation (4.69) becomes

$$\bar{\alpha}\, r^3 \left(g_0'(r) + \bar{\alpha}\, g_1'(r) + \dots \right) + \frac{r^3 \left(g_0'(r) + \bar{\alpha}\, g_1'(r) + \dots \right)}{\sqrt{4 + r^2 (g_0'(r) + \bar{\alpha}\, g_1'(r) + \dots)^2}}$$

$$= \bar{d}_0 + \bar{\alpha}\, \bar{d}_1 + \dots. \tag{4.81}$$

By expanding in $\bar{\alpha}$ equation (4.81) provides

$$\frac{r^3\, g_0'}{\sqrt{4 + r^2 (g_0')^2}} + \bar{\alpha}\, r^3 \left[g_0' + \left\{ \frac{4\, g_1'}{(4 + r^2 (g_0')^2)^{3/2}} \right\} \right] + O(\bar{\alpha}^2)$$

$$= \bar{d}_0 + \bar{\alpha}\, \bar{d}_1 + O(\bar{\alpha}^2). \tag{4.82}$$

The $O(1)$ equation is

$$\frac{r^3\, g_0'}{\sqrt{4 + r^2 (g_0')^2}} = \bar{d}_0. \tag{4.83}$$

94

Note that by renaming the function and constant in the equation (4.83) it can be seen that (4.83) is identical with (3.113). Hence the solution is

$$g_0(r) = \arctan\sqrt{\frac{r^4 - \bar{d}_0^2}{\bar{d}_0^2}} + \bar{c}_0. \tag{4.84}$$

Since attention is restricted to $|\psi_o - \psi_i| < \Psi_{\max} = \arccos(R_i^2\, R_o^2)$, it follows that $\bar{d}_0$ and $\bar{c}_0$ can be computed uniquely from the boundary conditions (2.17) as in Section 3.4. Indeed $\bar{d}_0$ and $\bar{c}_0$ are given by (viz. (3.118) and (3.119))

$$\bar{d}_0 = \frac{R_i^2 R_o^2 \sin\Psi}{\sqrt{R_i^4 + R_o^4 - 2R_i^2 R_o^2 \cos\Psi}}, \tag{4.85}$$

$$\bar{c}_0 = \psi_i - \arctan\sqrt{\frac{R_i^4 - \bar{d}_0^2}{\bar{d}_0^2}}. \tag{4.86}$$

At this point an important observation is that if $|\psi_o - \psi_i| > \Psi_{\max}$ then there is no $g_0(r)$ for which boundary conditions (2.17) are met. Hence the technique under consideration does not apply. Moreover from equation (4.84)

$$g_0'(r) = \frac{2}{r}\frac{\bar{d}_0}{\sqrt{r^4 - \bar{d}_0^2}}, \tag{4.87}$$

and using (4.85) in equation (4.87) gives

$$g_0'(R_i) = \frac{2R_o^2 \sin\Psi}{R_i(R_o^2 \cos\Psi - R_i^2)}, \tag{4.88}$$

where $\Psi = |\psi_o - \psi_i|$. Therefore $g_0'(R_i) \to \infty$ as $|\psi_o - \psi_i| \to \Psi_{\max}$. Hence for fixed $\bar{\alpha}$ if $|\psi_o - \psi_i| = (1 - \epsilon)\Psi_{\max}$ with $0 < \epsilon \ll 1$ then the first term, $\bar{\alpha}\, r^3\, g'(r)$, in equation (4.69) becomes large as $r \to R_i$. Thus the smallness of $\bar{\alpha}$ for a useful approximation must correlate with the closeness of $|\psi_o - \psi_i|$ to $\Psi_{\max}$, as discussed at the end of this section.

Deferring these issues for the present, the $O(\bar{\alpha})$ equation associated with (4.82) is

$$r^3 g_0' + \frac{4\, r^3\, g_1'}{[4 + r^2(g_0')^2]^{3/2}} = \bar{d}_1, \tag{4.89}$$

which can be solved for g_1'

$$g_1' = \frac{(\bar{d}_1 - r^3\, g_0')\, [4 + r^2(g_0')^2]^{3/2}}{4\, r^3}.$$

(4.90)

Substituting from (4.87) into (4.90) gives after some simplification

$$g_1' = 2\left[\frac{\bar{d}_1\, r^3}{[r^4 - \bar{d}_0^2]^{3/2}} - \frac{2\, \bar{d}_0\, r^5}{[r^4 - \bar{d}_0^2]^2}\right].$$

(4.91)

Therefore

$$g_1(r) = \frac{1}{2}\, \log\left|\frac{r^2 + \bar{d}_0}{r^2 - \bar{d}_0}\right| - \frac{\bar{d}_1\, \sqrt{r^4 - \bar{d}_0^2} - \bar{d}_0\, r^2}{r^4 - \bar{d}_0^2} + \bar{c}_1.$$

(4.92)

By using boundary conditions

$$g_1(R_i) = 0, \quad g_1(R_o) = 0,$$

(4.93)

constants $\bar{d}_1$ and $\bar{c}_1$ can be determined uniquely:

$$\bar{d}_1 = \left(0.5\, \log\left|\frac{R_o^2 + \bar{d}_0}{R_o^2 - \bar{d}_0}\right| - 0.5\, \log\left|\frac{R_i^2 + \bar{d}_0}{R_i^2 - \bar{d}_0}\right| + \frac{\bar{d}_0\, R_o^2}{R_o^4 - \bar{d}_0^2} - \frac{\bar{d}_0\, R_i^2}{R_i^4 - \bar{d}_0^2}\right)$$

$$\Big/ \left(\frac{1}{\sqrt{R_o^4 - \bar{d}_0^2}} - \frac{1}{\sqrt{R_i^4 - \bar{d}_0^2}}\right),$$

(4.94)

and

$$\bar{c}_1 = \frac{\bar{d}_1}{\sqrt{R_o^4 - \bar{d}_0^2}} - \frac{\bar{d}_0\, R_o^2}{R_o^4 - \bar{d}_0^2} - \frac{1}{2}\, \log\left|\frac{R_o^2 + \bar{d}_0}{R_o^2 - \bar{d}_0}\right|.$$

(4.95)

Consequently the perturbation expansion solution of (4.4) subject to (2.17) with $|\psi_o - \psi_i| < \Psi_{\text{max}}$ is given by

$$g(r) = g_0(r) + \bar{\alpha}\, g_1(r) + O(\bar{\alpha}^2)$$

(4.96)

where $g_0(r)$, $g_1(r)$ are given by respectively (4.84) and (4.92). This procedure can be continued to any order $\bar{\alpha}^n$ by further expansion of (4.82) to obtain a first order ODE for g_n containing d_n. Each such ODE for $n > 1$ is to be solved subject to $g_n(R_i) = g_n(R_o) = 0$. Thus truncation of the perturbation expansion at order n

Figure 4.5: One-term, two-term perturbation solutions and numeric solution with $\psi_i = 0$ and $\psi_o = 0.150826$ when $\bar{\alpha} = 0.1$. Here $R_i = 1$, $R_o = 4$ and $\Psi_{max} = 1.50826$ so that $\psi_o = 0.1\Psi_{max}$

results in an expansion that exactly satisfies the boundary conditions (2.17), but only solves the ODE (4.4) to $O(\bar{\alpha}^n)$.

Figure 4.5 shows the graph of one-term, two-term perturbation solutions and numeric solution with $\psi_i = 0$ and $\psi_o = 0.150826 = 0.1\Psi_{max}$ when $\bar{\alpha} = 0.1$, $R_i = 1$, $R_o = 4$. These three graphs look like almost identical. However if any part of the graph is enlarged then it becomes apparent that two-term perturbation solution, shown by the dotted line, is better than one-term perturbation solution, shown by the dashed line, as expected from general perturbation theory.

Figure 4.6 shows the graph of the one-term, the two-term perturbation solutions, and the numeric solution with $\psi_i = 0$ and $\psi_o = 1.3 = 0.862\Psi_{max}$ when $\bar{\alpha} = 0.01$, $R_i = 1$, $R_o = 4$. These three graphs again look like almost identical. However if any part of the graph is enlarged then it again becomes apparent that two-term perturbation solution, shown by the dotted line, is better than one-term perturbation solution, shown by the dashed line, as expected from general perturbation theory.

97

Figure 4.6: One-term, two-term perturbation solutions and numeric solution with $\psi_i = 0$ and $\psi_o = 1.3$ when $\bar{\alpha} = 0.01$. Here $R_i = 1$, $R_o = 4$ and $\Psi_{max} = 1.50826$ so that $\psi_o = 0.862\Psi_{max}$

As mentioned earlier the smallness of $\bar{\alpha}$ for a useful approximation is expected to correlate with the closeness of $|\psi_o - \psi_i|$ to Ψ_{max}. Numerical investigation of (4.96) gives useful insight about this correlation. In particular we note that the correction $g_1(R)$ involves $g_1{}'(R) < 0$. Thus the two term expansion for $g'(R)$ will involve $g'(R) < 0$ at some R if $\bar{\alpha}$ is sufficiently large. This breakdown first occurs at $R = R_i$. For fixed R_i, R_o, ψ_i and $\bar{\alpha}$ there is a critical value of ψ_o, say Ψ_{crit}, such that if $\psi_o \geq \Psi_{crit}$ then

$$g_0{}'(R_i) + \bar{\alpha}\, g_1{}'(R_i) \leq 0, \tag{4.97}$$

which is contrary to the physical expectation that $g(R_i)$ is an increasing function of ψ_o. Hence (4.97) provides an analytic expression to relate smallness of $\bar{\alpha}$ with ψ_o. Indeed by solving (4.97) numerically it has been found that $\Psi_{crit} = 1.0887 = 0.722\Psi_{max}$ when $R_i = 1$, $R_o = 4$, $\psi_i = 0$, $\bar{\alpha} = 0.1$ and that $\Psi_{crit} = 1.301 = 0.862\Psi_{max}$ when $R_i = 1$, $R_o = 4$, $\psi_i = 0$, $\bar{\alpha} = 0.01$.
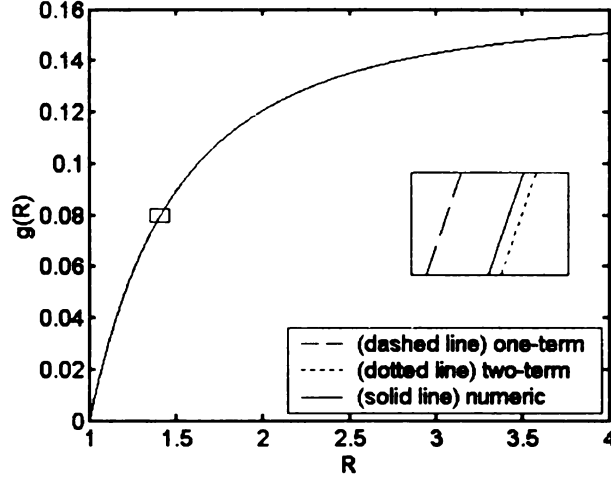
Figure 4.7: One-term, two-term perturbation solutions and numeric solution with $\psi_i = 0$ and $\psi_o = 0.97$ when $\bar{\alpha} = 0.1$. Here $R_i = 1$, $R_o = 4$ and $\Psi_{max} = 1.50826$ so that $\psi_o = 0.643\Psi_{max}$

Since $\Psi_{crit} = 1.0887$ when $R_i = 1$, $R_o = 4$, $\psi_i = 0$ and $\bar{\alpha} = 0.1$ the values of $\psi_o = 0.97$ and $\psi_o = 1.3$ are selected in the following graphs to emphasize the change in the nature of perturbation expansion. It can be seen from Figure 4.7 that the two-term perturbation solution, shown by the dotted line, is better than the one-term perturbation solution, shown by the dashed line, as expected from general perturbation theory. However as ψ_o increases through Ψ_{crit} the value of the derivative $g'(R_i)$ in the two term expansion becomes negative. For $\psi_o = 1.3$ this gives a graph for the two term expansion involving initially decreasing $g(R)$. (see Figure 4.8). As a result the two-term perturbation solution becomes a worse approximation to the numeric solution (shown by the solid line) than the one-term perturbation solution. On the other hand recall from Figure 4.6 that two-term perturbation solution is better than one-term perturbation solution when $\bar{\alpha} = 0.01$ and $\psi_o = 1.3$.
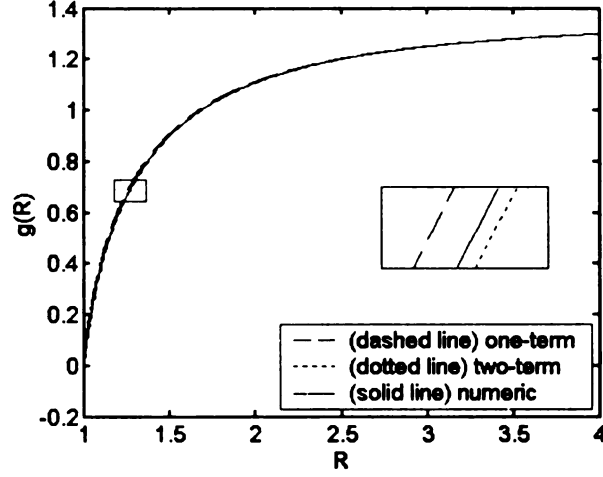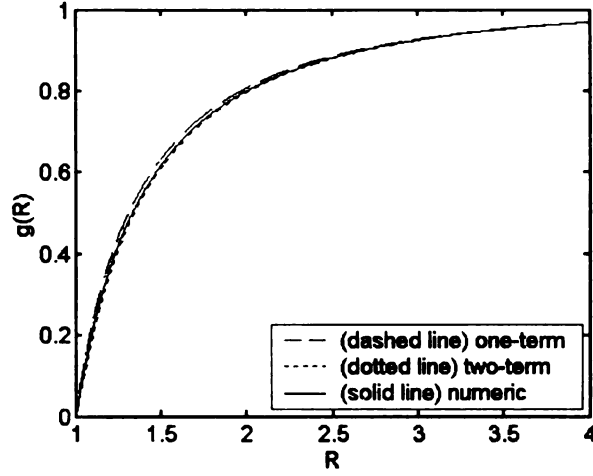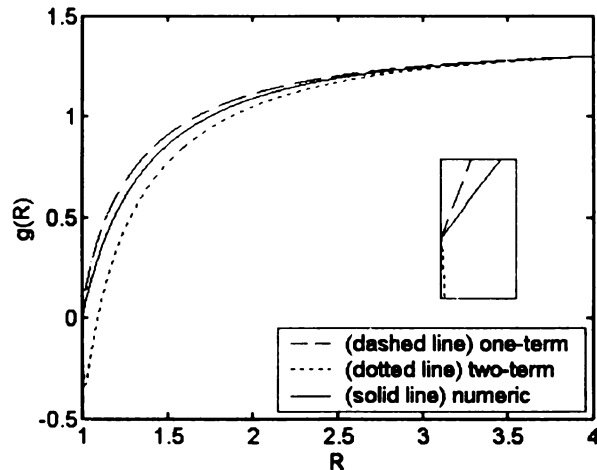
Figure 4.8: One-term, two-term perturbation solutions and numeric solution with $\psi_i = 0$ and $\psi_o = 1.3$ when $\bar{\alpha} = 0.1$. Here $R_i = 1$, $R_o = 4$ and $\Psi_{max} = 1.50826$ so that $\psi_o = 0.862\Psi_{max}$. Since $\psi_o > \Psi_{crit}$, the two term perturbation solution involves decrease of $g(R)$ when $R = R_i$

4.5 Boundary Layer Type Solution for the Extended Model

In this section the case $|\psi_o - \psi_i| > \Psi_{max}$ will be examined by means of perturbation theory for small $\bar{\alpha}$. This has the added benefit of clarifying the proper treatment of the case $|\psi_o - \psi_i| = (1 - \epsilon)\Psi_{max}$ with $0 < \epsilon \ll 1$. As discussed at the end of previous section if $|\psi_o - \psi_i| > \Psi_{max}$ then there is no $g_0(r)$ that satisfies the given boundary conditions so a regular perturbation treatment is not possible. Moreover if $|\psi_o - \psi_i| = (1 - \epsilon)\Psi_{max}$ with $0 < \epsilon \ll 1$ then the standard perturbation procedure does not yield a useful approximation if $\bar{\alpha}$ is not sufficiently small. To get a useful approximation in such cases we will proceed as follows: From (4.69) and (4.88) it follows that there is a region near $r = R_i$ in which $g(r)$ changes rapidly thus motivating a boundary layer type analysis. Indeed from (4.69) one can see that if $g'(r)$ is of order $1/\bar{\alpha}$

then the first term in (4.69) cannot be neglected while computing the first term of the perturbation expansion. i.e., there is a boundary layer at $r = R_i$. A boundary layer correction (inner solution) at $r = R_i$ will be constructed by using the stretching transformation

$$s = \frac{r - R_i}{\bar{\alpha}}.$$ (4.98)

This inner solution will be denoted $\zeta(r)$. Note that away from $r = R_i$, the first term in (4.69) is small, whereupon a standard perturbation can be used to get an approximate form of the outer solution. This outer solution will be denoted $G(r)$. However there will be only one boundary condition, namely $g(R_o) = \psi_o$, for the outer solution to meet. The additional integration constant generated by the outer solution will be determined by patching the outer solution with the inner solution so that

$$G_0(\bar{r}) = \zeta_0(\bar{r})$$ (4.99)

and

$$g_0{}'(\bar{r}) = \zeta_0'(\bar{r}),$$ (4.100)

for some $\bar{r} \in [R_i, R_o]$ where $G_0(r)$ is the first term of the outer solution and $\zeta_0(r)$ is the first term of the inner solution. Indeed it will be shown that if $\bar{\alpha}$ and $\bar{d}$ are suitably restricted, then $\bar{r}$ can be chosen uniquely. The geometric meaning of (4.99) and (4.100) is that the one-term outer and one-term inner solutions can be pieced up together smoothly; i.e., they have a common tangent at the point of contact. The terminology "patching" is used to indicate that the inner and outer solutions are reconciled at a single point, as opposed to some form of matching over a region [7], [8], [13].

We remark that the phenomena of interest are not associated with a singular perturbation in the usual sense. Namely, the small parameter $\bar{\alpha}$ does not annihilate higher order derivatives of the governing equations in the limit $\bar{\alpha} \to 0$.

If more terms are used in the outer and inner solutions, then patching can proceed as follows. For each new term that is added to the inner and outer solutions there will be one new integration constant. Now $\bar{r}$ and the constants (including the new one) can be chosen so that derivatives of the inner and outer solutions match up to one more order at $\bar{r}$. For example if a two-term inner and outer expansions are used we require that

$$(G_0 + G_1)(\bar{r}) = (\zeta_0 + \zeta_1)(\bar{r}) \tag{4.101}$$

and

$$(g_0{}' + g_1{}')(\bar{r}) = (\zeta_0' + \zeta_1')(\bar{r}) \tag{4.102}$$

and

$$(g_0{}'' + g_1{}'')(\bar{r}) = (\zeta_0'' + \zeta_1'')(\bar{r}), \tag{4.103}$$

where G_1 and ζ_1 are the second terms in the outer and inner solutions respectively. Note that $\bar{r}$ and all constants will be computed independently from any previous determination involving less terms in the expansions. In this sense this method is not iterative for computing patching constants. Technically, this process can be implemented for any order.

The procedure is illustrated with the two term form of the outer solution

$$G(r) = G_0(r) + \bar{\alpha}\,G_1(r) + O(\bar{\alpha}^2). \tag{4.104}$$

As usual we impose that

$$G_0(R_o) = \psi_o, \tag{4.105}$$

and

$$G_j(R_o) = 0, \quad j \geq 1. \tag{4.106}$$

102

The outer solution $G(r)$ must satisfy (4.69). By using the expansions (4.80) (for $\bar{d}$) and (4.104) in (4.69), the $O(1)$ equation is given by

$$\frac{r^3 G_o'}{\sqrt{4 + (rG_o')^2}} = \bar{d}_0.$$

(4.107)

Thus,

$$G_0(r) = \arctan \sqrt{\frac{r^4 - \bar{d}_0^2}{\bar{d}_0^2}} + \bar{C}_0,$$

(4.108)

where

$$\bar{C}_0 = \psi_o - \arctan \sqrt{\frac{R_o^4 - \bar{d}_0^2}{\bar{d}_0^2}}.$$

(4.109)

Hence it is found that the first term of the outer solution is given by (4.108) up to constant $\bar{d}_0$ which will be computed by patching.

Note for a given $\bar{d}_0$ that the maximal domain of the one-term outer solution, $G_0(r)$, is $[\sqrt{\bar{d}_0}, \infty)$. Moreover the derivative of $G_0(r)$ at $r = \sqrt{\bar{d}_0}$ is infinite. Therefore as $\bar{d}_0$ varies by virtue of a change in boundary conditions, the domain of the first term of the outer solution also changes. Indeed by using (4.108) and (4.109) the leftmost endpoints of the one-term outer solutions has the following coordinates as $\bar{d}_0$ varies between R_i^2 and R_o^2:

$$(r, g) = \left(\sqrt{\bar{d}_0}, \psi_o - \arctan \sqrt{\frac{R_o^4 - (\bar{d}_0)^2}{(\bar{d}_0)^2}} \ \right).$$

(4.110)

The graphs of the one-term outer solutions are depicted in Figure 4.9 for trial values $\bar{d}_0 = 1, 2.25, 4, 6.25, 9, 12.25$. Note that as the trial value $\bar{d}_0$ increases the graph of the one-term outer solutions move to the right. The dashed line gives (4.110) at which point each one-term outer solution has a vertical tangent.

The second term of the outer solution is now computed as follows. By using the expansions (4.80) and (4.104) in (4.69), the $O(\bar{\alpha})$ equation is given by

$$G_0' + \frac{4 G_1'}{[4 + r^2(G_0')^2]^{3/2}} = \frac{\bar{d}_1}{r^3},$$

(4.111)

103
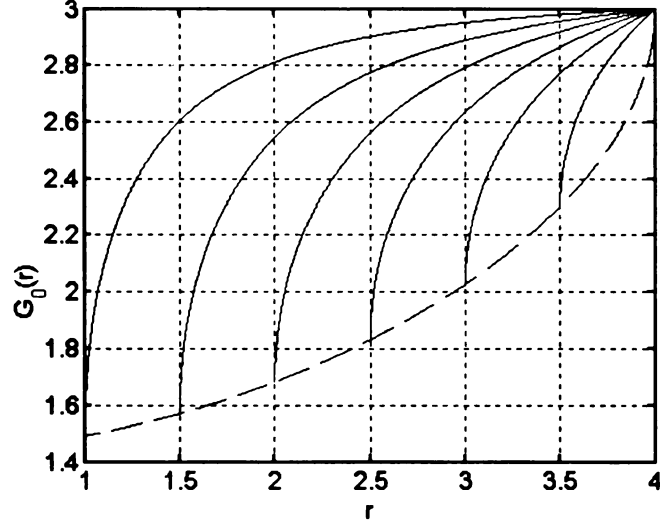
Figure 4.9: One-term outer solutions with $R_i = 1$, $R_o = 4$, $\psi_i = 0$ and $\psi_o = 3$ for the following six trial values $\bar{d}_0$, $\bar{d}_0 = 1, 2.25, 4, 6.25, 9, 12.25$. Here $\bar{d}_0 = 1$ is on the far left and $\bar{d}_0 = 12.25$ is on the far right. The curves order themselves sequentially in $\bar{d}_0$. The envelope of vertical tangency is shown as a dashed line

which can be solved for G_1'

$$G_1' = \frac{(\bar{d}_1 - r^3 \, G_0') \, [4 + r^2 (G_0')^2]^{3/2}}{4 \, r^3}. \tag{4.112}$$

Computing G_0' from (4.108) and then substituting into (4.112) gives after some simplification

$$G_1' = 2 \left[\frac{\bar{d}_1 \, r^3}{[r^4 - \bar{d}_0^2]^{3/2}} - \frac{2 \, \bar{d}_0 \, r^5}{[r^4 - \bar{d}_0^2]^2} \right]. \tag{4.113}$$

Therefore

$$G_1(r) = \frac{1}{2} \log \left| \frac{r^2 + \bar{d}_0}{r^2 - \bar{d}_0} \right| - \frac{\bar{d}_1 \, \sqrt{r^4 - \bar{d}_0^2} - \bar{d}_0 \, r^2}{r^4 - \bar{d}_0^2} + \bar{C}_1, \tag{4.114}$$

where $\bar{C}_1$ is an integration constant and is determined on the basis of boundary condition (4.106) yielding

$$\bar{C}_1 = \frac{\bar{d}_1}{\sqrt{R_o^4 - \bar{d}_0^2}} - \frac{\bar{d}_0 \, R_o^2}{R_o^4 - \bar{d}_0^2} - \frac{1}{2} \log \left| \frac{R_o^2 + \bar{d}_0}{R_o^2 - \bar{d}_0} \right|. \tag{4.115}$$

104

Note that (4.115) is the same as (4.95). Hence (4.114) is also same as (4.92). Hence two-term outer solution is given by

$$G(r) = \arctan \sqrt{\frac{r^4 - \bar{d}_0^2}{\bar{d}_0^2}} + \bar{C}_0 \tag{4.116}$$

$$+ \bar{\alpha} \left[\frac{1}{2} \log \left| \frac{r^2 + \bar{d}_0}{r^2 - \bar{d}_0} \right| - \frac{\bar{d}_1 \sqrt{r^4 - \bar{d}_0^2} - \bar{d}_0 \, r^2}{r^4 - \bar{d}_0^2} + \bar{C}_1 \right],$$

where $\bar{C}_0$ and $\bar{C}_1$ are given by (4.109) and (4.115) respectively.

The boundary layer equation (inner equation) can be found by substituting (4.98) in (4.69)

$$\zeta'(s) + \frac{\frac{\zeta'(s)}{\bar{\alpha}}}{\sqrt{4 + (R_i + \bar{\alpha} \, s)^2 \, (\frac{\zeta'(s)}{\bar{\alpha}})^2}} = \frac{\bar{d}}{(R_i + \bar{\alpha} \, s)^3}. \tag{4.117}$$

Let

$$\zeta(r) = \zeta_0(r) + \bar{\alpha} \, \zeta_1(r) + O(\bar{\alpha}^2) \tag{4.118}$$

be the form of the inner solution. Since $\bar{d}$ is a constant, the same value must apply to both inner and outer expansion. Thus $\bar{d}$ is again given by expansion (4.80). For the first term of the inner solution we set $\bar{\alpha} = 0$. The resulting equation is

$$\zeta_0'(s) + \frac{1}{R_i} = \frac{\bar{d}_0}{R_i^3}. \tag{4.119}$$

Thus,

$$\zeta_0(s) = \left(\frac{\bar{d}_0}{R_i^3} - \frac{1}{R_i} \right) s + \psi_i, \tag{4.120}$$

where the boundary condition $g(R_i) = \zeta_0(0) = \psi_i$ is used to determine the integration constant.

Note that by using (4.98) first term of the inner solution is given by

$$\zeta_0(r) = \left(\frac{\bar{d}_0}{R_i^3} - \frac{1}{R_i} \right) \left(\frac{r - R_i}{\bar{\alpha}} \right) + \psi_i. \tag{4.121}$$

The second term of the inner solution is computed as follows. By using the expansions (4.80) and (4.118) in (4.117), the $O(\bar{\alpha})$ equation is given by

$$\zeta_1'(s) = \frac{\bar{d}_1}{R_i^3} - \frac{3\,\bar{d}_0\,s}{R_i^4} + \frac{s}{R_i^2}. \tag{4.122}$$

Therefore

$$\zeta_1(s) = \frac{\bar{d}_1 s}{R_i^3} - \frac{3\,\bar{d}_0\,s^2}{2\,R_i^4} + \frac{s^2}{2\,R_i^2} + \bar{C}_1. \tag{4.123}$$

By using the boundary condition $\zeta_1(0) = 0$ it is found that $\bar{C}_1 = 0$. Again by using (4.98) the second term of the inner solution can be written as

$$\zeta_1(r) = \left(\frac{1}{2\,R_i^2} - \frac{3\,\bar{d}_0}{2\,R_i^4}\right)\left(\frac{r - R_i}{\bar{\alpha}}\right)^2 + \frac{\bar{d}_1}{R_i^3}\left(\frac{r - R_i}{\bar{\alpha}}\right). \tag{4.124}$$

Consequently the two-term inner solution is given by

$$\zeta(r) = \psi_i + \left(\frac{\bar{d}_0}{R_i^3} - \frac{1}{R_i}\right)\left(\frac{r - R_i}{\bar{\alpha}}\right) \tag{4.125}$$

$$+ \left(\frac{1}{2\,R_i^2} - \frac{3\,\bar{d}_0}{2\,R_i^4}\right)\frac{(r - R_i)^2}{\bar{\alpha}} + \frac{\bar{d}_1}{R_i^3}(r - R_i).$$

The patching procedure will be demonstrated for the one term case where $\zeta(r)$ is given by $\zeta_0(r)$ in (4.121) and $G(r)$ is given by $G_0(r)$ in (4.108) with $\bar{C}_0$ given by (4.109). At issue then is the determination of the single constant $\bar{d}_0$ which appears in both (4.108) and (4.121). Indeed it will be shown that if $\bar{\alpha}$ is sufficiently small then $\bar{d}_0$ is uniquely determined by patching the one-term inner and outer solutions so that (4.99) and (4.100) hold for some $\bar{r} \in [R_i, R_o]$. To begin for given R_i, R_o, ψ_i and ψ_o, let

$$\alpha_{max} = \frac{R_o^3}{R_i^3}\frac{1}{\sqrt{4 + m^2 R_o^2}} - \frac{1}{mR_i}, \tag{4.126}$$

and

$$d^* = \frac{mR_o^3}{\sqrt{4 + m^2 R_o^2}}. \tag{4.127}$$

106

where $m = (\psi_o - \psi_i)/(R_o - R_i)$.

α_{max} given by (4.126) is a consequence of the requirement that $G_0'(R_o) = m$ which in turn provides a natural upper bound for $\bar{\alpha}$ values. Note for an arbitrary $\psi_o - \psi_i$ that α_{max} given by (4.126) may not be positive. However if $|\psi_o - \psi_i| > \Psi_{max}$ or $|\psi_o - \psi_i| = (1 - \epsilon)\Psi_{max}$ with $0 < \epsilon \ll 1$, then $\alpha_{max} > 0$. The above restriction on $\psi_o - \psi_i$ once used in (4.127) also implies that $R_i^2 \leq d^*$. Finally it is easy to see from (4.127) that $d^* \leq R_o^2$. Therefore $R_i^2 \leq d^* \leq R_o^2$ if $|\psi_o - \psi_i| > (1 - \epsilon)\Psi_{max}$ for sufficiently small $\epsilon > 0$.

The following claim establishes that $\bar{d}_0$ can be chosen uniquely so that one-term inner and outer solutions can be patched on the basis of (4.99), (4.100).

Claim 4.5.1 If $0 < \bar{\alpha} \leq \alpha_{max}$, then there exists a unique $\bar{d}_0 \in [R_i^2, d^*]$ and a unique $\bar{r} \in [R_i, R_o]$ such that $G_0(\bar{r}) = \zeta_0(\bar{r})$ and $g_0'(\bar{r}) = \zeta_0'(\bar{r})$ for this unique $\bar{r} \in [R_i, R_o]$.

Proof of Claim 4.5.1: This claim will be proven in two steps.

Step 1: For each $\bar{d}_0 \in [R_i^2, d^*]$ there is a unique $\bar{r} \in [\sqrt{\bar{d}_0}, R_o]$ such that $G_0'(\bar{r}) = \bar{m}$, where $\bar{m}$ is the slope of the line passing through (R_i, ψ_i) and $(\bar{r}, G_0(\bar{r}))$.

Let $\bar{d}_0 \in [R_i^2, d^*]$ and let $S : [\sqrt{\bar{d}_0}, R_o] \to R^*$ be the function defined by

$$S(r) = G_0'(r)(r - R_i) - G_0(r) + \psi_i, \tag{4.128}$$

where the dependence of $G_0(r)$ on $\bar{d}_0$ follows from (4.108), (4.109). Equivalently

$$S(r) = \frac{2\bar{d}_0(r - R_i)}{r\sqrt{r^4 - \bar{d}_0^2}} - (\psi_o - \psi_i) \tag{4.129}$$

$$- \arctan\sqrt{\frac{r^4 - \bar{d}_0^2}{\bar{d}_0^2}} + \arctan\sqrt{\frac{R_o^4 - \bar{d}_0^2}{\bar{d}_0^2}}.$$

Clearly $S(r)$ is a continuous function for $r \in [\sqrt{\bar{d}_0}, R_o]$. Since $G_0(\sqrt{\bar{d}_0}) - \psi_i$ and $\sqrt{\bar{d}_0} - R_i$ are finite and $\lim_{r \to \sqrt{\bar{d}_0}^+} g_0'(r) = +\infty$, it follows that

$$\lim_{r \to \sqrt{\bar{d}_0}^+} S(r) = +\infty. \tag{4.130}$$

107

Also note that $\bar{d}_0 \leq d^*$ gives

$$\lim_{r \to R_0^-} S(r) = \frac{2\,\bar{d}_0\,(R_0 - R_i)}{R_0\,\sqrt{R_0^4 - \bar{d}_0^2}} - (\psi_o - \psi_i) \leq 0. \tag{4.131}$$

Hence by the *intermediate value theorem* there exists $\bar{r} \in [\sqrt{\bar{d}_0}, R_o]$ such that $S(\bar{r}) = 0$. This proves that there is a line passing through (R_i, ψ_i); that is, tangent to $G_0(r)$ at $(\bar{r}, G_0(\bar{r}))$.

Note that

$$S'(r) = \frac{-2\,\bar{d}_0}{r^2}\,\frac{3\,r^4 - \bar{d}_0^2}{(r^4 - \bar{d}_0^2)^{3/2}}\,(r - R_i) < 0. \tag{4.132}$$

Hence $S(r)$ is a strictly decreasing function. Thus $\bar{r}$ must be unique.

Step 2: Let $0 < \bar{\alpha} \leq \alpha^*$. Then there exists a $\bar{d}_0 \in [R_i^2, d^*]$ such that the one-term inner solution, $\zeta_0(r)$, coincides with the tangent line whose existence is guaranteed by step one. Moreover such a $\bar{d}_0$ is unique.

We introduce two families of rays, each family of which is centered at (R_i, ψ_i). The first family is the one-term inner solutions (4.120) where S is given by (4.98). The slope $\partial \psi / \partial R$ of any member of this family is

$$m_1(\bar{d}_0) = \frac{1}{\bar{\alpha}}\left(\frac{\bar{d}_0}{R_i^3} - \frac{1}{R_i}\right). \tag{4.133}$$

This family is parameterized by $\bar{d}_0$.

The second family consists of the rays passing through (R_i, ψ_i) that osculate with the one-term outer solution at $r = \bar{r} \in [\sqrt{\bar{d}_0}, R_o]$ (the existence of such a family is shown in step 1). This family is also parameterized by $\bar{d}_0$. The slope $\partial \psi / \partial R$ of any member of this family is

$$m_2(\bar{d}_0) = \frac{\psi_o - \psi_i}{\bar{r} - R_i} + \tag{4.134}$$

$$\frac{1}{\bar{r} - R_i}\left(\arctan\sqrt{\frac{\bar{r}^4 - \bar{d}_0^2}{\bar{d}_0^2}} - \arctan\sqrt{\frac{R_o^4 - \bar{d}_0^2}{\bar{d}_0^2}}\right),$$

108

where $r = \bar{r}$ is point of contact.

Let $U : [R_i^2, d^*] \to R^*$ be the function defined by

$$U(\bar{d}_0) = m_1(\bar{d}_0) - m_2(\bar{d}_0). \tag{4.135}$$

Clearly $U(\bar{d}_0)$ is a continuous function on $[R_i^2, d^*]$. Since $m_1(R_i^2) = 0$ and $m_2(R_i^2) = \infty$ it follows that

$$U(R_i^2) < 0. \tag{4.136}$$

Conversely

$$U(d^*) = \frac{1}{\bar{\alpha}} \left(\frac{d^*}{R_i^3} - \frac{1}{R_i} \right) - \tag{4.137}$$

$$\frac{1}{\bar{r} - R_i} \left(\psi_o - \psi_i + \arctan \sqrt{\frac{\bar{r}^4 - (d^*)^2}{(d^*)^2}} - \arctan \sqrt{\frac{R_o^4 - (d^*)^2}{(d^*)^2}} \right).$$

Since $\bar{r} \to R_o$ as $\bar{d}_0 \to d^*$, (4.137) gives

$$U(d^*) = \frac{1}{\bar{\alpha}} \left(\frac{d^*}{R_i^3} - \frac{1}{R_i} \right) - \frac{\psi_o - \psi_i}{R_o - R_i}, \tag{4.138}$$

or equivalently

$$U(d^*) = \frac{1}{\bar{\alpha}} \left(\frac{d^*}{R_i^3} - \frac{1}{R_i} \right) - m \geq 0, \tag{4.139}$$

where the inequality is a consequence of the restriction $0 < \bar{\alpha} \leq \alpha_{max}$. Hence again by the *intermediate value theorem* there exists a $\bar{d}_0 \in [R_i^2, d^*]$ for which $U(\bar{d}_0) = 0$, i.e. $m_1(\bar{d}_0) = m_2(\bar{d}_0)$. This proves that the one-term inner solution $\zeta_0(r)$ and the one-term outer solution $G_0(r)$ are tangent to each other at $(\bar{r}, G_0(\bar{r}))$ for this choice of $\bar{d}_0$. Moreover since

$$U'(\bar{d}_0) = \frac{1}{\bar{\alpha} \, R_i^3} - \left(\frac{1}{\bar{r} - R_i} \right) \left(\frac{1}{\sqrt{R_o^4 - \bar{d}_0^2}} - \frac{1}{\sqrt{\bar{r}^4 - \bar{d}_0^2}} \right) > 0, \tag{4.140}$$

109

ψ_o	$\bar{\alpha}$	$\bar{r}$	$\bar{d}_0$
1.5	0.1	1.220537	1.259226
1.5	0.01	1.055384	1.057055
1.5	0.001	1.012634	1.012155
3	0.1	1.289941	1.613179
3	0.01	1.089118	1.180059
3	0.001	1.027634	1.055379
15.0826	0.1	1.713057	2.929204
15.0826	0.01	1.246533	1.553191
15.0826	0.001	1.080849	1.168164

Table 4.1: Numerically computed values of $\bar{r}$ and $\bar{d}_0$ for one term patching for several ψ_o and $\bar{\alpha}$ values when $R_i = 1$, $R_o = 4$ and $\psi_i = 0$

such a $\bar{d}_0$ must be unique. This completes the proof of Claim 4.5.1 demonstrating that $\bar{d}_0$ can be chosen uniquely so that one-term inner and outer solutions can be patched on the basis of (4.99), (4.100). $\quad\square$

The Table 4.1 shows the values of $\bar{r}$ and $\bar{d}_0$ for one term patching for several ψ_o and $\bar{\alpha}$ values when $R_i = 1$, $R_o = 4$ and $\psi_i = 0$.

Figure 4.10 shows the one-term patched solution (dotted line), the one-term regular perturbation solution (dashed line) and the numerical solution (solid line) corresponding to the values $R_i = 1$, $R_o = 4$, $\psi_i = 0$, $\psi_o = 1.5$ and $\bar{\alpha} = 0.1$. Note that $\Psi_{max} \approx 1.50826$; hence $|\psi_o - \psi_i| = 0.995\Psi_{max}$. This suggests when $|\psi_o - \psi_i| \approx \Psi_{max}$ that this new construction gives a satisfactory result even with patching only one-term inner and outer solutions.

The patching procedure will be demonstrated for the two term case where $\zeta(r)$ is given by (4.125) and $G(r)$ is given by (4.116). At issue then is the determination of the constants $\bar{d}_0$ and $\bar{d}_1$, which appear in both (4.116) and (4.125), and the patching location $\bar{r} \in [R_i, R_o]$. The constants $\bar{d}_0$, $\bar{d}_1$ and $\bar{r}$ are computed numerically so that (4.101), (4.102) and (4.103) hold.

Figure 4.10: One-term patched, one-term regular perturbation and numeric solutions when $R_i = 1$, $R_o = 4$, $\psi_i = 0$, $\psi_o = 1.5 < \Psi_{max} \approx 1.50826$ and $\bar{\alpha} = 0.1$. The patching point is at $r = 1.220537$

ψ_o	$\bar{\alpha}$	$\bar{r}$	d_0	d_1
1.5	0.1	1.114935	0.769605	6.607128
1.5	0.01	1.007296	0.932538	16.428066
1.5	0.001	1.000533	0.984481	35.746076
3	0.1	1.233646	1.202777	8.082971
3	0.01	1.081715	1.094041	18.477852
3	0.001	1.029278	1.042663	39.633449
15.0826	0.1	1.586166	2.056238	26.629071
15.0826	0.01	1.245361	1.442835	50.379749
15.0826	0.001	1.093927	1.173599	87.871407

Table 4.2: Numerically computed values of $\bar{r}$, d_0 and d_1 for two term patching for several ψ_o and $\bar{\alpha}$ values when $R_i = 1$, $R_o = 4$ and $\psi_i = 0$
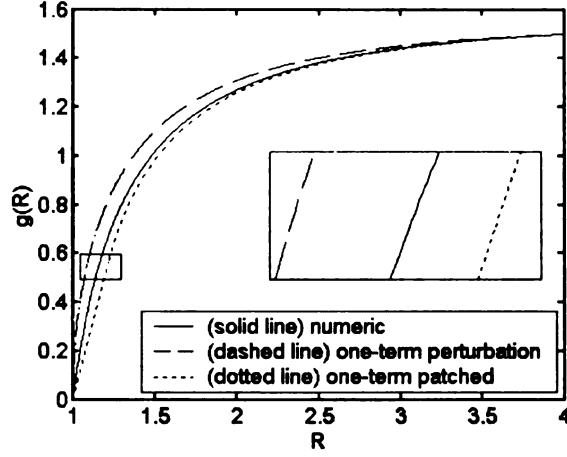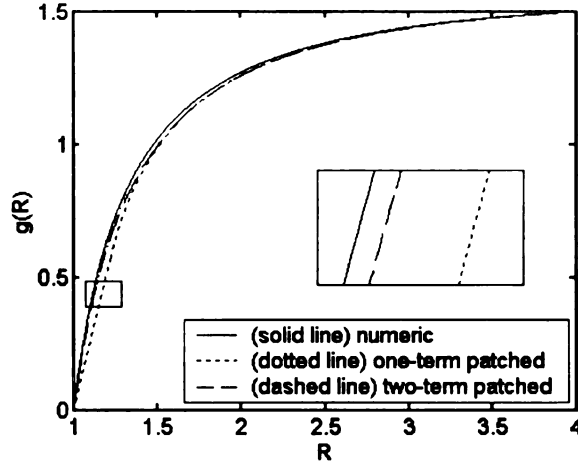
111

Figure 4.11: One-term patched, two-term patched and numeric solutions when $R_i = 1$, $R_o = 4$, $\psi_i = 0$, $\psi_o = 1.5 < \Psi_{max} \approx 1.50826$ and $\bar{\alpha} = 0.1$ The patching point is at $r = 1.220537$ for the one-term patched solution and the patching point is at $r = 1.114934699$ for the two-term patched solution

Table 4.2 shows the values of $\bar{r}$, $\bar{d}_0$ and $\bar{d}_1$ for two term patching for several ψ_o and $\bar{\alpha}$ values when $R_i = 1$, $R_o = 4$ and $\psi_i = 0$.

Figure 4.11 shows the one-term patched solution (dotted line), the two-term patched solution (dashed line), and the numeric solution (solid line) corresponding to the values $R_i = 1$, $R_o = 4$, $\psi_i = 0$, $\psi_o = 1.5$ and $\bar{\alpha} = 0.1$. It is clear from Figure 4.11 that two-term patched solution is better than the one-term patched solution.

Figure 4.12 shows the one-term patched solution (dotted line), the two-term patched solution (dashed line), and the numeric solution (solid line) corresponding to the values $R_i = 1$, $R_o = 4$, $\psi_i = 0$, $\psi_o = 3$ and $\bar{\alpha} = 0.1$. Note that $\psi_o = 3 > \Psi_{max} \approx 1.50826$ and hence regular perturbation cannot be used. However two-term patched solution (dotted line) gives an excellent approximation to numerical solution (solid line). The graphs of three solutions are enlarged around the patching point for the one term patched solution.

112

Figure 4.12: Two-term patched and numeric solution when $R_i = 1$, $R_o = 4$, $\psi_i = 0$, $\psi_o = 3 > \Psi_{max} \approx 1.50826$ and $\bar{\alpha} = 0.1$. The patching point is at $r = 1.2336459$
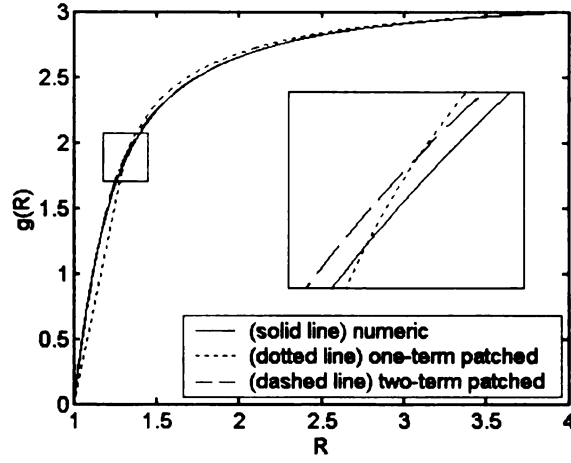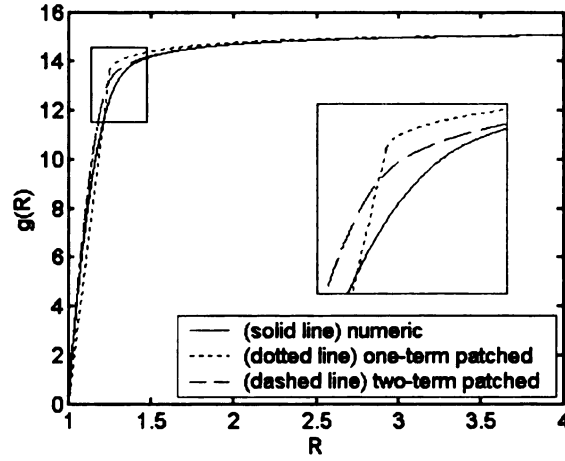

Figure 4.13: One-term patched, two-term patched and numeric solution when $R_i = 1$, $R_o = 4$, $\psi_i = 0$, $\psi_o = 10\Psi_{max}$ and $\bar{\alpha} = 0.01$. The patching point is at $r = 1.246533$ for the one-term patched solution and the patching point is at $r = 1.245361$ for the two-term patched solution

We close this section by depicting the graph of the one-term patched solution (dotted line), the two-term patched solution (dashed line), and the numeric solution (solid line) corresponding to the values $R_i = 1$, $R_o = 4$, $\psi_i = 0$, $\psi_o = 10\Psi_{\max}$ and $\bar{\alpha} = 0.01$. The two-term patched solution (dashed line) gives an excellent approximation to the numerical solution (solid line). The graphs of all three solutions are enlarged around the patching points.

4.6 Twist, Energy and Torque in the Extended Model

The relation between energy and twist in the extended model can be obtained by using the numerical solution discussed in Section 4.3. Recall that the strain-energy density in the extended material model is given by (4.1). Hence when $\hat{\alpha} = \alpha^*$ the potential energy functional (3.4) becomes

$$E = \pi h \int_{R_i}^{R_o} [\alpha(I_1 - 3) + \hat{\alpha}(I_1^* + \hat{I}_1 - 6)]\, r\, dr. \tag{4.141}$$

By using $I_1 = 3 + (rg')^2$ and $I_1^* = \hat{I}_1 = \sqrt{4 + (rg')^2} + 1$ it follows that (4.141) becomes

$$E = \pi h \int_{R_i}^{R_o} [\alpha\,(rg')^2 + \hat{\alpha}(2\sqrt{4 + (rg')^2} - 4)]\, r\, dr. \tag{4.142}$$

Letting $\bar{\alpha} = \alpha/\hat{\alpha}$, it follows from (4.142) that

$$E = \pi h \hat{\alpha} \int_{R_i}^{R_o} [\bar{\alpha}\,(rg')^2 + (2\sqrt{4 + (rg')^2} - 4)]\, r\, dr. \tag{4.143}$$

Divide the interval $[R_i, R_o]$ into N equal subintervals and label the end points as $R_i = r_0, r_1, \ldots, r_N = R_o$. For given ψ_i, ψ_o and $\bar{\alpha}$ the numerical solution presented in Section 4.3 provides the values of $g_j \equiv g(r_j)$. Once $g_j, j = 0, \ldots, N$ are known the centered difference approximation (4.71) can be used to estimate $g_j' \equiv g'(r_j)$. Then

Figure 4.14: Normalized energy $E/(2\pi h\hat{\alpha})$ versus twist when $R_i = 1$, $R_o = 4$ for the four values of $\bar{\alpha}$, $\bar{\alpha} = 0, 0.001, 0.01, 0.1$ are depicted as the curves E_1, E_2, E_3, E_4 respectively

(4.143) can be integrated numerically by using the standard composite Simpson's rule. The normalized energy (energy$/2\pi h\hat{\alpha}$) is computed by the outlined method for several values of ψ_o and $\bar{\alpha}$ when $R_i = 1$, $R_o = 4$ and $\psi_i = 0$. The normalized energy versus twist graph is depicted in the following figure for the values of $\bar{\alpha} = 0.1, 0.01, 0.001$. Note that since $\bar{\alpha} = 0$ corresponds to the material model discussed earlier in Part I it is possible to sketch the normalized energy versus twist and then compare with the extended material model. The energy versus twist graph is labeled as E_1, E_2, E_3, E_4 for $\bar{\alpha} = 0$, $0.001, 0.01, 0.1$ respectively. It is clear from Figure 4.14 that the stored energy is an increasing function of $\bar{\alpha}$ for a fixed amount of twist. This is to be expected since increasing $\bar{\alpha}$ at fixed $\hat{\alpha}$ represents an increase in energy penalization which would, in general, stiffen the material response.

Similarly the relation between torque and twist in the extended material model can be obtained as follows. *Torque M* acting on the outer surface is given by virtue
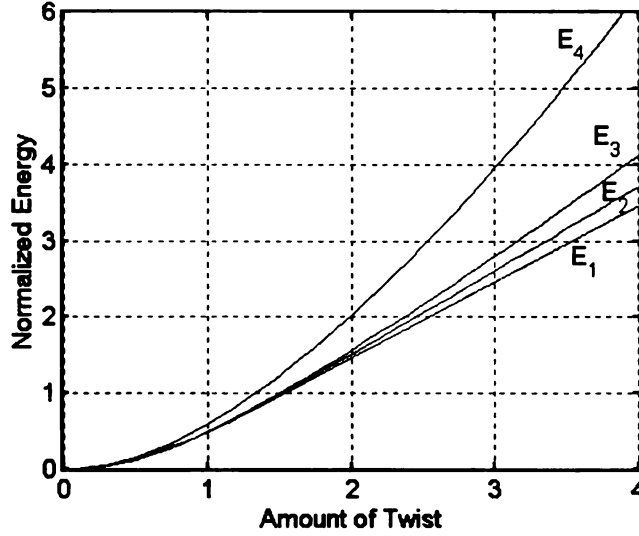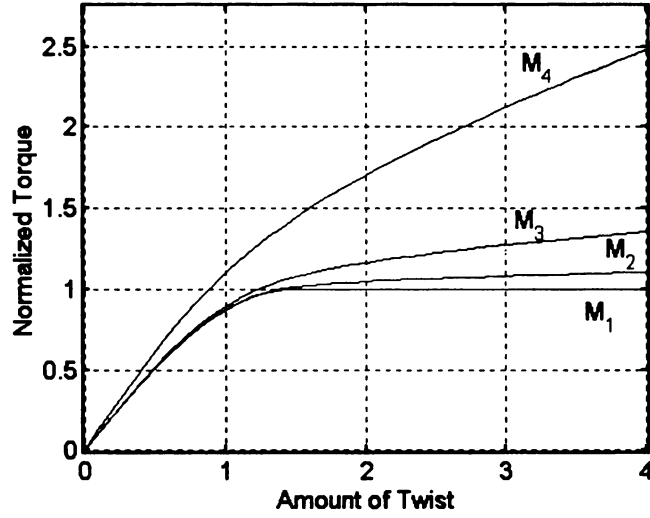
Figure 4.15: Normalized torque $M/(2\pi h\hat{\alpha})$ versus twist when $R_i = 1$, $R_o = 4$ for the four values of $\bar{\alpha}$, $\bar{\alpha} = 0, 0.001, 0.01,\ 0.1$ are depicted as the curves M_1, M_2, M_3, M_4 respectively

of (2.42), (4.2), (4.4) as

$$M = h \int_0^{2\pi} R_o^2\, \sigma_{\theta r}(R_o)\, d\theta = \tag{4.144}$$

$$h \int_0^{2\pi} R_o^2 \left[\alpha\, R_o\, g'(R_o) + \frac{\hat{\alpha}\, R_o\, g'(R_o)}{\sqrt{4 + (R_o g'(R_o))^2}} \right] d\theta.$$

Equivalently

$$M = 2\pi h\hat{\alpha} [\bar{\alpha}\, R_o^3\, g'(R_o) + \frac{R_o^3\, g'(R_o)}{\sqrt{4 + (R_o g'(R_o))^2}}]. \tag{4.145}$$

Since the torque acting on the outer surface $R = R_o$ depends on $g'(R_o)$, the value of $g'(R_o)$ must be estimated numerically. By using the numerical solution given in Section 4.3 and one sided centered difference the value of $g'(R_o)$ is estimated for fixed $R = R_i$, $R = R_o$, $\bar{\alpha}$, $\psi_i = 0$, and ψ_o.

The normalized torque (torque$/2\pi h\hat{\alpha}$) versus twist graph is depicted in Figure 4.15 for the values of $\bar{\alpha} = 0.1, 0.01, 0.001$. Note that since $\bar{\alpha} = 0$ corresponds to the

116

earlier material model it is possible to sketch normalized torque versus twist and then compare with the extended material model. The torque versus twist graph is labeled as M_1, M_2, M_3, M_4 for $\bar{\alpha} = 0,\ 0.001, 0.01, 0.1$ respectively. It is clear from the Figure 4.15 that torque is also an increasing function of $\bar{\alpha}$ for a fixed amount of twist.

CHAPTER 5

Conclusions and Discussions

In this concluding chapter the main work of this thesis is discussed and summarized.

A preliminary discussion from the well known conventional theory of hyperelasticity is presented at the outset. Then the solution of the pure azimuthal shear problem in this context is presented in order to provide context for this thesis.

In Chapter 3 the pure azimuthal shear problem is formulated in the new framework that is proposed by Pence and Tsai. This theory contains a material parameter $k = \hat{\alpha}/\alpha^*$ where $\hat{\alpha}$ can be viewed as a macroscopic stiffness and α^* can be viewed as a substructural stiffness. It is confirmed that if $k \to 0$, then the pure azimuthal shear problem in the new framework reduces to the standard pure azimuthal shear problem for a neo-Hookean material. Since the governing field equations are too complicated for a general k, the pure azimuthal shear problem is studied for small k by perturbation method and a numerical solution is presented for any k. The exact solution is also presented when $k = 1$ and a necessary restriction $|\Psi| \leq \Psi_{max}$ for a smooth solution is determined. A variational formulation of the problem is also presented and direct methods of the calculus of variations are used to investigate minimum energy configurations for arbitrarily large twist Ψ when $k = 1$.

In Chapter 4 a more generalized material model is considered. It is characterized by an additional stiffness parameter α. The first order nonlinear ODE governing the

pure azimuthal shear problem is derived by using equilibrium and internal balance equations. An existence and uniqueness result for the pure azimuthal shear problem for any $\alpha^* = \hat{\alpha} > 0$, $\alpha > 0$ and total twist $\Psi > 0$ is obtained by using the integral equation and initial value problems corresponding to the governing nonlinear ODE. A numerical solution is presented for any $\alpha/\hat{\alpha}$ and regular perturbation is used to investigate solution possibilities when $\alpha/\hat{\alpha}$ is small for three qualitatively different ranges of Ψ: either $\Psi < \Psi_{max}$ or $\Psi > \Psi_{max}$ or $\Psi = (1 - \epsilon)\Psi_{max}$ with $0 < \epsilon \ll 1$. A boundary layer type analysis is used to get a useful approximation for the latter two ranges of Ψ. In particular using the properties of inner and outer solutions a patching method is proposed. This patching method gives satisfactory agreement with the numerical solution. The relation between torque, twist and energy in the extended material model is also studied.

The pure azimuthal shear problem is complex in this new framework in either material model. The internal balance equation is a second order tensor equation. Even though it has been proved that the internal balance equation subject to requirement $\det \hat{\mathbf{B}} = 1$ has a unique solution the proof is not fully constructive. The nonlinear governing equations offer many conceptual, analytical and numerical challenges. In this thesis we have advanced in all of these areas and examined in depth many interesting phenomena such as occurrence of singular surfaces, boundary layer type behavior and uniqueness and regularity of the solution.

Appendix A

$g(r)$ given by (3.115) is a strong

local minimum of (3.168) if

$|\Psi| \leq \Psi_{max}$

Consider the basic problem of calculus of variations: Find a piecewise-smooth function $y(x)$ on the interval $[a, b]$ that minimizes the definite integral

$$J[y] = \int_a^b F(x, y(x), y'(x)) \, dx, \tag{A.1}$$

subject to

$$y(a) = A, \ y(b) = B. \tag{A.2}$$

The following are well-known from the calculus of variations [28]:

Theorem A.0.1 *For a general Lagrangian $F(x, y, y')$, the Legendre condition $\hat{F}_{,y'y'} \geq 0$ for all x in $[a, b]$ is a necessary condition for $\hat{y}$ to minimize $J[y]$.*

Proof: See [28], page 88. □

Let

$$I[h] \equiv \int_a^b [\hat{F}_{,yy}(x) \, h^2(x) + 2\hat{F}_{,yy'}(x) \, h(x) \, h'(x) + \hat{F}_{,y'y'}(x) \, h'(x)^2] \, dx. \tag{A.3}$$

Then it follows by direct calculation the *Euler-Lagrange Equation* associated with $I[h]$ is

$$[P(x) h'(x)]' - Q(x) h(x) = 0, \tag{A.4}$$

where

$$P(x) = \hat{F}_{,y'y'}(x), \ Q(x) = \hat{F}_{,yy}(x) - [\hat{F}_{,yy'}(x)]'. \tag{A.5}$$

The differential equation (A.4) is called *Jacobi's accessory equation.*

Definition A.0.2 *A point $c > a$ is said to be conjugate to point a relative to $\hat{y}(x)$ if there is a nontrivial extremal $\hat{h}(x)$ of $I[h]$ which vanishes at c as well as at a, i.e., $\hat{h}(a) = \hat{h}(c) = 0$.*

Because $P(x)$ and $Q(x)$ are defined for a particular $\hat{y}(x)$, conjugacy is relative to a given extremal $\hat{y}$.

Theorem A.0.3 *Let $J[y]$ attain a weak local minimum with the admissible extremal $\hat{y}(x)$ and let the strengthened Legendre condition $\hat{F}_{,y'y'} > 0$ hold for all x in $[a,b]$. Then there are no points in (a,b) conjugate to point a relative to $\hat{y}$.*

Proof: See [28], page 91. □

Let

$$E(x, y, v, w) = F(x, y, w) - F(x, y, v) - (w - v) F_{,y'}(x, y, v). \tag{A.6}$$

The quantity $E(x, y, v, w)$ is called the *Weierstrass excess function.*

Theorem A.0.4 *If, for the admissible extremal $\hat{y}$, $J[\hat{y}]$ is a strong local minimum for $J[y]$, it is necessary that*

$$E(x, \hat{y}(x), \hat{y}'(x), w) \geq 0, \tag{A.7}$$

for all x in $[a,b]$ and for all $|w| < \infty$. At a corner point, this equality is to hold for both $\hat{y}'_+$ and $\hat{y}'_-$.

Proof: See [28], page 116. □

The strengthened form of the above necessary conditions are useful in developing sufficiency conditions for minimizing $J[y]$:

(s1) $\hat{y}(x)$ is a piecewise-smooth (admissible) extremal. i.e., it is a solution of *Euler-Lagrange Equation* where it is smooth and satisfies the *Erdmann's corner conditions* at a corner point.

(s2) *Strengthened Legendre Condition:* $\hat{F}_{,y'y'} > 0$ on $[a, b]$.

(s3) *Strengthened Jacobi Condition:* $\hat{y}(x)$ has no conjugate points to a in $(a, b]$.

(s4) *Strengthened Weierstrass Condition:* $E(x, u, v, w) = F(x, u, w) - F(x, u, v) - (w - v)F_{,y'}(x, u, v) \geq 0$ for all (u, v) near $(\hat{y}, \hat{y}')$ and all $|w| < \infty$.

Theorem A.0.5 *If F is C^4 in its arguments and the admissible extremal $\hat{y}(x)$ satisfies $(s1)$, $(s2)$, $(s3)$, and $(s4)$, then $J[y]$ is a strong local minimum.*

Proof: See [28], page 128. □

Using the above theorem it will be proven that $g(r)$ given by (3.115) is a strong local minimum of (3.168) if $|\Psi| \leq \Psi_{\text{max}}$.

For (3.168) the *Lagrangian* F is

$$F(r, g, g') = r\sqrt{4 + (rg')^2} - 2r. \tag{A.8}$$

It is clear that F is C^4 in its arguments. By using the *Erdmann's Corner Conditions* ($\hat{F}_{,y'}$ and $\hat{F} - \hat{y}'\hat{F}_{,y'}$ must be continuous even at the corner points of $\hat{y}(x)$), it will be shown that any extremal of (3.168) must be smooth; i.e., there is no corner point. From (A.8)

$$\frac{\partial F}{\partial g'} = \frac{r^3 g'}{\sqrt{4 + (rg')^2}}. \tag{A.9}$$

Let $p = g'_+$ and $q = g'_-$ be the values of g' at the left and right side of a corner point respectively. Then by the first *Erdmann's corner condition*

$$\frac{r^3 p}{\sqrt{4 + (rp)^2}} = \frac{r^3 q}{\sqrt{4 + (rq)^2}}.$$ (A.10)

Since $r \neq 0$,

$$\frac{p}{\sqrt{4 + r^2 p^2}} = \frac{q}{\sqrt{4 + r^2 q^2}}.$$ (A.11)

By taking the squares of both sides in (A.11)

$$\frac{p^2}{4 + r^2 p^2} = \frac{q^2}{4 + r^2 q^2},$$ (A.12)

which leads to

$$p^2 = q^2.$$ (A.13)

If (A.13) is used in (A.11), then (A.13) simplifies to

$$p = q.$$ (A.14)

Therefore any extremal of (3.168) must be smooth. Note that in general the second *Erdmann's corner condition* is necessary to find the values of p and q. But in this case it is not necessary to check the second *Erdmann's corner condition*.

In Section 3.4 it was shown that $g(r)$ given by (3.115) is the only solution of the *Euler-Lagrange Equation* if $|\Psi| \leq \Psi_{\max}$ when $k = 1$. Therefore $(s1)$ is satisfied.

From (A.9) it follows that

$$\frac{\partial^2 F}{\partial g'^2} = \frac{4r^3}{(4 + r^2 g'^2)^{3/2}}.$$ (A.15)

Since $r > 0$, on $[R_i, R_o]$ (A.15) gives that

$$\frac{\partial^2 F}{\partial g'^2} = \frac{4 r^3}{(4 + r^2 g'^2)^{3/2}} > 0.$$ (A.16)

Hence $(s2)$ is satisfied. Note from (A.16) that an extremal $\hat{g}(r)$ must be at least C^2 by *Hilbert's Theorem*.

123

Jacobi's accessory equation (A.4) for the current problem may be written as

$$\frac{4\,r^3}{(4 + r^2 g'^2)^{3/2}}\, h'(r) = a_1,\tag{A.17}$$

where a_1 is a constant and $h(r)$ is a nontrivial function that vanishes at both c and R_i; i.e., $h(R_i) = h(c) = 0$. From (A.17) it follows

$$h'(r) = \frac{a_1\,(4 + r^2 g'^2)^{3/2}}{4\,r^3}.\tag{A.18}$$

Consequently (3.114) in (A.18) yields

$$h'(r) = \frac{2\,a_1\,r^3}{(r^4 - d_1^2)^{3/2}},\tag{A.19}$$

where d_1 is the constant given by (3.118). Hence

$$h(r) = \frac{-a_1}{\sqrt{r^4 - d_1^2}} + a_2,\tag{A.20}$$

where a_2 is another constant. By using $h(R_i) = 0$ from (A.20) it follows that

$$a_2 = \frac{a_1}{\sqrt{R_i^4 - d_1^2}}.\tag{A.21}$$

Whereupon (A.20) can be written as

$$h(r) = a_1 \left(\frac{1}{\sqrt{R_i^4 - d_1^2}} - \frac{1}{\sqrt{r^4 - d_1^2}} \right).\tag{A.22}$$

Now if $h(r) = 0$, then either $a_1 = 0$ giving $h(r) \equiv 0$ or

$$\frac{1}{\sqrt{R_i^4 - d_1^2}} = \frac{1}{\sqrt{r^4 - d_1^2}},\tag{A.23}$$

giving $r = R_i$. Therefore there is no conjugate points to R_i in $(R_i, R_o]$. Consequently $(s3)$ is satisfied.

One important remark is that the notion of being conjugate is defined relative to an extremal. Since there is no admissible extremal when $|\Psi| > \Psi_{\max}$ the outlined procedure cannot be used in that case.

It remains to show that *Strengthened Weierstrass Condition* ($s4$) is also satisfied. For the current problem the *Weierstrass excess function* E (A.6) becomes

$$E(r, u, v, w) = r\sqrt{4 + (rw)^2} - r\sqrt{4 + (rv)^2} - (w - v)\frac{r^3 v}{\sqrt{4 + (rv)^2}}, \quad \text{(A.24)}$$

or equivalently

$$E(r, u, v, w) = r\left(\sqrt{4 + (rw)^2} - \frac{(4 + r^2 vw)}{\sqrt{4 + (rv)^2}}\right). \quad \text{(A.25)}$$

Note that

$$(v - w)^2 \geq 0, \quad \text{(A.26)}$$

for all $|w| < \infty$. Then (A.26) can be written as

$$v^2 + w^2 \geq 2vw. \quad \text{(A.27)}$$

Multiplying both sides of (A.27) with $4r^2 (> 0)$ yields

$$(4r^2)v^2 + (4r^2)w^2 \geq (4r^2)2vw. \quad \text{(A.28)}$$

Adding $16 + r^4 v^2 w^2$ to both sides of (A.28) leads to

$$16 + 4r^2 v^2 + 4r^2 w^2 + r^4 v^2 w^2 \geq 16 + 8r^2 vw + r^4 v^2 w^2. \quad \text{(A.29)}$$

Note that (A.29) can be written as

$$\left(4 + r^2 v^2\right)\left(4 + r^2 w^2\right) \geq \left(4 + r^2 vw\right)^2, \quad \text{(A.30)}$$

or equivalently

$$\left(4 + r^2 w^2\right) \geq \frac{(4 + r^2 vw)^2}{(4 + r^2 v^2)}. \quad \text{(A.31)}$$

By taking square root of both sides of (A.31)

$$\sqrt{4 + (rw)^2} \geq \frac{(4 + r^2vw)}{\sqrt{4 + (rv)^2}}, \qquad (A.32)$$

or equivalently

$$\sqrt{4 + (rw)^2} - \frac{(4 + r^2vw)}{\sqrt{4 + (rv)^2}} \geq 0, \qquad (A.33)$$

giving that $E(r, u, v, w) \geq 0$ for all $|w| < \infty$.

This completes the proof of $(s4)$. Consequently $g(r)$ given by (3.115) is a strong local minimum of (3.168) if $|\Psi| \leq \Psi_{\text{max}}$. $\square$

Appendix B

Alternate Proof of Theorem 4.2.3

In Section 4.2 we presented a proof of the Theorem 4.2.3 based on maximal solution intervals for first order initial value problems. Here we present an alternative proof based on best existence and uniqueness result for first boundary value problem for second order nonlinear ODEs. By eliminating d, equation (4.4) can be written as

$$g''(r) + f(r, g'(r), \alpha, \hat{\alpha}) = 0, \tag{B.1}$$

where

$$f(r, g', \alpha, \hat{\alpha}) = \frac{g'}{r} \left[3 + \frac{2\,\hat{\alpha}\, r^2\, g'^2}{4\,\hat{\alpha} + \alpha\,[4 + r^2\, g'^2\,]^{3/2}} \right]. \tag{B.2}$$

Lemma B.0.6 $f(r, g', \alpha, \hat{\alpha})$ *is a Lipschitzian in* g' *on* $U \equiv [R_i, R_o] \times R \times R^+ \times R^+$. *i.e., there exists a nonnegative constant* L *such that*

$$|f(r, g'_1, \alpha, \hat{\alpha}) - f(r, g'_2, \alpha, \hat{\alpha})| \leq L\,|g'_1 - g'_2|, \tag{B.3}$$

for every $(r, g'_1, \alpha, \hat{\alpha})$ *and* $(r, g'_2, \alpha, \hat{\alpha})$ *in* U.

Proof: Note that if $f(r, g', \alpha, \hat{\alpha})$ has bounded partial derivative $\partial f / \partial g'$ in U then it is a Lipschitzian with lipschitz constant is given by

$$L = \sup_{(r, g', \alpha, \hat{\alpha}) \in U} \left| \frac{\partial f(r, g', \alpha, \hat{\alpha})}{\partial g'} \right|. \tag{B.4}$$

127

Now (B.2) gives

$$\frac{\partial f(r, g', \alpha, \hat{\alpha})}{\partial g'} = \frac{3}{r} + \frac{24\,\hat{\alpha}\,r\,g'^2\,[\hat{\alpha} + \alpha\,\sqrt{4 + r^2\,g'^2}\,]}{[4\,\hat{\alpha} + \alpha\,(4 + r^2\,g'^2\,)^{3/2}]^2}. \tag{B.5}$$

Note from (B.5) that $\partial f / \partial g'$ is an even function of g' and

$$\lim_{g' \to \pm \infty} \frac{\partial f}{\partial g'} = \frac{3}{r}. \tag{B.6}$$

By using the limit in (B.6) and the fact that $\partial f / \partial g'$ is continuous on U it can be proven that $\partial f / \partial g'$ is bounded on U.

For a given α and $\hat{\alpha}$, it is enough to find the supremum of $\partial f / \partial g'$ over the infinite strip $\Omega = \{(r, g') | r \in [R_i, R_o],\ g' \in (-\infty, \infty)\}$.

For each fixed $r \in [R_i, R_o]$ and $\epsilon > 0$, there exists $N > 0$ such that

$$\left| \frac{\partial f}{\partial g'} - \frac{3}{r} \right| < \epsilon \tag{B.7}$$

whenever $|g'| > N$, or equivalently

$$\frac{3}{r} - \epsilon < \frac{\partial f}{\partial g'} < \frac{3}{r} + \epsilon \tag{B.8}$$

whenever $|g'| > N$. Since $r \in [R_i, R_o]$,

$$\frac{3}{R_o} - \epsilon < \frac{\partial f}{\partial g'} < \frac{3}{R_i} + \epsilon \tag{B.9}$$

whenever $|g'| > N$. Let $m_1 = |(3/R_o) - \epsilon|$ and $m_2 = (3/R_i) + \epsilon$. Then (B.9) implies that

$$\left| \frac{\partial f}{\partial g'} \right| < M_1 \tag{B.10}$$

whenever $|g'| > N$ and $r \in [R_i, R_o]$, where $M_1 = \max\{m_1, m_2\}$. Consider the region $\Omega_0 = \{(r.g') | r \in [R_i, R_o],\ g' \in [-N, N]\}$. Since Ω_0 is a compact set and $\partial f / \partial g'$ is a continuous function, there exists a positive number M_2 such that

$$\left| \frac{\partial f}{\partial g'} \right| < M_2 \tag{B.11}$$

whenever $(r, g') \in \omega_0$. Let $L = \max\{M_1, M_2\}$. Then

$$\left| \frac{\partial f(r, g', \alpha, \hat{\alpha})}{\partial g'} \right| < L \tag{B.12}$$

for every $(r, g', \alpha, \hat{\alpha})$ in U. Thus $f(r, g', \alpha, \hat{\alpha})$ is a Lipschitzian in g' on U. This completes the proof of Lemma B.0.6 □

Lemma B.0.7 *Consider the following differential equation*

$$w''(r) + \frac{L}{\lambda} w'(r) = 0, \tag{B.13}$$

subject to

$$w(R_i) = w_i > 0, \quad w'(R_i) = m_i > 0, \tag{B.14}$$

where L is the lipschitz constant given by Lemma B.1 and λ is a positive real number less than 1. Then the solution $w(r)$ of (B.13), (B.14) and its derivative $w'(r)$ are strictly positive functions on $[R_i, \infty)$.

Proof: Clearly the solution of (B.13) satisfying (B.14) is given by

$$w(r) = w_i + \frac{\lambda m_i}{L} - \frac{\lambda m_i}{L} e^{L(R_i - r)/\lambda}. \tag{B.15}$$

Note that

$$w'(r) = m_i e^{L(R_i - r)/\lambda} > 0 \tag{B.16}$$

for every $r \in [R_i, \infty)$. Since $w'(r) > 0$ on $[R_i, \infty)$ and $w(R_i) = w_i > 0$, it follows that $w(r) > 0$ on $[R_i, \infty)$. Hence $w(r)$ and $w'(r)$ are strictly positive functions on $[R_i, \infty)$. This completes the proof of Lemma B.0.7. □

Proof of Theorem 4.2.3:

Note that the second boundary value problem (B.1), (4.15) is equivalent to following integral equation

$$g(r) = l(r) + \int_{R_i}^{R_o} H(r, s) \, f(s, g'(s)) \, ds \quad \text{for} \quad R_i \leq r \leq R_o, \tag{B.17}$$

and

$$g'(r) = m_o + \int_{R_i}^{R_o} H_r(r, s) \ f(s, g'(s)) \, ds, \tag{B.18}$$

where

$$l(r) = \psi_i + m_o \ (r - R_i), \tag{B.19}$$

and $H(r, s)$ is the Green's function given by

$$H(r, s) = \begin{cases} (s - R_i) & R_i \leq s \leq r \leq R_o \\ (r - R_i) & R_i \leq r \leq s \leq R_o, \end{cases} \tag{B.20}$$

and

$$H_r(r, s) = \frac{\partial}{\partial r} H(r, s). \tag{B.21}$$

Note that both H and H_r are nonnegative functions.

Let S be the space of continuously differentiable functions on $[R_i, R_o]$ with the norm

$$\|g(r)\| = \max \left\{ \max_{R_i \leq r \leq R_o} \frac{|g(r)|}{w(r)}, \max_{R_i \leq r \leq R_o} \frac{|g'(r)|}{w'(r)} \right\}, \tag{B.22}$$

where $w(r)$ is the positive weight function given by Lemma B.0.7. The space S is complete with this norm, and convergence in the norm of $g_n(r)$ to $g(r)$ implies uniform convergence of both $g_n(r)$ to $g(r)$ and $g'_n(r)$ to $g'(r)$. Let T be the operator defined by the right side of (B.17). In order to see that T maps S into S, we need to verify that $Tg(r)$ is continuously differentiable whenever $g(r)$ is. Observe that

$$\lim_{h \to 0} \frac{Tg(r + h) - Tg(r)}{h} = m_o + \int_{R_i}^{R_o} H_r(r, s) \ f(s, g'(s)) \, ds, \tag{B.23}$$

and that this limit function is continuous in r. To verify that T is a contraction mapping, consider

$$\frac{|Tg_1(r) - Tg_2(r)|}{w(r)} \leq \frac{1}{w(r)} \int_{R_i}^{R_o} H(r, s) \, |f(s, g'_1(s)) - f(s, g'_2(s))| \, ds. \tag{B.24}$$

130

By using the Lipschitz condition (B.3) equation (B.24) becomes

$$\frac{|Tg_1(r) - Tg_2(r)|}{w(r)} \leq \frac{1}{w(r)} \int_{R_i}^{R_o} H(r,s) \, L \, |g_1'(s) - g_2'(s)| \, ds \qquad \text{(B.25)}$$

or equivalently

$$\frac{|Tg_1(r) - Tg_2(r)|}{w(r)} \leq \frac{1}{w(r)} \int_{R_i}^{R_o} H(r,s) \, L \, w'(s) \, \frac{|g_1'(s) - g_2'(s)|}{w'(s)} \, ds, \quad \text{(B.26)}$$

and hence by (B.22)

$$\frac{|Tg_1(r) - Tg_2(r)|}{w(r)} \leq \qquad\qquad\qquad\qquad\qquad \text{(B.27)}$$

$$\frac{1}{w(r)} \int_{R_i}^{R_o} H(r,s) \, L \, w'(s) \, ds \quad \|g_1(r) - g_2(r)\|.$$

Note that since $w(r)$ is a solution of (B.13) with $w(R_i) > 0$ and $w'(R_i) > 0$, it is also a solution of the following integral equation

$$w(r) = w(R_i) + w'(R_i) \, (r - R_i) + \int_{R_i}^{R_o} H(r,s) \, \frac{L}{\lambda} \, w'(s) \, ds. \qquad \text{(B.28)}$$

Since $w(R_i) + w'(R_i) \, (r - R_i) \geq 0$, for every $r \in [R_i, R_o]$ equation (B.28) implies

$$w(r) \geq \int_{R_i}^{R_o} H(r,s) \, \frac{L}{\lambda} \, w'(s) \, ds, \qquad\qquad\qquad \text{(B.29)}$$

and since $w(r)$ and λ are positive, inequality (B.29) may be written as

$$\frac{1}{w(r)} \int_{R_i}^{R_o} H(r,s) \, L \, w'(s) \, ds \, \leq \lambda. \qquad\qquad\qquad \text{(B.30)}$$

Consequently substitution from (B.30) into (B.27) gives

$$\frac{|Tg_1(r) - Tg_2(r)|}{w(r)} \leq \lambda \, \|g_1(r) - g_2(r)\|. \qquad\qquad\qquad \text{(B.31)}$$

Similarly from (B.18) we obtain

$$\frac{|\frac{d}{dr}(Tg_1(r) - Tg_2(r))|}{w'(r)} \leq \qquad\qquad\qquad\qquad \text{(B.32)}$$

$$\frac{1}{w'(r)} \int_{R_i}^{R_o} H_r(r,s) \, |f(s, g_1'(s)) - f(s, g_2'(s))| \, ds,$$

131

which by virtue of (B.3) and (B.22) yields

$$\frac{|\frac{d}{dr}(Tg_1(r) - Tg_2(r))|}{w'(r)} \leq \tag{B.33}$$

$$\frac{1}{w'(r)} \int_{R_i}^{R_o} H_r(r,s) \, L \, w'(s) \, ds \quad \|g_1(r) - g_2(r)\|.$$

Now (B.28) supplies

$$w'(r) = w'(R_i) + \int_{R_i}^{R_o} H_r(r,s) \, \frac{L}{\lambda} \, w'(s) \, ds. \tag{B.34}$$

Since $w'(R_i) > 0$ for every $r \in [R_i, R_o]$, equation (B.34) implies

$$w'(r) > \int_{R_i}^{R_o} H_r(r,s) \, \frac{L}{\lambda} \, w'(s) \, ds. \tag{B.35}$$

Since $w'(r)$ and λ are positive, inequality (B.35) may be written as

$$\frac{1}{w'(r)} \int_{R_i}^{R_o} H_r(r,s) \, L \, w'(s) \, ds \; < \lambda. \tag{B.36}$$

Consequently substitution from (B.36) into (B.33) gives

$$\frac{|\frac{d}{dr}(Tg_1(r) - Tg_2(r))|}{w'(r)} < \lambda \; \|g_1(r) - g_2(r)\|. \tag{B.37}$$

Now (B.31) and (B.37) together imply that

$$\|Tg_1(r) - Tg_2(r)\| \leq \lambda \; \|g_1(r) - g_2(r)\|. \tag{B.38}$$

Since $0 < \lambda < 1$, T is a contraction mapping on S. Then by the contraction mapping theorem, T has a unique fixed point in S. Of course this means that the second boundary value problem, (B.1), (4.15) has a unique solution on $[R_i, R_o]$ for every $R_o > R_i > 0$. This completes the proof of Theorem 4.2.3. $\square$

BIBLIOGRAPHY

BIBLIOGRAPHY

[1] Akhiezer, N.I., The Calculus of Variation, Blaisdell Publishing Company, New York-London, 1962

[2] Antman, S.S., Nonlinear Problems of Elasticity, Applied Mathematical Sciences, 107, Springer Verlag, New York, 1995

[3] Atkin, R.J. and Fox N., An Introduction to the Theory of Elasticity, Longman Mathematical Texts, London, 1980

[4] Bailey, P.B., Shampine, L.F. and Waltman, P.E., Nonlinear Two Point Boundary Value Problems, New Academic Press, New York-London, 1968

[5] Ball, J.M., Discontinuous equilibrium solutions and cavitation in nonlinear elasticity, Philosophical Transactions of the Royal Society of London. Series A, (1982) vol. 306, pp. 557-610

[6] Beatty, M.F. and Jiang, Q., On Compressible Materials Capable of Sustaining Axisymmetric Shear Deformations. Part 2: Rotational Shear of Isotropic Hyperelastic Materials, Quarterly Journal of Mechanics and Applied Mathematics, (1997) vol. 50, pp. 211-237

[7] Bender, C.M. and Orszag, S.A., Advanced Mathematical Methods for Scientists and Engineers, McGraw-Hill Book Company, New York, 1978

[8] Bush, A.W., Perturbation Methods for Engineers and Scientists, CRC Press, Boca Raton, 1992

[9] Capriz, G., Continua with microstructure, Springer Tracts in Natural Philosophy, 35, Springer Verlag, New York, 1989

[10] Ericksen, J.L., Liquid crystals with variable degree of orientation, Archive for Rational Mechanics and Analysis, (1991) vol. 113, pp. 97-120

[11] Fu, Y.B. and Ogden, R.W., Nonlinear Elastic Deformations, Cambridge University Press, Cambridge, 2001

[12] Gurtin, M.E., Configurational forces as basic concepts of continuum physics, Applied Mathematical Sciences, 137, Springer Verlag, New York, 2000

[13] Holmes, M.H., Introduction to Perturbation Methods, Texts in Applied Mathematics, 20, Springer Verlag, New York, 1995

[14] Horgan C.O. and Polignone, D.A., Cavitation in nonlinear elastic solids: a review, Applied Mechanical Rewiev, (1995) vol. 48, pp. 471-485

[15] Jiang, X. and Ogden, R.W., On Azimuthal Shear of a Circular Cylindrical Tube of Compressible Elastic Material, Quarterly Journal of Mechanics and Applied Mathematics, (1998) vol. 51, pp. 143-158

[16] Johnson, L.W. and Riess, R.D., Numerical Analysis, Addison-Wesley Publishing Company, London, 1982

[17] Keller, H.B., Numerical Solution of Two Point Boundary Value Problems, Society for Industrial and Applied Mathematics, Philadelphia, 1976

[18] Mariano, P.M., Multifield theories in mechanics of solids, Adv. Appl. Mech, (2001) vol. 38, pp. 1-93

[19] Muller S. and Spector, S.J., An existence theory for nonlinear elasticity that allows for cavitation, Archive for Rational Mechanics and Analysis, (1995) vol. 131, pp. 1-66

[20] Murray, F.J. and Miller, K. S., Existence Theorems for Ordinary Differential Equations, Robert E. Krieger Publishing Company, New York, 1976

[21] Ogden, R.W., Nonlinear Elasticity Theory and Applications, Dover Publications, New York, 1997

[22] Pence, T.J. and Tsai, H., An Extended Theory of Elastic Material Response Under Prescribed Swelling, Research notes (2003) with publications in preparation

[23] Pence, T.J. and Tsai, H., On the cavitation of a swollen compressible sphere in finite elasticity, International Journal of Non-Linear Mechanics, (2005) vol. 40, pp. 307-321

[24] Rivlin, R.S., Large Elastic Deformations of Isotropic Materials. VI Further Results in the Theory of Torsion, Shear and Flexure, Philosophical Transactions of the Royal Society of London. Series A, Mathematical and Physical Sciences, (1949) vol. 242, pp. 173-195

[25] Shampine, L.F., Kierzenka J. and Reichelt M.W., Solving Boundary Value Problems for Ordinary Differential Equations in MATLAB with bvp4c, available at ftp://ftp.mathworks.com.pub/doc/papers/bvp/ 2000

[26] Tao, L., Rajagopal, K.R. and Wineman, A.S., Circular Shearing and Torsion of Generalized neo-Hookean Materials, IMA Journal of Applied Mathematics, (1992) vol. 48, pp. 23-37

[27] Triantafyllidis, N. and Bardenhagen, S., On higher order gradient continuum theories in 1-D nonlinear elasticity. Derivation from and comparison to the corresponding discrete models, Journal of Elasticity, (1993) vol. 33, pp. 259-293

[28] Wan, F.Y.M., Introduction to the Calculus of Variations and Its Applications, Chapman and Hall, New York, 1995